

THE IMPACT OF CLIMATE CHANGE ON STREAM FLOW

A DISSERTATION

*Submitted in partial fulfillment of the
requirements for the award of the degree*

of

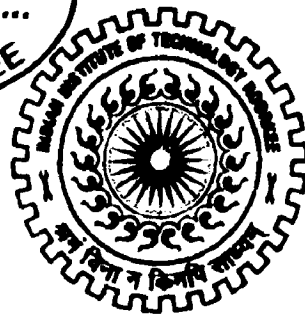
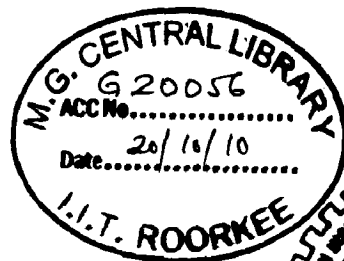
MASTER OF TECHNOLOGY

in

WATER RESOURCES DEVELOPMENT (CIVIL)

By

WISNU PRAMUDIO



**DEPARTMENT OF WATER RESOURCES DEVELOPMENT AND MANAGEMENT
INDIAN INSTITUTE OF TECHNOLOGY ROORKEE
ROORKEE -247 667 (INDIA)
JUNE, 2010**

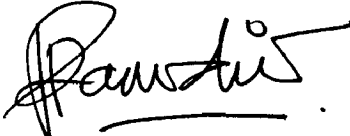
CANDIDATE'S DECLARATION

I hereby certify that the work, which is being presented in the dissertation entitled "**THE IMPACT OF CLIMATE CHANGE ON STREAM FLOW**" in partial fulfillment of the requirement for the award of degree of **Master of Technology in Water Resources Development** in the Department of Water Resources Development and Management of Indian Institute of Technology Roorkee, is an authentic record of my own work carried out during a period from July 2009 to June 2010 under the guidance of **Dr. Deepak Khare**, Professor of Water Resources Development and Management, Indian Institute of Technology Roorkee, India and **Dr. Sharad Kumar Jain**, NEEPCO Chair Professor of Water Resources Development and Management, Indian Institute of Technology Roorkee, India

I have not submitted the matter embodied in this dissertation for the award of any other degree.

Dated : June 3 , 2010


Place : Roorkee



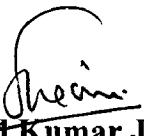
(WISNU PRAMUDIO)
Candidate

CERTIFICATE

This is to certify that the above mentioned statement made by the candidate is correct to the best of my knowledge.



Dr. Deepak Khare
Professor,
Department of Water Resources
Development and Management
I.I.T. Roorkee
Roorkee-247667
INDIA



Dr. Sharad Kumar Jain
NEEPCO Chair Professor,
Department of Water Resources
Development and Management
I.I.T. Roorkee
Roorkee-247667
INDIA

ACKNOWLEDGEMENT

First of all I want to express my thanks to my **God the Almighty ALLAH SWT**, who give me all the things I need: blessing every day that comfort me during awake or sleep.

I wish to express my heartiest thanks to my respected guides, **Dr. Deepak Khare**, Professor of Water Resources Development and Management Department, Indian Institute of Technology Roorkee and **Dr. Sharad Kumar Jain**, NEEPCO Chair Professor of Water Resources Development and Management Department, Indian Institute of Technology Roorkee, who helped and gave me invaluable assistance, guidance, collection of materials, and inspiration during the preparation of this dissertation. I have no words to express my indebtedness to my adviser for allowing me to fulfil my dreams and ambitions through this study.

I express my heartfelt thanks to **Dr. Nayan Sharma**, Professor and Head of Water Resources Development and Management Department, Indian Institute of Technology Roorkee, for his cooperation and facilities provided for this dissertation.

I am also grateful to other **Faculty Members** of Water Resources Development and Management Department, Indian Institute of Technology Roorkee, and my colleagues of **53rd WRD, 29th IWM Batch**, and all **Indonesian Trainees**, who have made it convenient to participate in the dissertation.

Unforgettable a special and sincerest thanks to my family (my father **Hary Yuswadi**, my mother **Tyas Danarini** and my brother **Danang Yudistiro**) for showering me with their unconditional love, persistent supports, encouragements and prayers throughout of my study in India, for giving me the privilege of free thinking, the opportunity to explore the world, and the freedom to make mistakes and learn from them.

The last, I would like to thank all persons who continuously gave me support during the preparation of this dissertation.

Roorkee - India, June 2010

Wisnu Pramudio

Enrollment No. 08548027

WRD & M 53rd Batch

ABSTRACT

Climate change as triggered by global warming is likely to significantly impact water resources and also the human life. As a result of global warming, snow is likely to melt at accelerated rates in many parts of the world, resulting in increased flow of rivers and rising sea levels. Extreme climate may cause increased flooding and drought in various regions. Increased flood and drought are causing many problems in human life and the decline in water quality.

A large number of hydrologic models have been developed to simulate the response of a catchment. Among the various model types, physically based distributed model are the best to study the impacts of climate and land use changes. Geographic information systems (GIS) and model-GIS interfaces aid in efficient creation of input data files required by such models as well as display/presentation of results. One such model widely used by water resources professionals is the Soil and Water Assessment Tool (SWAT). SWAT is a river basin or watershed scale model developed to predict the impact of climate and land management practices on water, sediment, and agricultural chemical yields in large, complex watersheds with varying soils, land use, and management conditions over long periods of time.

The study was aimed to evaluate the impact of climate change on stream flow in the Wonogiri catchment and on hydropower generation. The study was conducted using 20 years of records (1984–2003) of climate variables and 10 years (1994–2003) of discharge. SWAT calibration was performed for the period of 1994 through 1999, while the data for the period 2000–2003 was used for validation. Mann-Kendal statistical method was used in this study to do trend analysis and this together with IPCC (2007) recommendations for South-East Asia were used to create future climate scenarios. Two type of scenarios were conducted: corresponding to the maximum change and the minimum change in precipitation and temperature.

The conclusion of this study is that due to climate change, the stream flow at the Wonogiri catchment are likely to change by 0.4% to 0.37% in the medium-term (2024–2043) scenario and by 14.62% to -9.61% in the long-term (2074–2093) scenario. Changes in stream flow cause changes in the energy that can be generated by Wonogiri

hydropower plant. Accordingly, the energy generation is likely to change by 0.3% to - 0.33% in the medium-term (2024-2043) scenario and it will change by 5.03% to 0.85% in the long-term (2074-2093) scenario.

Mostly, the impact of climate change on the stream flow and hydropower generation at the study area is likely to increase, we can state that climate change impact need not always give negative impact.

CONTENT

CANDIDATE'S DECLARATION	i
ACKNOWLEDGEMENT	ii
ABSTRACT	iii
CONTENT	v
LIST OF TABLES	viii
LIST OF FIGURES	ix

CHAPTER I INTRODUCTION

1.1. General	1
1.2. Dissertation Objectives	4
1.3. Scope of Work	4
1.4. Dissertation Organization	4

CHAPTER II LITERATURE REVIEW

2.1. General	6
2.2. Basic Concept of Climate	
2.2.1. General	6
2.2.2. Monsoon	7
2.2.3. South Asian Monsoons	7
2.3. Climate Change	
2.3.1. General	8
2.3.2. Causes of Climate Change	
2.3.3.1. Natural causes	
A. Continental drift	9
B. Volcanoes	9
C. The earth's tilt	10
D. Ocean currents	11
2.3.3.2. Human causes	
A. Greenhouse gases and their sources	13
2.3.3. Climatic Change in the Recent Past	14
2.3.4. Climate Change in South Asia	
2.3.4.1. Regional characteristic	15
2.3.4.2. Climate trends and variability	15
2.3.5. Climate Change Impact in South Asia	18
2.4. Assessing Climate Change	
2.4.1. Special Report Emission Scenario (SRES)	19
2.4.2. General Circulation Models (GCMs)	21
2.4.3. Trend Analysis Using Mann-Kendall Method	
2.4.3.1. Calculation of the Mann-Kendall Statistic (S)	22
2.4.3.2. Calculation of Probability Associated with the Mann-Kendall Statistic	23
2.5. Impacts of Climate Change	
2.5.1. Impact of Climate Change on Hydrology	

2.5.1.1.	Change in Precipitation	24
2.5.1.2.	Change in Evaporation	24
2.5.2.	Impact of Climate Change on River Flow	24
2.5.3.	Impact of Climate Change on Ground Water	25
2.5.4.	Impact of Climate Change on Water Quality	26
2.5.5.	Impact of Climate Change on Agriculture and Fisheries	26
2.6.	Hydropower	
2.6.1.	Hydropower Potential	28
2.6.2.	Hydropower in the Past, at Present and in the Future	29
2.6.3.	Impact of Climate Change on Hydropower	30

CHAPTER III CATCHMENT MODELING USING SWAT MODEL

3.1.	Soil and Water Assessment Tool (SWAT) Model	33
3.2.	SWAT Modeling	
3.2.1.	Land Phase of the Hydrologic Cycle	34
3.2.2.	Climate.....	35
3.2.3.	Hydrology	
3.2.3.1.	Surface Runoff	36
3.2.3.2.	SCS Equation	36
3.2.3.3.	Green & Ampt Infiltration Method	37
3.2.3.4.	Peak Runoff Rate	40
3.2.3.5.	Time Concentration	40
3.3.	SWAT Calibration Techniques	
3.3.1.	General.....	41
3.3.2.	Basic Water Balance and Total Flow Calibration	
3.3.2.1.	Calibrate Surface Runoff	42
3.3.2.2.	Calibrate Subsurface Flow	42
3.3.3.	Temporal Flow Calibration	43
3.3.4.	Spatial Flow Calibration	44
3.3.5.	Evaluation of Model Performance	44

CHAPTER IV STUDY AREA AND DATA

4.1.	Study Area	46
4.2.	Topography	46
4.3.	Climate	
4.3.1.	Temperature	47
4.3.2.	Relative Humidity	48
4.3.3.	Wind Velocity	48
4.3.4.	Evaporation	48
4.4.	Hydrology	
4.4.1.	Rainfall	49
4.4.2.	Discharge	49
4.5.	Input Data for SWAT Model	50
4.6.	Principal Feature of Wonogiri Multipurpose Dam	50
4.7.	Power Generation at the Wonogiri Hydropower Station	51

CHAPTER V RESULT AND ANALYSIS

5.1. Assessment of Climate Change Scenario53

5.2. Watershed Modeling using SWAT Program

5.2.1. Watershed Deliniation

5.2.1.1. DEM (Digital Elevation Model) Processing56

5.2.1.2. Flow Direction56

5.2.1.3. Flow Accumulation56

5.2.2. Data Processing

5.2.2.1. Precipitation Data Processing59

5.2.2.2. Temperature Data Processing59

5.2.3. HRU (Hydrologic Response Unit) Processing

5.2.3.1. Land Use and Soil Definition64

5.2.4. SWAT Simulation

5.2.4.1. Initial Flow Simulation64

5.2.4.2. SWAT Calibration & Validation65

5.3. Climate Change Scenario76

5.4. Simulation of Reservoir Operation for Hydropower Generation78

CHAPTER VI CONCLUSIONS

6.1. Conclusions86

6.2. Suggestion for Future Research87

REFFERENCES

x

LIST OF TABLES

Table 2.1.	Summary of Past and Present Climate Trends and Variability	16
Table 2.2.	Extreme Climate in Asia	17
Table 3.1.	Example of SWAT Output and Observed Data.....	41
Table 4.1.	Mean Monthly Basin Rainfall	49
Table 4.2.	Data Source for Wonogiri Watershed	50
Table 4.3.	Principal Features of Wonogiri Multipurpose Dam and Reservoir	51
Table 5.1.	Statistical Description of Temperature and Precipitation	53
Table 5.2.	Result of Mann-Kendal Statistical Test.....	54
Table 5.3.	IPCC Projected Changes in Air Temperature and Precipitation	55
Table 5.4.	Comparison Result of Climate Change Projection	55
Table 5.5.	Subbasin Characteristic	58
Table 5.6.	Precipitation Data for SWAT Input	60
Table 5.7.	Temperature Data for SWAT Input	60
Table 5.8.	Measured Discharge for Keduang Subbasin	65
Table 5.9.	SWAT Output for Calibration Year (1994-1999) at Subbasin 3	65
Table 5.10.	Comparison of Observed and Modeling Discharge for Calibration Year	67
Table 5.11.	Statistical Calculation of Model Performance	67
Table 5.12.	Range of Parameter on SWAT Program	69
Table 5.13.	Adjusted Parameter	69
Table 5.14.	Comparison of Observed and Modeling Discharge After Calibration ..	71
Table 5.15.	Comparison of Observed and Modeling Discharge for Validation	72
Table 5.16.	Statistical Calculation of Model Performance after Correction	73
Table 5.17.	Land Use Change at Bengawan Solo Catchment	76
Table 5.18.	Climate Scenario used for Simulation	77
Table 5.19.	Statistical Description of Simulation Result based on Climate Scenario	77
Table 5.20.	Possible Firm Energy and Corresponding Firm Power of Wonogiri Hydropower Plant.....	79
Table 5.21.	(a) Reservoir Simulation : Critical Period for Observed Series (1984 – 2003)	79
	(b) Reservoir Simulation : Critical Period for Long-Term Period (2074 – 2093)	79
Table 5.22.	Simulation of Monthly Firm Energy Generated and Reliability	84
Table 6.1.	Result of Modeling of Wonogiri Catchment	87
Table 6.2.	Hydropower Generation at 0.90 Reliability	87

LIST OF FIGURES

Figure 2.1. Cause-Effect Chain from Emission to Impact	14
Figure 2.2. Location of Country Covered under South Asia	15
Figure 2.3. Seven Step in Climate Change Assessment	19
Figure 3.1. Hydrologic Cycle	34
Figure 3.2. Comparison of Moisture Content Distribution Modeled by Green-Ampt and a Typical Observed Distribution	38
Figure 3.3. Reasonable Peak	43
Figure 3.4. Peak of Simulation is High	44
Figure 4.1. Location Map	46
Figure 4.2. Mean Monthly Humidity and Temperature in the Study Area	48
Figure 4.3. Mean Monthly Wind Velocity and Evaporation in the Study Area	49
Figure 4.4. Water Level of Wonogiri Dam	51
Figure 5.1. Watershed Terrain Analysis using Grids	57
Figure 5.2. Subbasin Map	58
Figure 5.3. Rain Gauge and Weather Station Map	61
Figure 5.4. Land Use and Soil Classification Map	62
Figure 5.5. Land Slope and HRU Map	63
Figure 5.6. Comparison of Observed and Modeling Discharge for Calibration Year	66
Figure 5.7. R^2 of Observed and Modeling Discharge before Calibration Process	68
Figure 5.8. Stream Discharge of Observed and Simulation after Calibration Process	70
Figure 5.9. Stream Discharge of Observed and Simulation for Validation Year	72
Figure 5.10. R^2 for Observed and Modeling Discharge after Calibration Process	73
Figure 5.11. Yearly R^2 before Calibration (1994-1999)	74
Figure 5.12. Yearly R^2 after Calibration (1994-1999)	75
Figure 5.13. Reservoir Simulation Flow Chart for Determining Form Energy	82
Figure 5.14. Reservoir Simulation Flow Chart for Determining Energy Reliability	83
Figure 5.15. Monthly Energy Generated and Reliability	80

CHAPTER I INTRODUCTION

1.1. General

Society is now beginning to feel the impact of climate change in various places around the world, starting from rapid melting of glaciers, rising sea levels, bigger storms, higher floods, less snow in the mountains and droughts. While bigger individual events can not be conclusive evidence of significant climate change, some events, natural observation, the observations by people living close to nature reveal the early signs of a likely major change. Climate is the context for life on earth. Global climate change and the ripples of that change will affect every aspect of life, from municipal budgets for snowplowing to the spread of disease. Climate is already changing, and quite rapidly. With rare unanimity, the scientific community warns of more abrupt and greater change in the future. Today we start seeing impacts of climate change appearing in many places around the globe - be it melting glaciers, rising sea levels, stronger storms, higher floods, less snow in the north and more drought in the south. While individual events cannot be proof of a serious climate change, the multiple events, the observations in nature, the observations by people living close to nature tell the tale.

The earth's climate is dynamic and always changing through a natural cycle. What the world is more worried about is that the changes that are occurring today have been speeded up because of man's activities. These changes are being studied by scientists all over the world by collecting evidences from diverse sources such as pollen samples, ice cores, and sea sediments. The causes of climate change can be divided into two categories - those that are due to natural causes (such as continental drift, volcanoes, the earth's tilt, ocean currents, etc.) and those that are induced by human/anthropogenic causes (industrialization, land use and land cover change, transportation, etc.). Many studies show that anthropogenic causes have contributed more to the global warming in recent past. Among the human activities those that involve burning of fossil fuel have contributed to a rise in greenhouse gases in the atmosphere.

The increase in the average temperature of the earth is called global warming. Many of the scientists who study Earth's climate record have opined that human actions, especially the higher emission of greenhouse gases from the industrial, transportation, energy sector and deforestation are the main causes of global warming.

Estimated shows that nearly 72% of the totally emitted greenhouse gases is carbon dioxide (CO₂), 18% Methane and 9% Nitrous oxide (NO_x). Consequently, the concentration of CO₂ in the atmosphere is rapidly increasing. Carbon dioxide (CO₂) emissions, therefore, are the most important cause of global warming. CO₂ is inevitably released by burning of fossil fuels. One of the major sources of carbon dioxide is thermal power stations. Which emit large amount of carbon dioxide from burning of fossil fuels. Meanwhile, around twenty percent of carbon dioxide emitted to the atmosphere comes from burning of gasoline in the vehicle engine.

Scientist over the world are trying to assess the negative impacts of global warming and the connecting of event (e.g. melting of glaciers, sea level increase, etc) which have taken place in some decades as an warning to global warming. An increase in earth's temperature in turn can cause to change of ecology, including an increasing of sea level and modify rainfall pattern and quantity. This modification can boost concentration and occurrence of extreme of climate event, like floods, famines, heat waves, hurricane, and cyclone. Other consequence may happen at increase or decreasing of agricultural production, degradation of stream flows at summer, species extinctions and improvement of disease.

A modification of the present climate especially of temperature, solar radiation and wind velocity can affect the hydrological regime. Besides, changes in land use and land cover by human activities also affects hydrological regime, especially the pattern and magnitude of discharge. The most vulnerable industries, settlements and societies are generally those located in coastal areas and river flood plains, and those whose economies are closely linked with climate sensitive natural resources.

Currently there is considerable uncertainty about climate change. As a result of climate change, the pattern and intensity of precipitation, amount and temporal distribution are likely to change.

As a consequence of climate change, air and water quality are being degraded, added again with improvement in waste and consumption in consequence of exponential growth in the area with environment problems. Increased extreme precipitation and flooding will increase erosion rates and wash soil based pollutants and toxins into waterways. Coastal surface and groundwater resources are likely to be contaminated due to sea level rise, resulting in saltwater intrusion into rivers, deltas, and aquifers. Increase in water temperatures will lead to more algal and bacterial blooms that further contaminate water supplies and contribute to environmental health risks associated with water. For instance, changes in precipitation patterns are likely to increase flooding, and as a result mobilize more pathogens and contaminants. It is estimated that by 2030 the risk of diarrhea will be up to 10 percent higher in some countries due to climate change.

The records of stream flows can be reflective of climate variation on the river basin as well as changes in land use / land cover. Dynamics of stream flows do not directly show the respond to existing atmospheric conditions but it can be represent a dampened account of meteorological action due to watershed. The most significant ability of stream flow records are to reflect variations climate condition with any anthropogenic activities, such as flow diversion, reduction of base flow by excessive pumping of groundwater reserves, regulation of stream flow by some containment structure, or other effects to the watershed such as widespread changes in land use/land cover by, for example, urbanization or clear cutting. Anthropogenic activity effects on stream flow have to get more attention if stream flow records are used to reflect climate variability and changes.

The impacts of climate change on groundwater are far reaching and need to be investigated, especially in the area where most people rely on groundwater as a source of potable water and for other domestic uses. Groundwater is a vital water resource and awareness needs to be raised on its vulnerability to overexploitation, pollution and, most importantly, climate change. A few research studies have explored the effects of climate change on groundwater. Future simulations also indicate some seasonal variations in flows, whereby in the dry seasons almost all the river runoff will be entirely contributed by base flow. It is simulated that the recharge will intensify in the future, this being

caused by the predicted intensification of rainfall. The mean annual daily discharge is expected to increase by 40–100% from the current in the coming 20–80 years.

The world is faced with considerable risk and uncertainty about climate change. Particular attention has been paid increasingly to hydropower generation in recent years because it is renewable energy. However, hydropower is among the most vulnerable industries to changes in global and regional climate. Due to climate change, precipitation pattern in terms of intensity, annual magnitude and time distribution is likely to change. The hydrological regime of a basin is influenced strongly by water accumulation in the form of snow and ice and the corresponding melt process.

1.2. Objectives of Study

The objectives of this study are:

- i. To review literature related to climate change with particular emphasis on South Asia
- ii. To construct future climate scenario
- iii. To analyze the impact of climate changes on stream flow.
- iv. To analyze the impact of climate changes on hydropower generation for a project.

1.3. Scope of the Work

The scope of study includes the modeling of a catchment by employing ARC GIS 9.3 and SWAT (2005) model. The simulation will focus on stream flows in case of climate change. Calibration will be done by comparing the outputs of the SWAT program with observed data.

1.4. Dissertation Organization

This dissertation is organized into six chapters. Below is the brief description of each chapter.

Chapter 1 – Introduction

An overview introduces the topic of the dissertation, including background, dissertation objectives and scope of the work.

Chapter 2 – Literature Review

This chapter presents a review of the literature pertaining to dissertation topic. The chapter provides review of introduction of a climate change and climate change impacts.

Chapter 3 – Catchment Modeling using SWAT Model

The chapter provides an overview of the SWAT program, and modeling of catchments.

Chapter 4 –Study Area and Data

This chapter describes the study area and the data used in this study

Chapter 5 – Result and Analysis

The results of the SWAT program will be presented in this chapter. It also analyzes the impact of climate change on hydropower generation.

Chapter 6 – Conclusion

This chapter draws conclusions from the dissertation and gives suggestions for further research.

CHAPTER II LITERATURE REVIEW

2.1. General

While no one event is conclusive evidence of climate change, the relentless pace of severe weather — prolonged droughts, intense heat waves, violent windstorms, more wildfires and more frequent “100-year” floods — is indicative of a changing climate. Although the associations among greater weather volatility, natural cycles and climate change are debated, the rise in mega-catastrophes and prolonged widespread heat waves is, at the very least, a harbinger of what we can expect in a changing and unstable climate.

Global Warming is defined as the increase of the average temperature on Earth. As the Earth is getting hotter, disasters like hurricanes, droughts and floods are getting more frequent. It is happening because of climatic effect of an increasing concentration of “greenhouse” gases, primarily carbon dioxide (CO₂), methane and nitrous oxide. In the most general terms, these gases are transparent to incoming short-wave radiation, but they block outgoing long-wave radiation, leading to increase in both surface radiation and surface temperature. These increases in turn, it is hypothesized, lead to changes in climate.

Climate change is the general term for any persistent change in climate, occurring over decades. Global warming is one particular type of climate change.

2.2. Basic Concept of Climate Change

2.2.1. General

Climatic conditions significantly vary from one region to the other. In other words, there are spatial variations in the combinations of elements of weather and climate (wind, temperature, air pressure, humidity, etc.) and hence different climate types are originated. The climate system is a complex, interactive system consisting of the atmosphere, land surface, snow and ice, oceans and other bodies of water, and living things. The atmospheric component of the climate system most obviously characterizes climate; climate is often defined as ‘average weather’. Climate is usually described in

terms of the mean and variability of temperature, precipitation and wind over a period of time, ranging from months to millions of years. (IPCC,2007b)

Weather is the short-term and continually changing conditions in the atmosphere over a certain location that we experience on a daily basis. Weather events or phenomena include rain, sunshine, thunderstorms, and blizzards. The current weather is the result of meteorological conditions that quickly emerge and dissipate like a low-pressure system or a prevailing warm weather front. General weather situations are the weather conditions over large areas such as Europe or East Asia. Observed atmospheric conditions over a few days are also known as weather. Reliable weather forecasts are only possible for a few days and maximum up to a week. Climate refers to the characteristic developments in weather at a specific location or area over a longer period of time. Climate is therefore a statistic of weather in which short-lived fluctuations have little bearing. But climate is not just the “average” weather. Climate also takes into account the frequency of extreme weather events. Climate always refers to a particular place.

2.2.2. Monsoon

The word ‘monsoon’ is used to indicate the winds in the areas where they change their direction twice each year. On this basis, the word monsoon was applied to all those winds of the globe which had directional change from summer season to winter season and vice-versa. The regions that dominated by monsoon winds are called ‘monsoon climatic regions’ which are more developed in Indian sub-continent, south-east Asia, parts of China and Japan.

According to Singh (2005) monsoon is surface convective system which are originated due to differential heating and cooling of the land and water (oceans) and thermal variations. Regionally, monsoons are divided into 3 broad categories, namely, (i) Asian monsoons, (ii) African monsoons and (iii) American monsoons (Singh,2005). In the present study, our focus is on Asian monsoon.

2.2.3. South Asian Monsoons

The Asian monsoons are, on average, the outcome of large-scale seasonal shifting of pressure and associated wind belts and humidity. Asian monsoons are further divided into (1) South Asia monsoons, (2) South-East Asia monsoons and (3) East Asia

monsoons. Some significant variations in South Asian and South-East Asian monsoons are as follows.

- (1) There are variations in summer and winter monsoons over South and East Asia depending upon geographical locations. South Asian monsoons are located in tropical and sub tropical zones.
- (2) The Himalayas and their branches become effective barriers in protecting the Indian subcontinent from the cold polar air masses originating from Siberian and Central Asian high pressure system during winter season.
- (3) The summer monsoons are much stronger in South Asia and are weak in East Asia because of maritime tropical air masses. In fact summer monsoon winds in South Asia are warmer, more humid and unstable. They yield torrential rainfall when they are forced to ascend by mountain barrier (the Himalayas and their chains).

2.3. Climate Change

2.3.1. General

Climate change is defined as variation and shifts in weather condition over space and time of different scales and magnitude. In fact, climatic change refers to drastic or secular change in heat balance of the earth-atmosphere system, moisture, cloudiness and precipitation caused by either external or internal factor (Singh,2005).

The climochronology (history of paleoclimates) reveals the fact that climates have changed in the geological past and hence it is opined that the world's climates have changed in the past, are changing now and there is every reason to expect that they will change in future. The change of climate may be slow and gradual, rapid and catastrophic, periodic, semi-periodic or non-periodic, short-term or long term, may be at local, regional and global scales, it may be due to natural factors or anthropogenic factors.

2.3.2. Causes of Climate Change

The earth's climate is dynamic and always changing through a natural cycle. What the world is more worried about is that the changes that are occurring today have been speeded up because of man's activities. These changes are being studied by scientists all over the world who are finding evidence from tree rings, pollen samples, ice cores, and

sea sediments. The causes of climate change can be divided into two categories - those that are due to natural causes and those that are created by man.

2.3.3.1. Natural causes

There are a number of natural factors responsible for climate change. Some of the more prominent ones are continental drift, volcanoes, ocean currents, the earth's tilt, and comets and meteorites.

A. Continental drift

We may have noticed something peculiar about South America and Africa on a map of the world, they seem to fit into each other like pieces in a jigsaw puzzle. About 200 million years ago they were joined together. Scientists believe that back then, the earth was not as we see it today, but the continents were all part of one large landmass. Proof of this comes from the similarity between plant and animal fossils and broad belts of rocks found on the eastern coastline of South America and western coastline of Africa, which are now widely separated by the Atlantic Ocean. The discovery of fossils of tropical plants (in the form of coal deposits) in Antarctica has led to the conclusion that this frozen land at some time in the past, must have been situated closer to the equator, where the climate was tropical, with swamps and plenty of lush vegetation.

The continents that we are familiar with today were formed when the landmass began gradually drifting apart, millions of years back. This drift also had an impact on the climate because it changed the physical features of the landmass, their position and the position of water bodies. The separation of the landmasses changed the flow of ocean currents and winds, which affected the climate. This drift of the continents continues even today; the Himalayan range is rising by about 1 mm (millimeter) every year because the Indian land mass is moving towards the Asian land mass, slowly but steadily.

B. Volcanoes

When a volcano erupts it throws out large volumes of sulphur dioxide (SO₂), water vapor, dust, and ash into the atmosphere. Although the volcanic activity may last only a few days, yet the large volumes of gases and ash can influence climatic patterns for years. Millions of tones of sulphur dioxide gas can reach the upper levels of the atmosphere (called the stratosphere) from a major eruption. The gases and dust particles

partially block the incoming rays of the sun, leading to cooling. Sulphur dioxide combines with water to form tiny droplets of sulphuric acid. These droplets are so small that many of them can stay aloft for several years. They are efficient reflectors of sunlight, and screen the ground from some of the energy that it would ordinarily receive from the sun. Winds in the upper levels of the atmosphere, called the stratosphere, carry the aerosols rapidly around the globe in either an easterly or westerly direction. Movement of aerosols north and south is always much slower. This should give you some idea of the ways by which cooling can be brought about for a few years after a major volcanic eruption.

Mount Pinatoba, in the Philippine islands erupted in April 1991 emitting thousands of tones of gases into the atmosphere. Volcanic eruptions of this magnitude can reduce the amount of solar radiation reaching the Earth's surface, lowering temperatures in the lower levels of the atmosphere (called the troposphere), and changing atmospheric circulation patterns. The extent to which this occurs is an ongoing debate.

Another striking example was in the year 1816, often referred to as "the year without a summer." Significant weather-related disruptions occurred in New England and in Western Europe with killing summer frosts in the United States and Canada. These strange phenomena were attributed to a major eruption of the Tambora volcano in Indonesia, in 1815.

Recent phenomenon is erupted of E15 volcano in Iceland on end of April 2010. As release by The Philadelphia Inquirer at April 23rd 2010, many scientist believed that E15 eruption will not cause any large-scale climate change because they have not been lofted high enough. The other eruptions, such as Pinatubo in 1991 sent sulfur dioxide into stratosphere that causes dramatic sunset and a drop of 1°F in global temperatures (www.philly.com).

C. The earth's tilt

The earth makes one full orbit around the sun each year. It is tilted at an angle of 23.5° to the perpendicular plane of its orbital path. For half of the year the northern hemisphere tilts towards the sun and experiences summer. In the other half when it is winter, the earth is tilted away from the sun. If there was no tilt we would not have experienced seasons. Changes in the tilt of the earth can affect the severity of the seasons

- more tilt means warmer summers and colder winters; less tilt means cooler summers and milder winters.

The Earth's orbit is somewhat elliptical, which means that the distance between the earth and the Sun varies over the course of a year. We usually think of the earth's axis as being fixed, after all, it always seems to point toward Polaris (also known as the Pole Star and the North Star). Actually, it is not quite constant: the axis does move, at the rate of a little more than a half-degree each century. So Polaris has not always been, and will not always be, the star pointing to the North. When the pyramids were built, around 2500 BC, the pole was near the star Thuban (Alpha Draconis). This gradual change in the direction of the earth's axis, called precession is also responsible for changes in the climate.

D. Ocean currents

The oceans are a major component of the climate system. They cover about 71% of the Earth and absorb about twice as much of the sun's radiation as the atmosphere or the land surface. Ocean currents move vast amounts of heat across the planet - roughly the same amount as the atmosphere does. But the oceans are surrounded by land masses, so heat transport through the water is through channels.

Winds push horizontally against the sea surface and drive ocean current patterns. Certain parts of the world are influenced by ocean currents more than others. The coast of Peru and other adjoining regions are directly influenced by the Humboldt Current that flows along the coastline of Peru. The El Niño event in the Pacific Ocean can affect climatic conditions all over the world. El Niño is considered as a significant weather event which occurs off the west coast of South America, mainly off the Peru Coast. While the occurrence of La Nina event is strengthens Southern Oscillation and walker circulation at the eastern Pacific Ocean off the Peru coast is characterized by more precipitation at south and south-east Asia (Singh,2005).

Another region that is strongly influenced by ocean currents is the North Atlantic. If we compare places at the same latitude in Europe and North America the effect is immediately obvious. For example some parts of coastal Norway have an average temperature of -2°C in January and 14°C in July; while places at the same latitude on the Pacific coast of Alaska are far colder: -15°C in January and only 10°C in July. The warm

current along the Norwegian coast keeps much of the Greenland-Norwegian Sea free of ice even in winter. The rest of the Arctic Ocean, even though it is much further south, remains frozen.

Ocean currents have been known to change direction or slow down. Much of the heat that escapes from the oceans is in the form of water vapor, the most abundant greenhouse gas on Earth. Yet, water vapor also contributes to the formation of clouds, which shade the surface and have a net cooling effect.

Any or all of these phenomena can have an impact on the climate, as is believed to have happened at the end of the last Ice Age, about 14,000 years ago.

2.3.3.2. Human causes

Whether, and to what extent, one also changes the factors governing climate is a subject currently being hotly disputed. Probably people in earlier times already influenced the climate. An example of this is the complete clearance of timberland areas in middle Europe by the Greeks, Phoenicians, and later mainly by the Romans (ship building). However, the influence on the climate remained regionally limited; global effects cannot be deduced from this.

But the basic changes caused by the developments in the wake of the Industrial Revolution in the 19th century saw the large-scale use of fossil fuels for industrial activities. These industries created jobs and over the years, people moved from rural areas to the cities. This trend is continuing even today. More and more land that was covered with vegetation has been cleared to make way for houses. Natural resources are being used extensively for construction, industries, transport, and consumption. Consumerism (our increasing want for material things) has increased by leaps and bounds, creating mountains of waste. Also, our population has increased to an incredible extent. Up until this point in time, people for many centuries did not have many energy sources available. They used muscle power or draft animals, wind and water power (sailing boats, windmills, etc.) as well as firewood which were used as further sources of energy. The use of fossil fuels opened up a completely new dimension. Steam engines, combustion engines, the production and use of electricity as well as numerous other technical innovations replaced handicrafts; wind and water power, and caused an

largely to a rise in temperature, particularly during the summer and normally drier months.

Table 2.2. Extreme Climate in Asia

COUNTRY	KEY TREND
Heat waves	
Russia	Heat waves broke past 22-year record in May 2005
Mongolia	Heat wave duration has increased by 8 to 18 days in last 40 years; coldwave duration has shortened by 13.3 days
China	Increase in frequency of short duration heat waves in recent decade, increasing warmer days and nights in recent decades
Japan	Increasing incidences of daily maximum temperature >35°C, decrease in extremely low temperature
Korea	Increasing frequency of extreme maximum temperatures with higher values in 1980s and 1990s; decrease in frequency of record low temperatures during 1958 to 2001
India	Frequency of hot days and multiple-day heat wave has increased in past century; increase in deaths due to heat stress in recent years
South-East Asia	Increase in hot days and warm nights and decrease in cold days and nights between 1961 and 1998
Intense Rains and Floods	
Russia	Increase in heavy rains in western Russia and decrease in Siberia; increase in number of days with more than 10 mm rain; 50 to 70% increase in surface runoff in Siberia
China	Increasing frequency of extreme rains in western and southern parts including Changjiang river, and decrease in northern regions; more floods in Changjiang river in past decade; more frequent floods in North-East China since 1990s; more intense summer rains in East China; severe flood in 1999; seven-fold increase in frequency of floods since 1950s
Japan	Increasing frequency of extreme rains in past 100 years attributed to frontal systems and typhoons; serious flood in 2004 due to heavy rains brought by 10 typhoons; increase in maximum rainfall during 1961 to 2000 based on records from 120 stations
South Asia	Serious and recurrent floods in Bangladesh, Nepal and north-east states of India during 2002, 2003 and 2004; a record 944 mm of rainfall in Mumbai, India on 26 to 27 July 2005 led to loss of over 1,000 lives with loss of more than US\$250 million; floods in Surat, Barmer and in Srinagar during summer monsoon season of 2006; 17 May 2003 floods in southern province of Sri Lanka were triggered by 730 mm rain
South-East Asia	Increased occurrence of extreme rains causing flash floods in Vietnam; landslides and floods in 1990 and 2004 in the Philippines, and floods in Cambodia in 2000
Droughts	
Russia	Decreasing rain and increasing temperature by over 1°C have caused droughts; 27 major droughts in 20th century have been reported
Mongolia	Increase in frequency and intensity of droughts in recent years; droughts in 1999 to 2002 affected 70% of grassland and killed 12 million livestock
China	Increase in area affected by drought has exceeded 6.7 Mha since 2000 in Beijing, Hebei Province, Shanxi Province, Inner Mongolia and North China; increase in dust storm affected area
South Asia	50% of droughts associated with El Niño; consecutive droughts in 1999 and 2000 in Pakistan and N-W India led to sharp decline in water tables; consecutive droughts between 2000 and 2002 caused crop failures, mass starvation and affected ~11 million people in Orissa; droughts in N-E India

	during summer monsoon of 2006
South-East Asia	Droughts normally associated with ENSO years in Myanmar, Laos, Philippines, Indonesia and Vietnam; droughts in 1997 to 98 caused massive crop failures and water shortages and forest fires in various parts of Philippines, Laos and Indonesia
Cyclones/Typhoons	
Philippines	On an average, 20 cyclones cross the Philippines Area of Responsibility with about 8 to 9 landfall each year; with an increase of 4.2 in the frequency of cyclones entering PAR during the period 1990 to 2003
China	Number and intensity of strong cyclones increased since 1950s; 21 extreme storm surges in 1950 to 2004 of which 14 occurred during 1986 to 2004
South Asia	Frequency of monsoon depressions and cyclones formation in Bay of Bengal and Arabian Sea on the decline since 1970 but intensity is increasing causing severe floods in terms of damages to life and property
Japan	Number of tropical storms has two peaks, one in mid 1960s and another in early 1990s, average after 1990 and often lower than historical average

Source : IPCC, 2007c

2.3.5. Climate change impact in South Asia

Asia is the largest continent on Earth and spreads over four climatic zones (boreal, arid and semi-arid, tropical and temperate). The region faces formidable environmental and socio-economic challenges in its effort to protect valuable natural resources. Land and ecosystems are being degraded, threatening to undermine food security. In addition, water and air quality are deteriorating while continued increases in consumption and associated waste have contributed to the exponential growth in the region's existing environmental problems. Furthermore, the region is highly subject to natural hazards, such as the 2004 Indian Ocean Tsunami, the 2005 Pakistan Earthquake, and the 2006 landslides in the Philippines.

There is evidence of prominent increases in the intensity and/or frequency of many extreme weather events such as heat waves, tropical cyclones, prolonged dry spells, intense rainfall, tornadoes, snow avalanches, thunderstorms, and severe dust storms in the region. Impacts of such disasters range from hunger and susceptibility to disease, to loss of income and livelihoods, affecting human survival and well-being. For example the extreme weather events in China during 2006 included major storms and flooding in the east and south, as well as heat and drought in central, western and northeastern regions, killing more than 2700 people and causing USD 20 billion in damages. Climate change will affect many sectors, including water resources, agriculture and food security, ecosystems and biodiversity, human health and coastal zones. Many environmental and developmental problems in Asia will be exacerbated by climate change (UNFCCC, 2007).

2.4. Assessing Climate Change

Climate change assessments are estimates of what might happen under specified scenarios. As such, they must be based on rigorous, well-documented methodology, and all the stages in the process must be credible and scientifically-supportable. In general framework for conducting a climate change impact assessment was prepared, under the auspices of the IPCC, by Carter *et al* (1994). They defined seven steps as shown on Figure 2.3. (Kates, 1985; Carter *et al.*, 1994; Arnell, 1997).

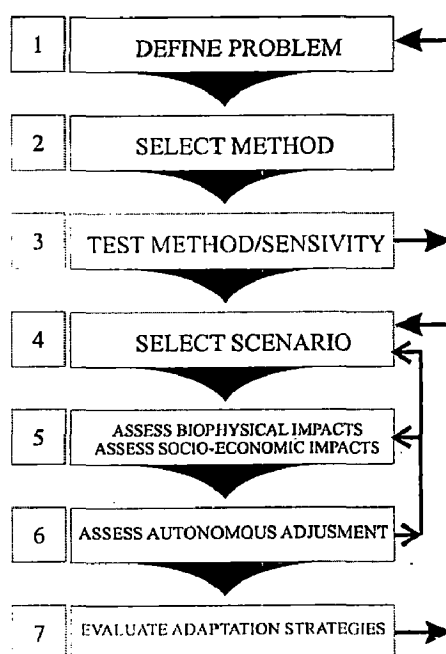
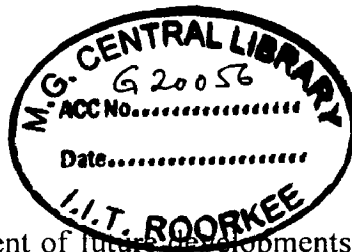


Figure 2.3. Seven Steps in Climate Change Assessment
(Sources : Arnell, 1997)

2.4.1. Special Report on Emission Scenario (SRES)

Scenarios are images of the future, or alternative futures. They are neither predictions nor forecasts. Rather, each scenario is one alternative image of how the future might unfold. A set of scenarios assists in the understanding of possible future developments of complex systems. Some systems, those that are well understood and for which complete information is available, can be modeled with some certainty, as is frequently the case in the physical sciences, and their future states predicted. However, many physical and social systems are poorly understood, and information on the relevant variables is so incomplete that they can be appreciated only through intuition and are best communicated by images and stories.



Scenarios help in the assessment of future developments in complex systems that are either inherently unpredictable, or that have high scientific uncertainties. In all stages of the scenario-building process, uncertainties of different nature are encountered. A large uncertainty surrounds future emissions and the possible evolution of their underlying driving forces, as reflected in a wide range of future emissions paths in the literature. The uncertainty is further compounded in going from emissions paths to climate change, from climate change to possible impacts and finally from these driving forces to formulating adaptation and mitigation measures and policies. The uncertainties range from inadequate scientific understanding of the problems, data gaps and general lack of data to inherent uncertainties of future events in general. Hence the use of alternative scenarios to describe the range of possible future emissions.

For the current SRES scenarios, the following sources of uncertainties are identified:

- *Choice of Storylines.* Freedom in choice of qualitative scenario parameter combinations, such as rainfall combined with discharge data, contributes to scenario uncertainty.
- *Authors Interpretation of Storylines.* Uncertainty in the individual modeler's translation of narrative scenario storyline text in quantitative scenario drivers. Two kinds of parameters can be distinguished:
 - Harmonized drivers such as population, GDP, and final energy. Inter-scenario uncertainty is reduced in the harmonized runs as the modeling teams decided to keep population and GDP within certain agreed boundaries.
 - Other assumed parameters were chosen freely by the modelers, consistent with the storylines.
- *Translation of the Understanding of Linkages between Driving Forces into Quantitative Inputs for Scenario Analysis.* Often the understanding of the linkages is incomplete or qualitative only. This makes it difficult for modelers to implement these linkages in a consistent manner.

- *Methodological Differences.*
 - Uncertainty induced by conceptual and structural differences in the way models work (model approaches) and in the ways models are parameterized.
 - Uncertainty in the assumptions that underlie the relationships between scenario drivers and output, such as the relationship between average income and diet change.
- *Different Sources of Data.* Data differ from a variety of well-acknowledged scientific studies, since "measurements" always provide ranges and not exact values. Therefore, modelers can only choose from ranges of input parameters for. For example:
 - Base year data.
 - Historical development trajectories.
 - Current investment requirements.
- *Inherent Uncertainties.* These uncertainties stem from the fact that unexpected "rare" events or events that a majority of researchers currently consider to be "rare future events" might nevertheless occur and produce outcomes that are fundamentally different from those produced by SRES model runs.

2.4.2. General Circulation Models (GCMs)

Numerical models (General Circulation Models or GCMs), representing physical processes in the atmosphere, ocean, cryosphere and land surface, are the most advanced tools currently available for simulating the response of the global climate system to increasing greenhouse gas concentrations. While simpler models have also been used to provide globally- or regionally-averaged estimates of the climate response, only GCMs, possibly in conjunction with nested regional models, have the potential to provide geographically and physically consistent estimates of regional climate change which are required in impact analysis.

2.4.3. Trend Analysis Using Mann-Kendall Method

The Mann-Kendall test was performed to evaluate the trend of precipitation at rain gauge station

2.4.3.1. Calculation of the Mann-Kendall Statistic (S)

The Mann-Kendall test is a non-parametric test for identifying trends in time series data. The test compares the relative magnitudes of sample data rather than the data values themselves (Gilbert, 1987). One benefit of this test is that the data need not conform to any particular distribution. Moreover, data reported as non-detects can be included by assigning them a common value that is smaller than the smallest measured value in the data set. The procedure that will be described in the subsequent paragraphs assumes that there exists only one data value per time period. When multiple data points exist for a single time period, the median value is used. The data values are evaluated as an ordered time series. Each data value is compared to all subsequent data values. The initial value of the Mann-Kendall statistic, S, is assumed to be 0 (e.g., no trend). If a data value from a later time period is higher than a data value from an earlier time period, S is incremented by 1. On the other hand, if the data value from a later time period is lower than a data value sampled earlier, S is decremented by 1. The net result of all such increments and decrements yields the final value of S.

Let x_1, x_2, \dots, x_n represent n data points where x_j represents the data point at time j.

Then the Mann-Kendall statistic (S) is given by

$$S = \sum_{k=1}^{n-1} \sum_{j=k+1}^n \text{sign}(x_j - x_k) \dots\dots\dots(2.1)$$

where :

$$\begin{aligned} \text{sign}(x_j - x_k) &= 1 \quad \text{if } x_j - x_k > 0 \\ &= 0 \quad \text{if } x_j - x_k = 0 \dots\dots\dots(2.2) \\ &= -1 \quad \text{if } x_j - x_k < 0 \end{aligned}$$

A very high positive value of S is an indicator of an *increasing* trend, and a very low negative value indicates a *decreasing* trend. However, it is necessary to compute the probability associated with S and the sample size, n, to statistically quantify the significance of the trend.

2.4.3.2. Calculation of Probability Associated with the Mann-Kendall Statistic

Kendall (1975, p55) describes a normal-approximation test that could be used for datasets with *more than 10 values*, provided there are not many tied values within the data set.

The test procedure is as follows:

- Calculate S as described
- Calculate the variance of S, VAR(S), by the following equation:

$$VAR(S) = \frac{1}{18} \left[n(n-1)(2n+5) - \sum_{p=1}^g t_p(t_p-1)(2t_p+5) \right] \dots\dots\dots(2.3)$$

where n is the number of data points, g is the number of tied groups (a tied group is a set of sample data having the same value), and t_p is the number of data points in the p^{th} group.

- Compute a normalized test statistic Z as follows:

$$\begin{aligned} Z &= \frac{S-1}{[VAR(S)]^{1/2}} \quad \text{if } S > 0 \\ &= 0 \quad \text{if } S = 0 \quad \dots\dots\dots(2.4) \\ &= \frac{S+1}{[VAR(S)]^{1/2}} \quad \text{if } S < 0 \end{aligned}$$

- Compute the probability associated with this normalized test statistic. The probability density function for a normal distribution with a mean of 0 and a standard deviation of 1 is given by the following equation:

$$f(z) = \frac{1}{\sqrt{2\pi}} e^{-\frac{z^2}{2}} \dots\dots\dots(2.5)$$

Microsoft Excel function, *NORMSDIST()*, was used to calculate this probability.

- Decide on a probability level of significance (95% typically).
- The trend is said to be *decreasing* if Z is negative and the computed probability is greater than the level of significance. The trend is said to be *increasing* if the Z is positive and the computed probability is greater than the level of significance. If the computed probability is less than the level of significance, there is *no trend*.

2.5. Impacts of Climate Change

2.5.1. Impacts of climate change on hydrology

The greatest attention has been directed towards changes in the mean climate, the variability of climatic inputs to the hydrological system are also likely to change. A simple rise in the mean of an input – such as precipitation – would affect the mean value of the output – such as stream flow – and could also affect the variance of the output because of the non-linear relationships between input and output.

2.5.1.1. Change in precipitation

Precipitation is the major driving force of the hydrological system. Changes in the amount, intensity, duration and timing during the year will all affect river flows and groundwater recharge, but to what degree will depend on the amount of change and the type of catchments.

2.5.1.2. Change in evaporation

Potential evapotranspiration is the evaporation and transpiration that would occur from an extensive short grass crop with unlimited supply of water. It is controlled by meteorological demand – as determined by inputs of net radiation, the ability of the air to hold moisture and the rate of renewal of air above the evaporating surface – and plant physiological properties, which include aerodynamic resistance and stomatal conductance. Global warming will alter potential evaporation. The most immediate effect will be an increase in the air's ability to absorb water as temperature rises.

2.5.2. Impacts of climate change on river flow

Climate change will have wide-ranging effects on the environment, and on socio-economic and related sectors, including water resources, agriculture and food security, human health, terrestrial ecosystems and biodiversity and coastal zones. Changes in rainfall pattern are likely to lead to severe water shortages and/or flooding. Melting of glaciers can cause increasing in river discharge, flooding and soil erosion.

Many catchments and rivers are heavily modified by human activities, which will complicate the effect of global warming. The most obvious human interventions are structures and procedures to manage the water (particularly reservoir and interbasin transfer) and abstraction from and return to water courses (all have direct impacts, intentional and unintentional on river flows). Human activities also effect catchments

land use, and these also can have significant effect on river regimes and water quality of the river. Land use decisions may be affected by global warming, farmers may alter cropping patterns or crop mixes (or at the extreme, abandon land or cultivate new land), different amounts of agricultural chemicals may be applied, and a policy of afforestation for carbon sequestration would affect catchment water balances.

The variability in extreme discharges for climate change conditions increases with respect to the simulations for current climate conditions. This variability results both from the stochasticity of the precipitation process and the differences between the climate models. The total uncertainty in river flooding with climate change (over 40%) is much larger than the change with respect to current climate conditions (less than 10%). However, climate changes are systematic changes rather than random changes and thus the large uncertainty range will be shifted to another level corresponding to the changed average situation. (Booij,2005).

2.5.3. Impact on Ground Water

The impacts of climate change on groundwater are far reaching and need to be investigated, especially in the area where most people rely on groundwater as a source of potable water and for other domestic uses. Groundwater is a vital water resource and awareness needs to be raised on its vulnerability to overexploitation, pollution and, most importantly, climate change. However, there are still few research studies that have explored the effects of climate change on groundwater. Future simulations also indicate some seasonal variations in flows, whereby in the dry seasons almost all the river runoff will be entirely contributed by base flow. It is simulated that the recharge will intensify in the future, this being caused by the predicted intensification of rainfall. The mean annual daily discharge is expected to increase by 40–100% from the current in the coming 20–80 years (Dragoni, 2008). Corresponding increases in mean annual daily base flows were found to range between 30 and 90% from the current base flow (69% of total runoff) (Dragoni, 2008). The results from their study Nyenje and Batelaan (2009) suggest that, in the future, the region will experience increased annual flooding and rising groundwater levels, especially in the wet seasons, due to climate change. Thus, there is need for more hydrogeological studies in order to ensure more reliable recharge estimates.

2.5.4. Impact on Water Quality

As a consequence of climate change, air and water quality are being degraded, moreover with improvement in waste and consumption in consequence of exponential growth in the area with environment problems. Increase extreme precipitation and flooding, which will increase erosion rates and wash soil based pollutants and toxins into waterways. Contaminate coastal surface and groundwater resources due to sea level rise, resulting in saltwater intrusion into rivers, deltas, and aquifers. Increase water temperatures, leading to more algal and bacterial blooms that further contaminate water supplies. Contribute to environmental health risks associated with water. For instance, changes in precipitation patterns are likely to increase flooding, and as a result mobilize more pathogens and contaminants. It is estimated that by 2030 the risk of diarrhea will be up to 10 percent higher in some countries due to climate change. Any change in precipitation regime will in turn have an effect on freshwater ecosystems. The functional responses of each ecosystem class in regard to climate change will differ due to the underlying differences in the structure and flow dynamics of such systems (Polhemus, 2009).

2.5.5. Impacts of Climate Change on Agriculture and Fisheries

At present, 40% of the Earth's land surface is managed for cropland and pasture. Natural forests cover another 30% (3.9 billion ha) of the land surface with just 5% of the natural forest area (FAO, 2000) providing 35% of global roundwood. In developing countries, nearly 70% of people live in rural areas where agriculture is the largest supporter of livelihoods. Growth in agricultural incomes in developing countries fuels the demand for non-basic goods and services fundamental to human development. The United Nations Food and Agriculture Organization (FAO) estimates that the livelihoods of roughly 450 million of the world's poorest people are entirely dependent on managed ecosystem services. Fish provide more than 2.6 billion people with at least 20% of their average per capita animal protein intake, but three-quarters of global fisheries are currently fully exploited, overexploited or depleted (FAO, 2004c).

Global warming will confound the impact of natural variation on fishing activity and complicate management. The sustainability of the fishing industries of many countries will depend on increasing flexibility in bilateral and multilateral fishing

agreements, coupled with international stock assessments and management plans. Increases in seawater temperature have been associated with increases in diseases and algal blooms in the aquaculture industry.

Under climate change, predicted rainfall increases over most of Asia, particularly during the summer monsoon, could increase flood-prone areas in East Asia, South Asia and Southeast Asia. In Central and South Asia, crop yields are predicted to fall by up to 30 per cent, creating a very high risk of hunger in several countries. Global warming is causing the melting of glaciers in the Himalayas. In the short term, this means increased risk of flooding, erosion, mudslides and GLOF in Nepal, Bangladesh, Pakistan, and north India during the wet season. Because the melting of snow coincides with the summer monsoon season, any intensification of the monsoon and/or increase in melting is likely to contribute to flood disasters in Himalayan catchments. In the longer term, global warming could lead to a rise in the snowline and disappearance of many glaciers causing serious impacts on the populations relying on the 7 main rivers in Asia fed by melt water from the Himalayas. Throughout Asia one billion people could face water shortage leading to drought and land degradation by the 2050s (UNFCCC:2007).

In recent years, enormous pressures have been put on Asia's ecosystems to support the ever growing demand for natural resources. The most affected areas are coastal and marine ecosystems, forests and mountainous regions and the flora and fauna within them. Climate change will have a profound effect on the future distribution, productivity, and health of forests throughout Asia, for example northeast China may become deprived of conifer forest.¹⁷ Grassland productivity is expected to decline by as much as 40 – 90 per cent for an increase in temperature of 2 – 3° C, combined with reduced precipitation, in the semi-arid and arid regions of Asia.

Fisheries in both fresh water and sea water could be affected. Fisheries at higher elevations are likely to be adversely affected by lower availability of oxygen due to a rise in surface air temperatures. In the plains, the timing and amount of precipitation could also affect the migration of fish species from the river to the floodplains for spawning, dispersal, and growth (FAO 2003). Sea level rise and changes in sea water temperature, salinity, wind speed and direction, strength of upwelling, mixing layer thickness and predator response to climate change have the potential to substantially alter fish breeding

habitats and food supply for fish and ultimately the abundance of fish populations in Asian waters with associated effects on coastal economies.(UNFCC:2007;IPCC:2007c)

2.6. Hydropower

Hydropower generation follows a simple concept: water falling under the force of gravity turns the blades of a turbine, which is connected to a generator. The rotating generator produces electricity. The pre-historic man was aware of the energy contained in falling water. One of the earliest devices to utilize this energy was the water wheel. The Romans used the energy of falling water to do many useful things. They had constructed paddle wheels that turned with the river flow and lifted water to troughs built higher than river level. Before 2000 B.C., the Egyptians and the Greeks knew how to harness the power of river currents to turn wheels and grind grain. More efficient water wheels were built for milling grain in the middle ages. The basic elements of potential water power are river or stream flow and available head or fall trough which the stream flow may be utilized in the development of power in hydropower plant.

2.6.1. Hydropower Potential

Before any power plant is contemplated it is essential to assess the inherent power available from the discharge of the river and the head available at the site. Let P (mkg/sec) be the potential power for a stream having a head of H (m) and a discharge carrying capacity of Q (m³/sec). The theoretical potential power can be expressed as :

$$P = wQH \text{ (m kg / sec)} \dots\dots\dots(2.6)$$

where w , the specific weight of water = 1000 kg/m³. This expression written in term of “horse power” and kW would be :

$$P = \frac{1000QH}{75} = 13.33QH \text{ (hp)} \dots\dots\dots(2.7)$$

or

$$P = 0.736(13.33)QH = 9.81QH \text{ (kW)} \dots\dots\dots(2.8)$$

Then total energy that can be produce is:

$$E = \frac{P}{3600} = \frac{9.81QH}{3600} = 0.002725QH \text{ (kWH)} \dots\dots\dots(2.9)$$

The total kilowatt-hours of energy, that produce from equation (2.9) is assuming 100% efficiency in conversion of potential to electrical energy, than the energy that produce using a given plant efficiency is:

$$E = 0.002725 QHe \dots\dots\dots(2.10)$$

with e as plant efficiency.

2.6.2. Hydropower in the Past, at Present and in the Future

Hydropower projects have been built successfully for over a hundred years. During this long period societal attitudes and needs have changed and science has made good progress. This impacted on the planning, construction and operation of hydropower projects. The first generation hydropower plants were wooden water wheels used for motive power. Around 1880 the first small single purpose hydroelectric plants were built. Over the years more and more projects became multipurpose, making best use of dam projects for irrigation, hydropower, water supply, and flood control. With progress in technology and increasing electricity demand, the maximum size of hydro projects increased. After World War II the pace at which hydro plants were built accelerated, first in the industrialized world and China, and 10–15 years later also in developing countries. Worldwide, most hydro projects were commissioned between 1955 and 1985.

Electricity generation from hydropower makes a substantial contribution to meeting today’s increasing world electricity demands. In the mid-1990s hydropower plants accounted for about 19% (or approx. 2500TWh/a) of total electricity production worldwide and reached 22% (or approx. 700GW) of the total installed capacity for electricity generation (EIA, 1999; IEA, 1999). The role of hydropower, along with other renewable energy sources, is expected to become increasingly important in future. World production of hydroelectricity has grown steadily by about 2.3% per year on average since 1980 (European Commission, 2000).

Looking into the future, there are good reasons to expect a revival for hydro in the medium to long term: (Oud, 2002)

- The depletion of oil and natural gas deposits will lead to higher generation costs for thermal plant in the future, putting hydro in a relatively better position.

- By offsetting thermal generation, hydropower is a leading technology in efforts to reduce greenhouse gases. With the introduction of carbon trading, thermal plant will become more expensive, improving the chances of hydro development.
- HVDC (high voltage direct current) transmission over long distances is becoming cheaper and electricity networks are getting interconnected and growing, improving the prospects for large scale hydro plants in remote areas.
- The ancillary services in electrical networks¹ that can be provided by hydro are increasingly acknowledged and financially rewarded. This adds to the revenues and makes hydro more attractive.
- Due to the growth of the world population, especially in developing countries, new dams will have to be built for irrigation and water supply. The addition of a hydropower component to such a project is economic and has practically no additional environmental or social impacts.
- It is widely believed that, as part of the long-term changes in the energy sector, hydrogen is the fuel of the future. Remote hydro can become one of the major carbon-free financially viable producers of hydrogen.

2.6.3. Impact of Climate Change on Hydropower

Hydropower generation depends on availability of water and effective head. The climate change has significant contribution to changes in rainfall intensity and distribution. These changes lead to change in discharge and effective head that caused a change in hydropower production. A search of literature showed only limited studies that have investigated the impact of climate change on hydropower generation.

Lehner et al. (2005) reviewed the potential of hydroelectric power generation in Europe in terms of present, mid-and long-term prospects. Assessments of European hydropower potential presented in the study are based on flow calculations as provided by WaterGAP (Water-Global Assessment and Prognosis) model. This model provides a study of current and the future climate and the water use conditions to the river flow time series. The model allows for the analysis of the combined effects of climate change and the demographic, socio-economic and technological trends in large-scale discharge regime. WaterGAP model consists of two main components: the Global Hydrology Model and the Global Water Use Model. The Global Hydrology Model simulates the

characteristic macro-scale behavior of the terrestrial water cycle and estimates of natural water availability that is defined as the total river discharge, which is a combination of surface runoff and groundwater recharge. While, the Global Water Use Model consists of four submodels which calculate the water use for household-sector, industry, irrigation, and livestock. The main results of the model simulations can be summarized as follows:

- Based on climate projections from two different GCMs and a set of scenarios, for the future water use, it is likely that there will be increased availability of water in north and northeast Europe and decrease availability in large parts of southern and southeastern Europe.
- Reduction of water resources could occur due to a shift towards a drier climate or a significant increase in water use by humans. The latter is assumed to have a significant effect in Eastern Europe.
- Results from GCM projections for 2070 for Scandinavia and northern Russia show an increase in developed hydropower potential of 15-30% and above. Areas most vulnerable to decline in hydropower potential are Portugal and Spain in the southwest of Europe, as well as Ukraine, Bulgaria and Turkey in the southeast, with decreases of 20-50% or more. In the western and central Europe, the United Kingdom and Germany, a stable developed hydropower potential will be noticed compared with other European countries.
- For the whole of Europe, the gross hydropower potential is estimated to decline by about 6% by the 2070s, while the developed hydropower potential shows a decrease of 7–12%.

Harrison et al. (2007) developed a model to assess the relationship between climate change and the viability, technical and financial, of the hydro development. Batoka Gorge scheme that is planned on the River Zambezi was used as a case study to validate the model and to predict the impact of climate change on river flows, electricity production schemes and financial performance.

Harrison et al. (2007) used three different scenarios of climate change (all available from the IPCC Data Distribution Center). Two of them are HadCM2 GCM and HadCM2-S developed by the Hadley Center in the UK Meteorological Office, HadCM2-S combines the effects of aerosols which have a tendency to cool the atmosphere. The

third scenario is the ECHAM4 GCM developed by the Max Planck Institut fur Meteorologie. All the data used to represent the conditions projected for the 2080s and consists of changes in rainfall and temperature relative to the control results which represent the current conditions. Comparison between GCM simulation with the current scenario and potential future climate will illustrate the sensitivity of the case study schemes to climate change.

CHAPTER III CATCHMENT MODELING USING SWAT MODEL

3.1. Soil and Water Assessment Tool (SWAT) Model

SWAT is a river basin or watershed scale model developed to predict the impact of land management practices on water, sediment, and agricultural chemical yields in large, complex watersheds with varying soils, land use, and management conditions over long periods of time. The model is physically based and computationally efficient, uses readily available inputs and enables users to study long-term impacts. The SWAT model can be applied to support various watershed and water quality modeling studies. SWAT can be used to simulate a single watershed or a system of multiple hydrologically connected watersheds. Each watershed is first divided into subbasins and then in hydrologic response units (HRUs) based on the land use and soil distributions.

3.2. SWAT Modeling

SWAT allows a number of different physical processes to be simulated in watershed. For modeling purposes, a watershed may be partitioned into a number of subwatersheds or subbasins. The use of subbasins in a simulation is particularly beneficial when different areas of watershed are dominated by land uses or soil dissimilar enough in properties to impact hydrology. By partitioning the watershed into subbasins, we can reference different areas of the watershed to one another spatially.

Input information for each subbasin is grouped or organized into the following categories :

1. climate
2. hydrologic response unit (HRU)
3. wetlands
4. ground water
5. main channel

Hydrologic response unit are lumped land areas within the subbasin that are comprised of unique land cover, soil and management combinations.

Simulation of the hydrology of a watershed can be separated into two major divisions. The first division is the land phase of the hydrologic cycle (Figure. 3.1). The land phase of the hydrologic cycle controls the amount of water loadings to the main channel in each subbasin. The second division is the water routing phase of the hydrologic cycle which can be defined as the movement of water, sediment, etc. through the channel network of the watershed to the outlet.

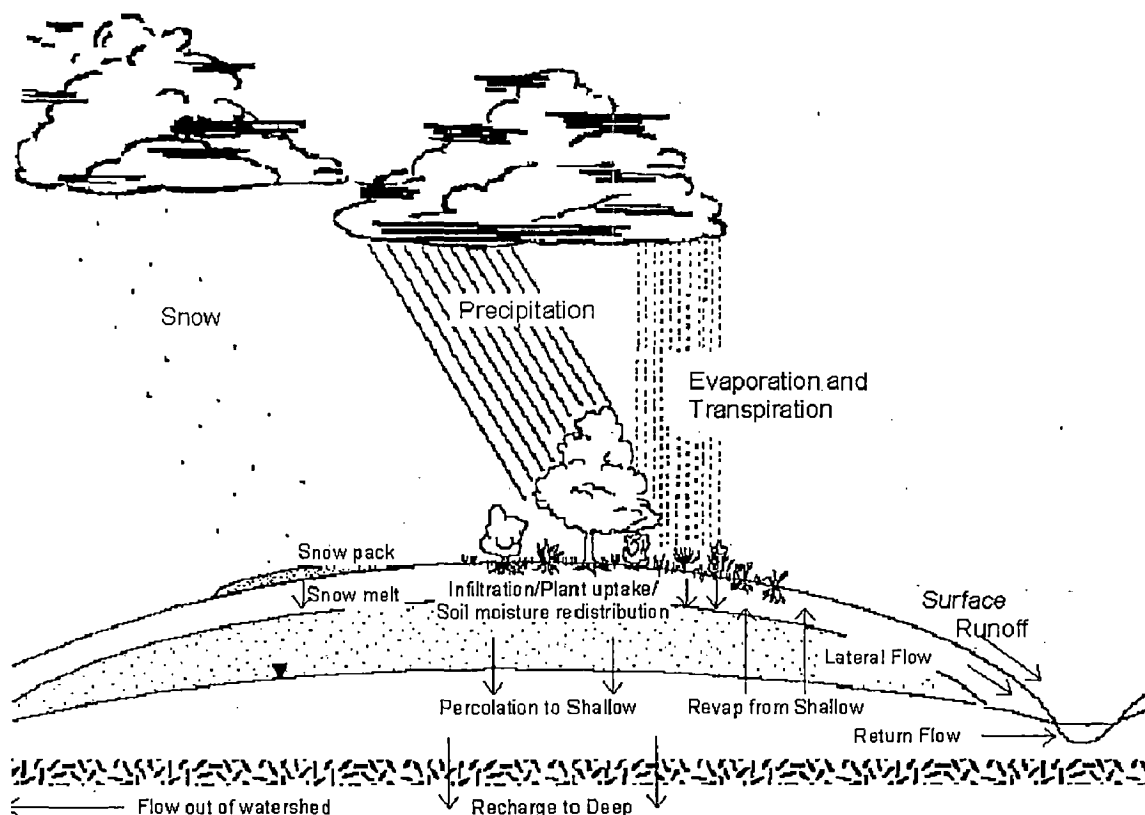


Figure 3.1: Hydrologic Cycle

3.2.1. Land Phase of the Hydrologic Cycle

The hydrologic cycle as simulated by SWAT is based on the water balance equation :

$$SW_t = SW_0 + \sum_{i=1}^t (R_{day} - Q_{surf} - E_a - w_{seep} - Q_{gw}) \dots\dots\dots(3.1)$$

where :

- SW_t = final soil water content (mm H₂O)
- SW_0 = initial soil water content on day i (mm H₂O)
- t = time (days)

- R_{day} = amount of precipitation on day i (mm H₂O)
- Q_{surf} = amount of surface runoff on day i (mm H₂O)
- E_a = amount of evapotranspiration on day i (mm H₂O)
- w_{seep} = amount of water entering the vadose zone from the soil profile on day i (mm H₂O)
- Q_{gr} = amount of return flow on day i (mm H₂O)

The subdivision of the watershed enables the model to reflect differences in evapotranspiration for various crops and soil. Runoff is predicted separately for each HRU and routed to obtain the total runoff for the watershed. This increases accuracy and gives a much better physical description of the water balance.

3.2.2. Climate

The climate of watershed provides the moisture and energy inputs that control the water balance and determine the relative importance of the different component of the hydrologic cycle.

The climatic variables required by SWAT consist of daily precipitation, maximum/minimum air temperature, solar radiation, wind speed and relative humidity to be input from records of observed data or generated during simulation.

The impact of global climate change on water supply is a major area of research. Climate change can be simulated with SWAT by manipulating the climatic input that is read into the model (precipitation, temperature, and other weather parameters). A less time-consuming method is to set adjustment factors for the various climatic inputs.

SWAT will allow to adjust precipitation, temperature, solar radiation, relative humidity, and carbon dioxide levels in each subbasin. The alteration of precipitation and temperature are straightforward:

$$R_{day} = R_{day} \left(1 + \frac{adj_{pcp}}{100} \right) \dots\dots\dots (3.2)$$

where R_{day} is the precipitation falling in the subbasin on a given day (mm H₂O), and adj_{pcp} is the % change in rainfall.

$$T_{mx} = T_{mx} + adj_{imp} \dots\dots\dots (3.3)$$

where T_{mx} is the daily maximum temperature ($^{\circ}\text{C}$), and adj_{imp} is the change in temperature ($^{\circ}\text{C}$).

$$T_{mn} = T_{mn} + adj_{imp} \dots\dots\dots(3.4)$$

where T_{mn} is the daily minimum temperature ($^{\circ}\text{C}$), and adj_{imp} is the change in temperature ($^{\circ}\text{C}$).

SWAT allows the adjustment terms to vary from month to month so that for change the daily data, we must change on the climate input database.

3.2.3. Hydrology

As precipitation descends, it may be intercepted and held in the vegetation canopy or fall to the soil surface. Water on the soil surface will infiltrate into the soil profile or flow overland as runoff. Runoff moves relatively quickly toward a stream channel and contributes to short-term stream response. Infiltrated water may be held in the soil and later evapotranspired or may slowly make its way to the surface-water system via underground paths. The potential pathways of water movement simulated by SWAT in the HRU are illustrated in Figure 3.1.

3.2.3.1. Surface Runoff

Surface runoff occurs whenever the rate of water application to the ground surface exceeds the rate of infiltration. When water is initially applied to a dry soil, the infiltration rate is usually very high. However, it will decrease as the soil becomes wetter. When the application rate is higher than the infiltration rate, surface depressions begin to fill. If the application rate continues to be higher than the infiltration rate once all surface depressions have filled, surface runoff will commence. SWAT provides two methods for estimating surface runoff: the SCS curve number procedure and the Green & Ampt infiltration method (Neitsch, 2005).

3.2.3.2. SCS Equation

The SCS runoff equation is an empirical model that came into common use in the 1950s. It was the product of more than 20 years of studies involving rainfall-runoff relationships from small rural watersheds across the U.S. The model was developed to provide a consistent basis for estimating the amounts of runoff under varying land use and soil types (Mishra, 2003). The SCS curve number equation is (Mishra, 2003):

$$Q_{surf} = \frac{(R_{day} - I_a)^2}{(R_{day} - I_a + S)} \dots\dots\dots(3.5)$$

where Q_{surf} is the accumulated runoff or rainfall excess (mm H₂O), R_{day} is the rainfall depth for the day (mm H₂O), I_a is the initial abstractions which includes surface storage, interception and infiltration prior to runoff (mm H₂O), and S is the retention parameter (mm H₂O). The retention parameter varies spatially due to changes in soils, land use, management and slope and temporally due to changes in soil water content. The retention parameter is defined as:

$$S = 25.4 \left(\frac{1000}{CN} - 10 \right) \dots\dots\dots(3.6)$$

where CN is the curve number for the day. The initial abstractions, I_a , is commonly approximated as 0.2S and equation (3.6) becomes

$$Q_{surf} = \frac{(R_{day} - 0.2S)^2}{(R_{day} + 0.8S)} \dots\dots\dots(3.7)$$

3.2.3.3. Green & Ampt Infiltration Method

The Green & Ampt equation was developed to predict infiltration assuming excess water at the surface at all times. The equation assumes that the soil profile is homogenous and antecedent moisture is uniformly distributed in the profile. As water infiltrates into the soil, the model assumes the soil above the wetting front is completely saturated and there is a sharp break in moisture content at the wetting front. Figure 3.2 illustrates the difference between the moisture distribution with depth modeled by the Green & Ampt equation and what occurs in reality.

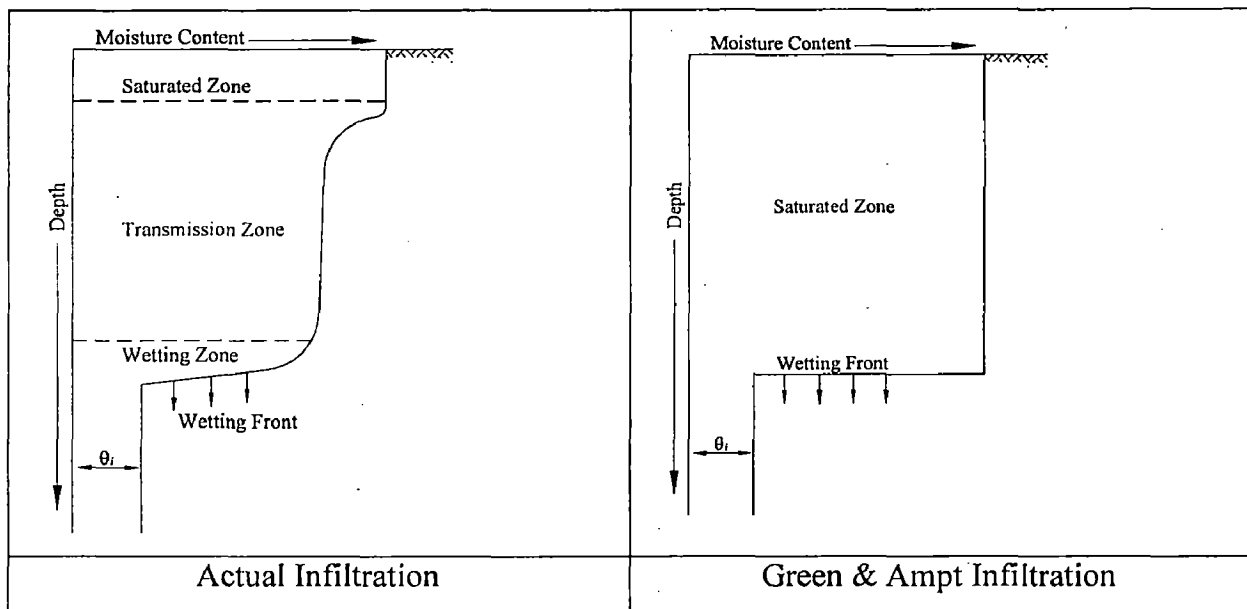


Figure 3.2. Comparison of moisture content distribution modeled by Green & Ampt and a typical observed distribution

Source : Neitsch, 2005

Mein and Larson (1973) developed a methodology for determining ponding time with infiltration using the Green & Ampt equation. The Green-Ampt Mein-Larson excess rainfall method was incorporated into SWAT to determining surface runoff. The Green-Ampt Mein-Larson infiltration rate is defined as (Neitsch, 2005):

$$f_{inf,t} = K_e \left(1 + \frac{\Psi_{wf} \cdot \Delta\theta_v}{F_{inf,t}} \right) \dots\dots\dots(3.8)$$

where f_{inf} is the infiltration rate at time t (mm/hr), K_e is the effective hydraulic conductivity (mm/hr), Ψ_{wf} is the wetting front matric potential (mm), $\Delta\theta_v$ is the change in volumetric moisture content across the wetting front (mm/mm) and F_{inf} is the cumulative infiltration at time t (mm H₂O).

When the rainfall intensity is less than the infiltration rate, all the rainfall will infiltrate during the time period and the cumulative infiltration for that time period is calculated:

$$F_{inf,t} = F_{inf,t-1} + R_{\Delta t} \dots\dots\dots(3.9)$$

where, $F_{inf,t}$ is the cumulative infiltration for a given time step (mm H₂O), $F_{inf,t-1}$ is the cumulative infiltration for the previous time step (mm H₂O), and $R_{\Delta t}$ is the amount of rain falling during the time step (mm H₂O).

The infiltration rate defined by equation (3.8) is a function of the infiltrated volume, which in turn is a function of the infiltration rates in previous time steps. To avoid numerical errors over long time steps, f_{inf} is replaced by dF/dt_{inf} in equation (3.8) and integrated to obtain.

$$F_{inf,t} = F_{inf,t-1} + K_e \cdot \Delta t + \Psi_{wf} \cdot \Delta \theta_v \cdot \ln \left[\frac{F_{inf,t} + \Psi_{wf} \cdot \Delta \theta_v}{F_{inf,t-1} + \Psi_{wf} \cdot \Delta \theta_v} \right] \dots\dots\dots(3.10)$$

Equation (3.10) must be solved iteratively for $F_{inf,t}$, the cumulative infiltration at the end of the time step. A successive substitution technique is used.

The Green-Ampt effective hydraulic conductivity parameter, K_e , is approximately equivalent to one-half the saturated hydraulic conductivity of the soil, K_{sat} (Bouwer, 1969). Nearing et al. (1996) developed an equation to calculate the effective hydraulic conductivity as a function of saturated hydraulic conductivity and curve number. This equation incorporates land cover impacts into the calculated effective hydraulic conductivity. The equation for effective hydraulic conductivity is:

$$K_e = \frac{56.82 \cdot K_{sat}^{0.286}}{1 + 0.051 \cdot \exp(0.062 \cdot CN)} - 2 \dots\dots\dots(3.11)$$

where K_e is the effective hydraulic conductivity (mm/hr), K_{sat} is the saturated hydraulic conductivity (mm/hr), and CN is the curve number.

Wetting front matric potential, Ψ_{wf} , is calculated as a function of porosity, percent sand and percent clay (Neitsch, 2005):

$$\Psi_{wf} = 10 \cdot \exp \left[6.5309 - 7.32561 \cdot \phi_{soil} + 0.001583 \cdot m_c^2 + 3.809479 \cdot \phi_{soil} + 0.000344 \cdot m_s \cdot m_c - 0.049837 \cdot m_s \cdot \phi_{soil} + 0.001608 \cdot m_s^2 \cdot \phi_{soil}^2 + 0.001602 \cdot m_c^2 \cdot \phi_{soil}^2 - 0.0000136 \cdot m_s^2 \cdot m_c - 0.003479 \cdot m_c^2 \cdot \phi_{soil} - 0.000799 \cdot m_s^2 \cdot \phi_{soil} \right] \dots\dots\dots(3.12)$$

where ϕ_{soil} is the porosity of the soil (mm/mm), m_c is the percent clay content, and m_s is the percent sand content.

The change in volumetric moisture content across the wetting front is calculated at the beginning of each day as:

$$\Delta \theta_v = \left(1 - \frac{SW}{FC} \right) \cdot (0.95 \cdot \phi_{soil}) \dots\dots\dots(3.13)$$

where $\Delta\theta_v$ is the change in volumetric moisture content across the wetting front (mm/mm), SW is the soil water content of the entire profile excluding the amount of water held in the profile at wilting point (mm H₂O), FC is the amount of water in the soil profile at field capacity (mm H₂O), and ϕ_{soil} is the porosity of the soil (mm/mm). If a rainfall event is in progress at midnight, $\Delta\theta_v$ is then calculated:

$$\Delta\theta_v = 0.001 * (0.95 * \phi_{soil}) \dots\dots\dots(3.14)$$

For each time step, SWAT calculates the amount of water entering the soil. The water that does not infiltrate into the soil becomes surface runoff.

3.2.3.4. Peak Runoff Rate

The peak runoff rate is the maximum runoff flow rate that occurs with a given rainfall event. The peak runoff rate is an indicator of the erosive power of a storm and is used to predict sediment loss. SWAT calculates the peak runoff rate with a modified rational method.

The rational method is widely used in the design of ditches, channels and storm water control systems. The rational method is based on the assumption that if a rainfall of intensity i begins at time $t = 0$ and continues indefinitely, the rate of runoff will increase until the time of concentration, $t = t_{conc}$, when the entire subbasin area is contributing to flow at the outlet. The rational formula is:

$$q_{peak} = \frac{C.i.Area}{3.6} \dots\dots\dots(3.15)$$

where q_{peak} is the peak runoff rate (m³s⁻¹), C is the runoff coefficient, i is the rainfall intensity (mm/hr), $Area$ is the subbasin area (km²) and 3.6 is a unit conversion factor.

3.2.3.5. Time Concentration

The time of concentration is the amount of time from the beginning of a rainfall event until the entire subbasin area is contributing to flow at the outlet (Neitsch, 2005). In other words, the time of concentration is the time for a drop of water to flow from the remotest point in the subbasin to the subbasin outlet. The time of concentration is calculated by summing the overland flow time (the time it takes for flow from the remotest point in the subbasin to reach the channel) and the channel flow time (the time it takes for flow in the upstream channels to reach the outlet):

$$t_{conc} = t_{ov} + t_{ch} \dots\dots\dots(3.16)$$

where t_{conc} is the time of concentration for a subbasin (hr), t_{ov} is the time of concentration for overland flow (hr), and t_{ch} is the time of concentration for channel flow (hr).

3.3. SWAT Calibration Techniques

3.3.1. General

To calibrate the water balance and streamflow it need to have proper understanding of the actual conditions occurring in the watershed. Ideally, one has the data from a stream gauge located within or at the outlet of the watershed. Calibration for water balance and stream flow is first done for average annual conditions. Once the run is calibrated for average annual conditions, it can be shifted to monthly or daily records to fine-tune the calibration. The example of average annual observed and simulated results could be summarized in Table 3.1:

Table 3.1. Example of SWAT Output and Observed Data

	Total Water Yield	Baseflow	Surface Flow
Observed	200 mm	80 mm	120 mm
SWAT	300 mm	20 mm	280 mm

Following are some ways to make improvement in the output of SWAT to obtain a better match with the observed output:

- For calibrating at the watershed outlet, the SWAT values are provided in the .std file. These values are listed in the table titled "Ave Annual Basin Values" located near the end of the file.
- For calibrating at a gauge located within the watershed, the total water yield can be calculated from the FLOW_OUT variable in the reach (.rch) file.
- The values for baseflow and surface flow have to be estimated from the HRU output (.sbs) file or the subbasin output file (.bsb).
- To estimate the contributions by baseflow and streamflow, the annual values for GWQ, SURQ and WYLD need to be averaged, so that a weighted value bae on area of the drainage is obtained.
- The values for GWQ and SURQ cannot be used directly because in-stream precipitation, evaporation, transmission losses, etc. will alter the net water yield from that predicted by the WYLD variable in the HRU or Subbasin Output files.

There are a number of methods available for partitioning observed stream flow into fractions contributed by baseflow and surface runoff. If daily stream flow is available, a baseflow filter program can be run which performs this analysis.

3.3.2. Basic Water Balance and Total Flow Calibration

3.3.2.1. Calibrate Surface Runoff

Step 1: Adjust the curve number (CN2 in .mgt) until surface runoff is acceptable. If surface runoff values are still not reasonable after adjusting curve numbers, adjust: -soil available water capacity (± 0.04) (SOL_AWC in .sol) and/or -soil evaporation compensation factor (ESCO in .bsn or .hru).

3.3.2.2. Calibrate Subsurface Flow

Step 2: Once surface runoff is calibrated, compare measured and simulated values of baseflow.

- If simulated baseflow is too high:
 - increase the groundwater "revap" coefficient (GW_REVAP in .gw file) the maximum value that GW_REVAP should be set at is 0.20.
 - decrease the threshold depth of water in the shallow aquifer for "revap" to occur (REVAPMN in .gw file) the minimum value that REVAPMN should be set at is 0.0.
 - increase the threshold depth of water in the shallow aquifer required for base flow to occur (GWQMN in .gw file) the maximum value that GWQMN should be set.
- If simulated baseflow is too low, check the movement of water into the aquifer.
- If groundwater recharge (GWQ in .sbs file or .bsb file) is greater than the desired baseflow:
 - decrease the groundwater "revap" coefficient (GW_REVAP in .gw)—the minimum value that GW_REVAP should be set at is 0.02.
 - increase the threshold depth of water in the shallow aquifer for "revap" to occur (REVAPMN in .gw).

- o decrease the threshold depth of water in the shallow aquifer required for base flow to occur (GWQMN in .gw)—the minimum value that GWQMN should be set at is 0.0.

Step 3: Repeat steps 1 and 2 until values are acceptable. It may take several iterations to get the surface runoff and baseflow correct.

3.3.3. Temporal Flow Calibration

Once average annual and annual surface runoff and baseflow are realistic, the temporal flow should look reasonable as well. A few problems that may still be present include:

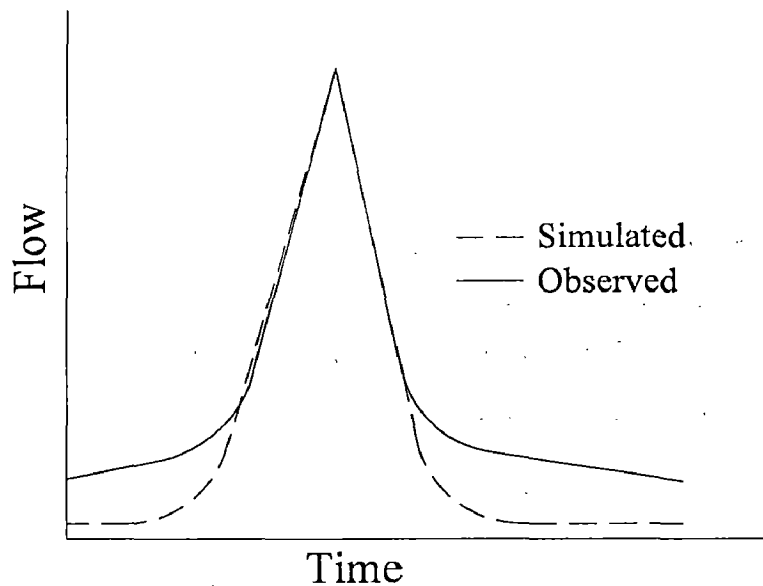


Figure 3.3. Reasonable Peak

1. Peaks are reasonable, but the recessions "bottom out" (Figure 3.3): Check the transmission losses/values for channel hydraulic conductivity (CH_K in .rte). The value for channel hydraulic conductivity is an *effective* hydraulic conductivity for movement of water out of the stream bed. For perennial streams receiving groundwater contribution to flow, the groundwater enters the stream through the sides and bottom of the stream bed, making the effective hydraulic conductivity of the channel beds to water losses equal to zero. The only time the channel hydraulic conductivity would be greater than zero is for ephemeral and transient streams that do not receive continuous groundwater contributions to streamflow.

A second variable that will affect the shape of the hydrograph is the baseflow alpha factor (ALPHA_BF in .gw).

2. In snow melt months, the peaks are too high and recessions are too low (Figure 3.4) : Check the values for maximum and minimum melt rates for snow (SMFMX and SMFMN in .bsn). These values may need to be lowered. Another variable that will impact snow melt is the temperature lapse rate (TLAPS in .sub). These values may need to be increased.
3. Finally, the baseflow alpha factor may need to be modified (ALPHA_BF in .gw).

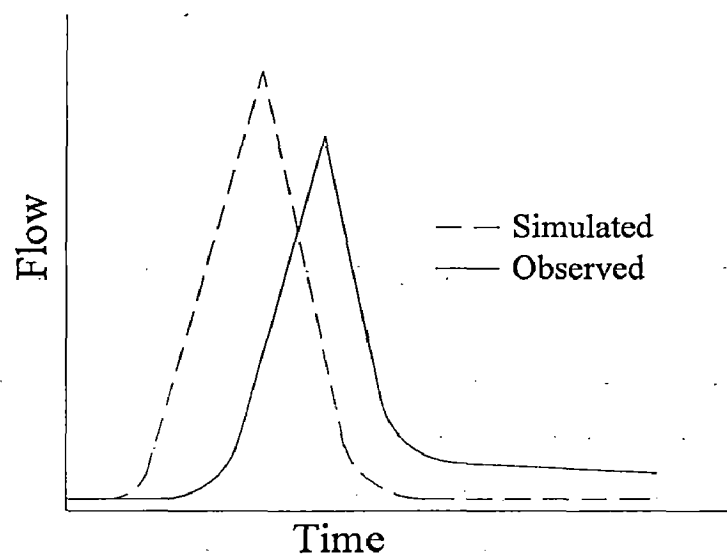


Figure 3.4. Peak of Simulation is High

3.3.4. Spatial Flow Calibration

Calibrating a watershed with multiple stream gauges, calibrate streamflow for the gauge furthest upstream. Once that gauge is calibrated, move downstream to the next gauge and calibrate for that area. It is important that, as it calibrates downstream gauges, but it is no need to change parameters within the files associated with the drainage area of the upstream gauges already calibrated.

3.3.5. Evaluation of Model Performance

In SWAT model, three statistical measures were included to evaluate the goodness of a calibration (White, 2005). SWAT model calibration was performed by minimizing the Relative Error (RE in percent) at the gauge locations :

$$(RE\%) = \left| \frac{(O - P)}{O} \right| \times 100 \dots\dots\dots(3.17)$$

where O is the measured value and P is the predicted output. The SWAT model was further calibrated monthly using the Nash-Sutcliffe coefficient (E), which is defined as :

$$E = 1 - \frac{\sum_{i=1}^n (O_i - P_i)^2}{\sum_{i=1}^n (O_i - O_{avg})^2} \dots\dots\dots(3.18)$$

where O_i are the measured values, P_i are the predicted outputs, O_{avg} is the average of measured value and i equals the number of values. Monthly coefficient of determination (R^2) was also calculated. A significance test can be performed when conducting a linear regression analysis with a null hypothesis that the coefficient of determination is equal to 0. The R^2 statistic is calculated as :

$$R^2 = \left(\frac{\sum_{i=1}^n (O_i - O_{avg})(P_i - P_{avg})}{\left[\sum_{i=1}^n (O_i - O_{avg})^2 \sum_{i=1}^n (P_i - P_{avg})^2 \right]^{0.5}} \right)^2 \dots\dots\dots(3.19)$$

The aim of a model calibration is to minimize relative error (RE%) and to maximize Nash-Sutcliffe coefficient (E) and coefficient of determination.

CHAPTER IV STUDY AREA AND DATA

4.1. Study Area

The study area covers the entire catchment of the Wonogiri dam (reservoir area of 90 km² and remaining catchment area of 1,260 km²). The Wonogiri multipurpose dam is the only large dam on the mainstream of the Bengawan Solo River, which is the largest river in the Java with a catchment area of around 16,100 km² and a length of about 600 km.



Figure 4.1 Location Map
Source : PBS

4.2. Topography

The Bengawan Solo River rises on southwest slope of mountain. Rahtawu in Tertiary Volcanic mountains area, and flows westward along the mountains series. The Solo River runs northward receiving Alang River, Temon River, Tirutomoyo River and Keduang River immediately upstream of the Wonogiri Dam. After the confluence, the Solo River clockwise flows around mountain Lawu throw alluvial basin of Surakarta City and Sragen City, and runs eastward to Ngawi City. After the confluence with the Madiun

River the Solo River flows northward to Cepu City and changes the direction to the east northeast and flows into the Jawa .

The catchment area of Wonogiri Dam is topographically divided into the following three mountain regions extending east and west, and one plain area surrounding Wonogiri reservoir (Figure 4.1). Southern area forms karst tableland with many small mountains of about 400 m elevation. Almost entire rainfall on the tableland infiltrates into underground, and there is no obvious runoff. There are some springs along the foot of the tableland. Middle area is characterized by EL.500 m-EL.1200 m ranging mountains and steep valleys extending east-west with dendritic drainage feature. Northern area, mountain Semilir (EL. 2,023 m) on the south slope of mountain Lawu is the highest of the catchment area, forms a volcanic cone with deep V-shape valleys running radially. Relatively wide plains spread around the confluence of Bengawan Solo River and Alang River, and downstream region of along Tirtomoyo River.

4.3. Climate

The climate of the study area is tropical and is subject to the tropical monsoon. The south-west to north-west winds prevail from November to April in ordinary year and they bring rains to the river basin, while the period from July to October is the dry season, in which the basin area is dried up by the south and south-east winds.

Six meteorological stations are scattered in the study area. The data observation works is carryout by several agencies such as *Proyek Bengawan Solo* (PBS), *Badan Meteorologi dan Geofisika* (BMG) and Indonesian Air Force. The oldest station is Panasan which is in operation since 1972. Most of the stations have period of the record from 1984 to 2003 with some interruption.

Hydro-meteorological data used for this study was collected from PBS and Irrigation Services, and also taken from previous water resources development project reports.

4.3.1. Temperature

Mean annual temperature at the Wonogiri dam is approximately 29.3°C and it fluctuates from the minimum mean monthly temperature of 28.3°C in July to the maximum mean monthly temperature of 30.4°C on October. Temperature in the dry

season (especially from June through August) is relatively low. Mean monthly temperature is graphically shown in Figure 4.2(a).

4.3.2. Relative Humidity

Annual mean relative humidity is approximately 77.4% in the dam catchment (Baturetno). The maximum mean monthly relative humidity is 79.7% in December, while the minimum of that is 75.4% in October at Baturetno. Mean monthly relative humidity is graphically shown in Figure 4.2.(b).

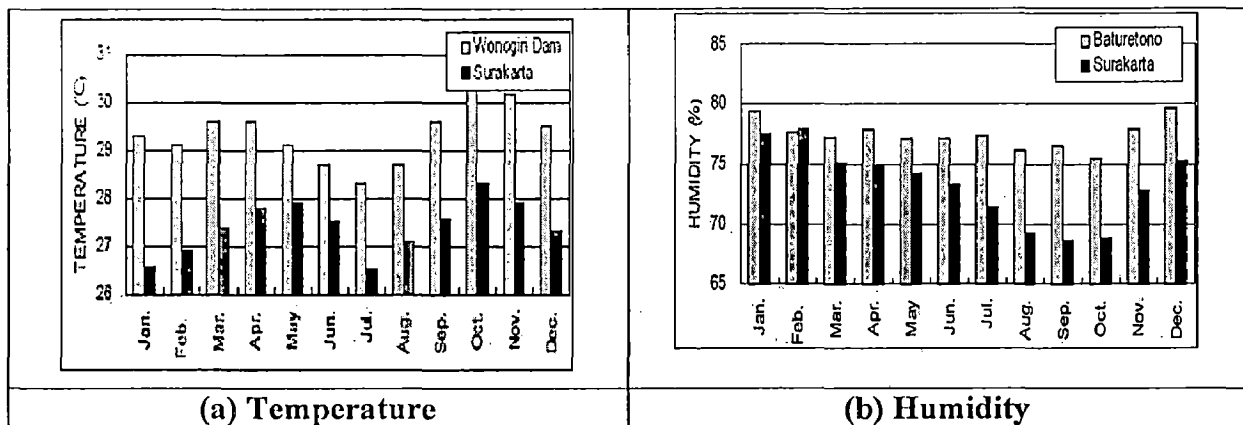


Figure 4.2. Mean Monthly Humidity and Temperature in the Study Area

4.3.3. Wind Velocity

Annual mean wind velocity (Figure 4.3.(a)) in the dam catchment (Baturetno) is 2.31 m/s. Maximum mean monthly wind velocity at Baturetno is 3.47 m/s in October, while the minimum is 1.53 m/s in April.

4.3.4. Evaporation

Annual mean evaporation rate at the Wonegiri dam is 5.3 mm/day. Evaporation in the dry season of July to November is relatively higher than that in the wet season of December to June. Monthly mean daily evaporation rate is graphically shown in Figure 4.3 (b).

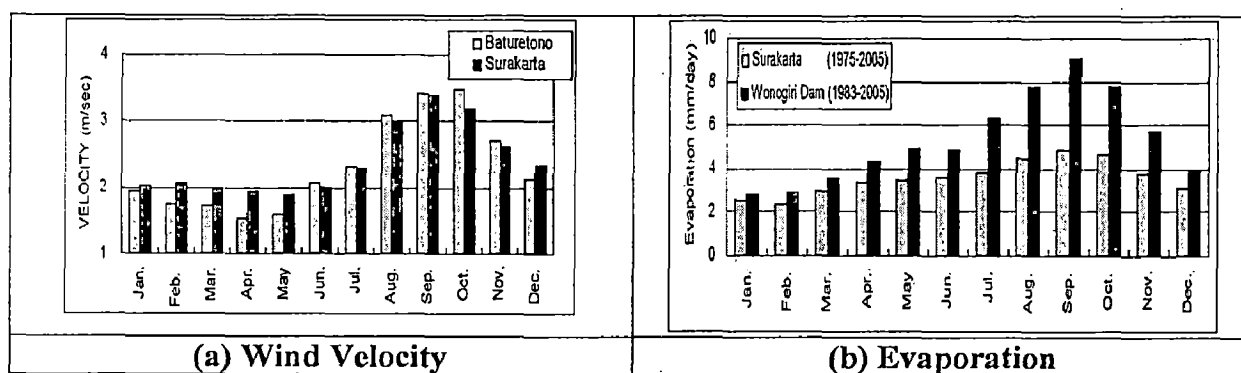


Figure 4.3. Mean Monthly Wind Velocity and Evaporation in the Study Area

4.4. Hydrology

4.4.1. Rainfall

The rainfall data on the study area are available from a number of sources the primary one being the irrigation services and other sources belong to PBS and BMG offices which operate rainfall monitoring stations in the study area.

Based on availability and reliability of data in and around the Wonogiri dam catchment, seven rainfall stations are selected to analyze the rainfall condition of the study area.

The basin average rainfall for each tributary is estimated by arithmetical mean method. Table 4.1 shows the estimated mean monthly basin rainfall for five (5) major tributaries. The annual rainfalls in the two (2) tributary basins, the Keduang and Tirtomoyo River basins, are considerably higher than those in other three (3) major tributary basins.

Table 4.1. Mean Monthly Basin Rainfall

Tributary Basin	Month												Annual
	J	F	M	A	M	J	J	A	S	O	N	D	
Keduang	393	353	326	215	90	62	32	22	30	104	236	287	2150
Tirtomoyo	394	374	340	229	90	72	32	13	22	72	205	282	2125
Temon	339	326	289	181	75	57	21	10	14	61	160	274	1807
Bengawan Solo	340	317	276	170	84	61	22	12	19	58	155	243	1757
Alang	326	289	256	154	66	61	24	10	18	51	159	237	1651
Remaining Area	341	315	283	181	85	61	32	15	17	77	167	236	1810
Whole Catchment	369	336	307	201	89	64	31	16	24	82	198	274	1991

4.4.2. Discharge

The observation of river water level had been carried out in many places along the Bengawan Solo and its tributaries. Two types of gauges i.e., ordinary staff gauge and

automatic water level recorder (AWLR) are commonly installed to measure the river stage. The staff gauges are normally read three times a day, in the morning, afternoon and evening, and the average of these three values is taken as daily water level record. Further, in the Wonogiri dam catchment, river water level records were collected from a number of agencies, the primary one is the PBS office and the other sources belong to the Watershed Management Technology Center of Surakarta (BTPDAS) and Balai Pengelolaan Sumber Daya Air (Balai PSDA).

4.5. Input Data for SWAT Model

Data used in SWAT model is shown in Table 4.2. Initially, the watershed was delineated into subbasin by using digital elevation map (DEM), land use and soil map were overlaid. SWAT simulated different land uses in each sub basin, the SWAT input data and procedure shown in Figure 6.

Table 4.2. Data Source for Wonogiri Watershed

Data Type	Scale	Data Description
Topographic Map	1 : 250000	Elevation
Soil Map	1 : 250000	Soil Classification
Land Use Map	1 : 250000	Land Used Classification
Precipitation	Daily	Daily Precipitation
Weather : - Temperature	Monthly	Maximum and Minimum Air Temperature

4.6. Principal Feature of Wonogiri Multipurpose Dam

The principal feature, allocation of the storage capacity and designated water levels of the Wonogiri Multipurpose Dam Reservoir is summarized in Table 4.3. and shown in Figure 4.4.

Table 4.3. Principal Features of Wonogiri Multipurpose Dam and Reservoir

Dam type	Rockfill	Normal Water Level	EL. 136.0 m
Dam height	40 m	Design Flood Level	EL. 138.3 m
Crest length	830m	Extra Flood Water Level	EL. 139.1 m
Embankment volume	1,223,300 m ³	Spillway (Radial gate)	7.5 m x 7.8 m x 4 nos.
Catchment area	1,260 km ²	Crest height	EL. 131.0 m
Reservoir area	90 km ²	Flood inflow discharge	4,000 m ³ /s
Gross storage capacity	735 x 106 m ³	Flood outflow discharge	400 m ³ /s
Active storage capacity	615 x 106 m ³	Design flood discharge	5,100 m ³ /s
Flood control storage capacity	220 x 106 m ³	PMF	9,600 m ³ /s
Irrigation & hydro power storage capacity	440 x 106 m ³	Installed capacity	12.4 MW
Sediment storage capacity	120 x 106 m ³	Design head	20.4 m
Sediment deposit level	EL. 127.0 m	Max. discharge	75 m ³ /s
Limited water level in flood during flood season	EL. 135.3 m	Annual energy output	50,000 MWh

Source: PBS

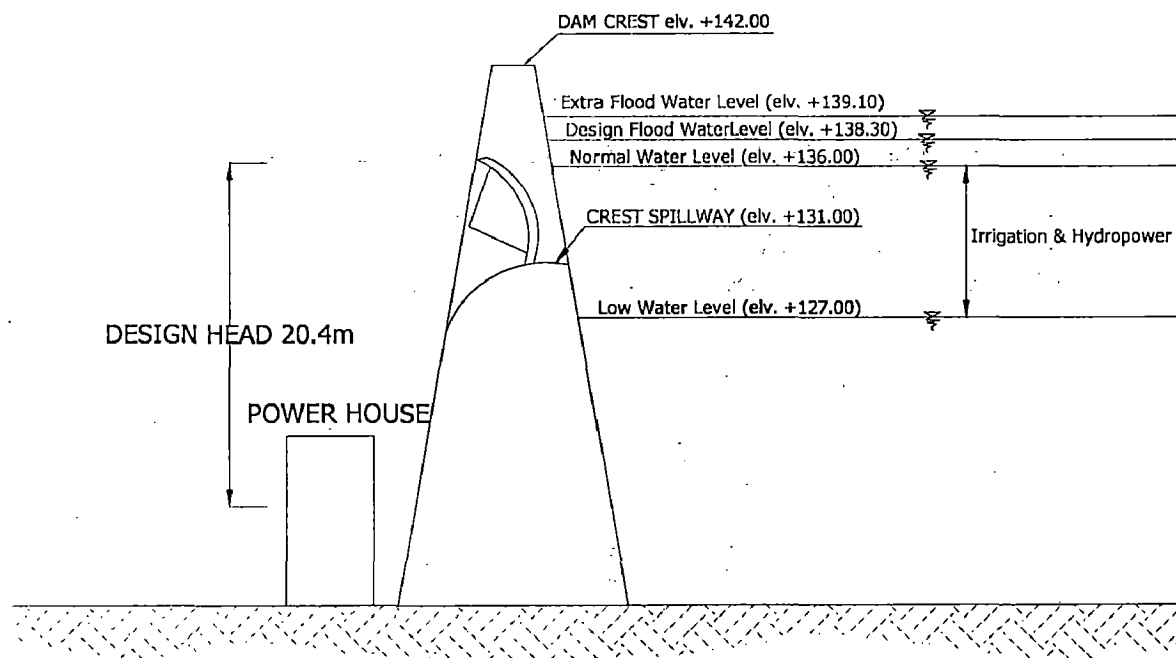


Figure 4.4. Water Levels of Wonogiri Dam

Source: PBS

4.7. Power Generation at the Wonogiri Hydropower Station

The power house is located just downstream of the Wonogiri Dam. It accommodates the generating equipment with an installed capacity of 12.4 MW to produce annual energy output of 55,000 MWh. The maximum discharge for power generation is 75 m³/s. In the dry season of May-November, around 50-60 million m³ of the stored water in reservoir is used for power generation. In terms of a mean monthly

discharge, they are around 20-25 m³/sec. Power generation is of no consumptive water use. Thus the majority of released water through power generation is then used for irrigation water taken at the Colo weir. The lowest reservoir water level for power generation is currently at El. 127.00.

CHAPTER V ANALYSIS OF RESULT

5.1. Assessment of Climate Change Scenario

Monthly temperature and precipitation records from the recording stations were averaged to obtain average annual for each year. Monthly and annual time series were analyzed statistically by using Mann Kendall (MK) test.

The statistics for annual temperature and precipitation are given in Table 5.1, which shows that the annual temperature ranges from 20.9 – 33.3°C, with an average 27.2°C. The annual precipitation in study area ranges from 1191-2670 mm, with an average 2054.4 mm during the study period from 1984-2003.

Table 5.1. Statistical Description of Temperature and Precipitation

Statistical Descriptive	Wonogiri		Jakarta
	(1984-2003)		(1946-1995)
	Temperature	Precipitation	
Mean (Monthly)	27.202	171.220	152.590
Standard Error	0.084	7.252	3.899
Median	27.169	165.503	153.917
Standard Deviation	0.373	32.430	27.567
Sample Variance	0.139	1051.697	759.956
Skewness	-0.026	0.023	0.320
Minimum	20.881	115.823	97.750
Maximum	33.291	225.938	235.833

Rainfall data at Wonogiri taken from 5 rain gauge stations and 3 weather stations at the study area, while at Jakarta the data that was collected at Jakarta rain gauge station.

Monitoring precipitation data collected between 1946 and 1995 at Jakarta rain gauge station was used to perform the analysis for long period precipitation. The reason of selecting Jakarta rain gauge station is because the rain gauge stations in the study area did not have enough length of data to predict climate changes. Hence to help in predicting climate changes, we selected the closest rain gauge stations that has sufficient data. The data collected from Jakarta rain gauge station is monthly data.

From the data statistical description (Table 5.1.) shows that the precipitation data for the study area are relatively similar to the precipitation data from Jakarta rain gauge

station. This condition indicates that the data from Jakarta rain gauge station can be used for climate change prediction in the study area.

In this study assessment of climate change was perform using Mann-Kendall statistical tests to determine the trend of climate change. The Mann-Kendall test is a non-parametric test for identifying trends in time series data. The results of statistical analysis using the Mann-Kendall method are given in Table 5.2.

Table 5.2. Result of Mann-Kendall Statistical Test

Scenario		Year	Parameter	DJF	MAM	JJA	SON
Temperature	Medium Term	1984-2003	Zmk	0.94	0.13	-1.30	0.55
			Q	-0.1	+0.4	-0.5	+0.7
Precipitation	Medium Term	1984-2003	Zmk	-0.78	0.93	-0.50	-0.19
			Q (mm)	-7.82	4.58	-0.63	-3.19
			Q (%)	-3	3	1	-3
	Long Term	1946-1995	Zmk	-0.55	-1.42	-0.39	-0.69
			Q (mm)	-31.69	-1.55	-1.93	-9.97
			Q (%)	-12	-1	-3	-9

Note: Zmk = Statistical value of Mann-Kendall test, Q = Sen's slope estimator, (-) indicate decreasing trend and (+) indicate increasing trend, DJF = December, January, February, MAM = March, April, May, JJA = June, July, August, SON = September, October, November

From time series statistical test using Mann-Kendall method (Table 5.2) for medium-term scenario using the data from rain gauge station and weather station at Wonogiri cathcment area and for long-term scenario using data from Jakarta rain gauge station. For medium-term scenario temperature changing varies between -0.5°C – 0.7°C and precipitation varies between -7.82 mm – 4.58 mm or -3% - 3% . Whereas for long-term scenarios, changes in precipitation between -31.69 mm – -1.55 mm or -12% - -1% , while for the temperatures there are not enough data to predict long-term changes.

Recommendations from the IPCC in 2007 also used in this study to obtain more comprehensive analysis about the impact of climate change at the study area base on calculation that is done at the study area and base on IPCC 2007 that is represented South-East Asia region. Changes in rainfall and temperature as a recommendation from IPCC 2007 for South-East Asia region are shown in Table 5.3. Using the values from Table 5.2 and Table 5.3 we have prepared climate change projection for use in this study. These are shown in Table 5.4.

Table 5.3. IPCC Projected Changes in Air Temperature and Precipitation

Sub Region	Season	2010 to 2039		2040 to 2069		2070 to 2099	
		Temperature °C	Precipitation %	Temperature °C	Precipitation %	Temperature °C	Precipitation %
South-East Asia (10S-20N;100E-150E)	DJF	0.86	-1	2.25	2	3.92	6
	MAM	0.92	0	2.32	3	3.83	12
	JJA	0.83	-1	2.13	0	3.61	7
	SON	0.85	-2	1.32	-1	3.72	7

Source : IPCC 2007b

Table 5.4 Comparison Result of Climate Change Projection

Scenario		Year	Seasons	Calculation		IPCC 2007	
				Precipitation (%)	Temperature (°C)	Precipitation (%)	Temperature (°C)
I	Observed	1984 - 2003	DJF	Observed	Observed	Observed	Observed
			MAM	Observed	Observed	Observed	Observed
			JJA	Observed	Observed	Observed	Observed
			SON	Observed	Observed	Observed	Observed
II	Medium	2024 - 2043	DJF	(-3)	(-0.1)	(-1) - (+2)	(+0.86) - (+2.25)
			MAM	(+3)	(+0.4)	0 - (+3)	(+0.92) - (+2.32)
			JJA	(+1)	(-0.5)	(-1) - 0	(+0.83) - (+2.13)
			SON	(-3)	(+0.7)	(-2) - (-1)	(+0.85) - (+1.32)
III	Long	2074 - 2093	DJF	(-12)	NO DATA	(+6)	(+3.92)
			MAM	(-1)	NO DATA	(+12)	(+3.83)
			JJA	(-3)	NO DATA	(+7)	(+3.61)
			SON	(-9)	NO DATA	(+7)	(+3.72)

From Table 5.4, it can be seen that calculation results given less deviation than IPCC 2007 projection. This is because the climate projection from IPCC 2007 are for larger area and more complex data than the calculation. But both these results do not show too much difference except on the long-term scenario. The data for long-term temperature projection is not available, than for next calculation we use the result from IPCC 2007 as a projection for temperature in the long-term scenario.

5.2. Watershed Modeling using SWAT Program

There are 7 basic steps in the modeling work using ARCSWAT program :

1. Watershed Delineation, this process is aimed to develop site boundary modeling limits. Boundary modeling based on the concept of geo-hydrology science, namely the limit resulting from the formation of a region catchment area / watershed. Then the user of this application software must provide data: altitude map in grid format (DEM / Digital Elevation Model),

2. Parameterization Landuse and Soil Type on ARCSWAT modeling analysis is using GIS system base, that is system with one interface between an image map and table attributes. Because it was necessary to determine the parameters of watershed, land use map, and soil type and its data properties.
3. Calculating boundary map modeling and parameter values and catchment land use or soil type is called Processing HRU (Hydrologic Response Unit)
4. Input Data Base
5. Edit data base which has been listed as the properties of land, location modeling studies.
6. Run Simulation.
7. Calibration and verification process.

5.2.1. Watershed Deliniation

5.2.1.1. DEM (Digital Elevation Model) Processing

The use of DEM is to represent the physical characteristics or relief of the surface of the earth. Data base used is a digital contour map with a scale of 1: 25,000 produced by Bakosurtanal (National Coordinating Agency for Surveys and Mapping). DEM is used to identify the flow direction that will occur, flow accumulation and the flow length from the furthest point of the outlet in a watershed area.

5.2.1.2. Flow Direction

Flow direction is a very important parameter for hydrologic modeling. This flow direction map derived from DEM modification with eight neighbor deterministic methods or commonly abbreviated with the D8 in which each cell of the land surface will identify the direction of flow in accordance with 8 (eight) directions are defined by numbers according to the numbering convention grid direction of flow as in Figure 5.1.

5.2.1.3. Flow Accumulation

Flow accumulation can be derived from the flow direction map. Basically, if each cell has defined the direction of flow, accumulated flow from each cell would lead to cells that have the lowest elevation, the cells that have the lowest elevation compared to the surrounding will form a stream network (drainage network) in the watershed.

Furthermore the combination of flow direction map with a flow accumulation map will be give synthetic streams (stream that is obtain from SWAT process) from a

watershed, where the result is verified by comparison of synthetic river network from SWAT with the river network of the Bakosurtanal map, from this comparison it can be seen that the synthetic stream represents the real condition.

Based on the results of analysis of spatial process (interface with the modeling ARCSWAT 2005), for the purpose of modeling accuracy of the analysis of flow direction and flow accumulation both land and in the river and ends at the boundary of watershed, Wonogiri watershed area is divided into 20 sub-watersheds or 20 stream outlets, shown in Figure 5.2. The results of the Wonogiri watershed delineation yielded characteristic values of Wonogiri watershed area as shown in Table 5.5.

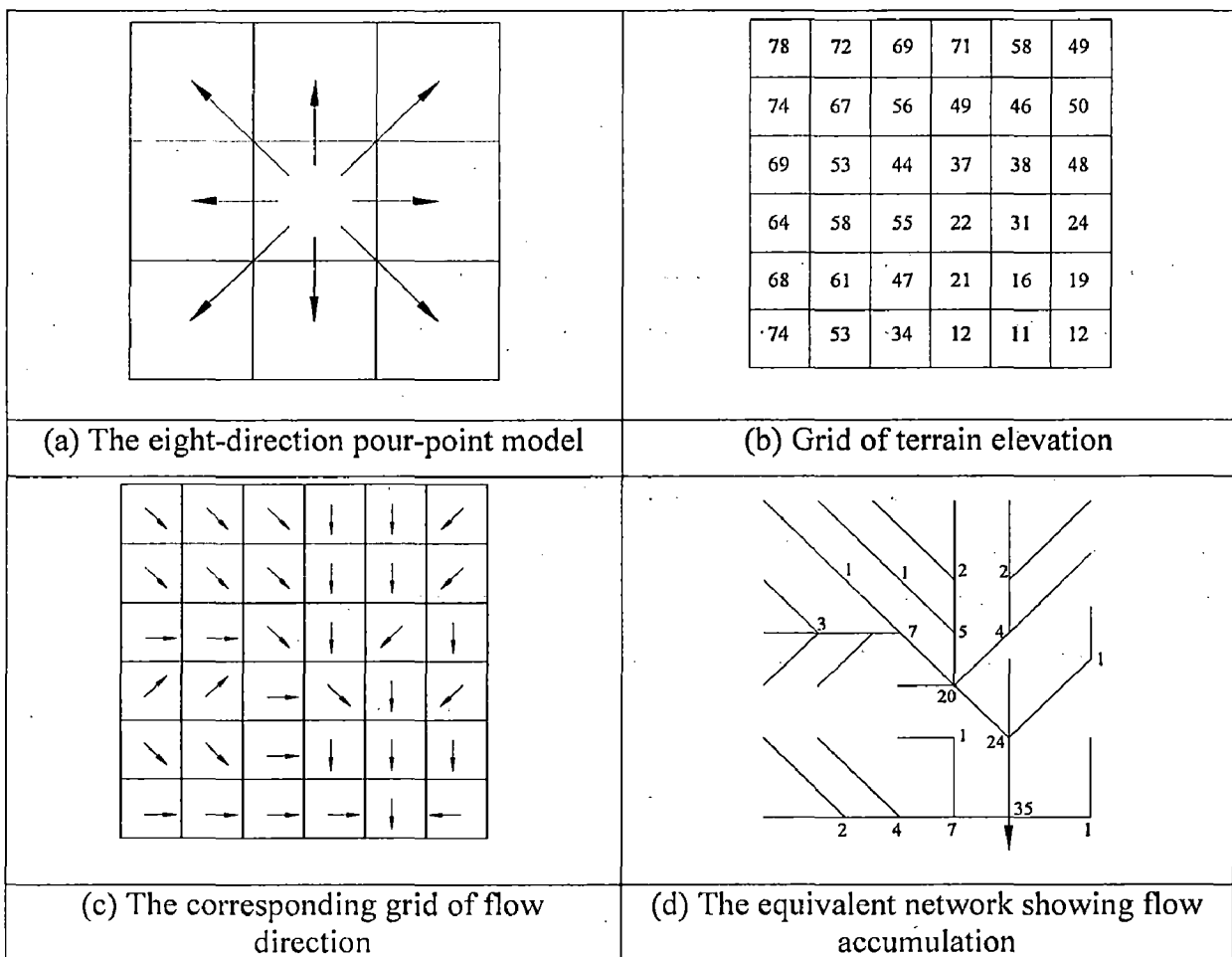


Figure 5.1: Watershed Terrain Analysis using Grids

Source: Adapted from Jain (2003)

Table 5.5. Subbasin Characteristic

Sub basin	Subbasin Area (km ²)	Stream Length (m)	Stream Slope (%)	Stream Width (m)	Sub basin	Subbasin Area (km ²)	Stream Length (m)	Stream Slope (%)	Stream Width (m)
1	1253.11059	357.20	0.100	93.193	11	231.2970179	8937.31	0.933	13.439
2	404.5837104	7368.01	0.100	47.293	12	49.69186358	20331.65	0.907	29.017
3	368.245167	7490.58	0.100	73.736	13	179.2409599	7505.45	0.100	17.119
4	848.1766282	295.91	0.100	84.299	14	74.38456054	3092.19	0.808	12.530
5	509.352547	2648.32	0.100	54.295	15	44.21919138	5613.58	0.100	44.849
6	509.2649842	7768.54	0.125	11.654	16	370.3466731	3240.14	0.100	28.392
7	39.18433295	6898.76	0.040	14.274	17	172.8488788	5816.66	0.015	29.030
8	54.94562889	3622.72	0.100	14.653	18	179.372304	6653.62	0.376	27.634
9	57.39738603	1760.59	0.100	50.206	19	165.2309191	7541.35	0.305	26.755
10	446.9640839	10644.05	0.014	33.814	20	156.5622063	10261.47	0.487	44.696

Source : SWAT Output

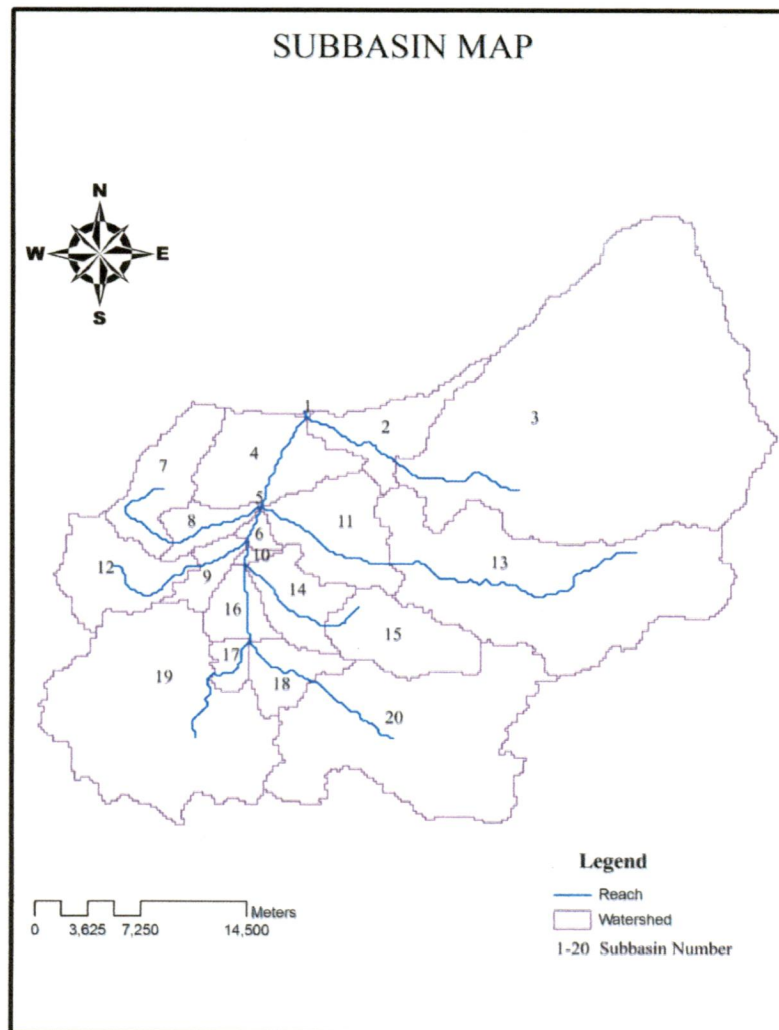


Figure 5.2: Subbasin Map

5.2.2. Data Processing

The purpose of data processing is to remove errors from the data and arrange them in a format that can be read by the program. Data preparation must be done before modeling. Here, the data that must be prepared is daily precipitation data for 20 years (1984-2003), daily temperature data for 20 years (1984-2003), the position coordinates of the stations, the distribution of land use and soil type of study locations. All the data must be prepared in database format (.dbf) and the map with the identification and attributes of each map.

5.2.2.1. Precipitation Data Processing

Precipitation data is needed in the ARCSWAT 2005 program to obtain the value of precipitation, evaporation, transpiration, surface flow, lateral flow, and the flow of the river.

Precipitation data that is used in this study is the data from rain gauge stations in the area of Wonogiri watershed recorded by BMG (meteorology and geophysical bureau). The total of rain gauge station that is used in this study is 5 stations, with a period of 20 years (1984-2003). An example of data formats that is used in the SWAT program is shown in the Table 5.6 and Figure 5.3 (a).

5.2.2.2. Temperature Data Processing

When measured temperature data are to be used, a table is required to provide the locations of the temperature gauges. Temperature data is needed in the ARCSWAT 2005 program to obtain the value of evapotranspiration in the hydrological cycle modeling. Temperature data that is used in this study is the data from weather station in the area of Wonogiri watershed recorded by BMG. The temperature data table is used to store the daily maximum and minimum temperatures for a weather station. This table is required if the climate station option is chosen for temperature in the weather data dialog box. There will be one temperature data table for every location listed in the climate station location table. The amount of weather station that is used in this study is 3 stations, with a period of 20 years (1984-2003). The examples of data formats that is used in the SWAT program is shown in the Table 5.7 and Figure 5.3 (b).

Table 5.6. Precipitation Data for SWAT Input

DATE	PCP
1/1/1984	0.0
1/2/1984	3.0
1/3/1984	22.0
1/4/1984	38.0
1/5/1984	18.0
1/6/1984	0.0
1/7/1984	6.0
1/8/1984	0.0
1/9/1984	6.0
↓	↓

ID	NAME	XPR	YPR	ELEVATION
1	NAWANGAN	489064.58	9110448.80	230.00
2	WONOGIRIDAM	490310.56	9135279.48	141.00
3	TAWANGMANGU	513628.26	9153079.25	1000.00
4	NGANCAR	503464.03	9115116.49	275.00
5	WONOGIRI	491762.30	9136615.02	136.00

(a) Form of Daily Precipitation Data	(b) Form of Rain Gauge Station
--------------------------------------	--------------------------------

Table 5.7 Temperature Data for SWAT Input

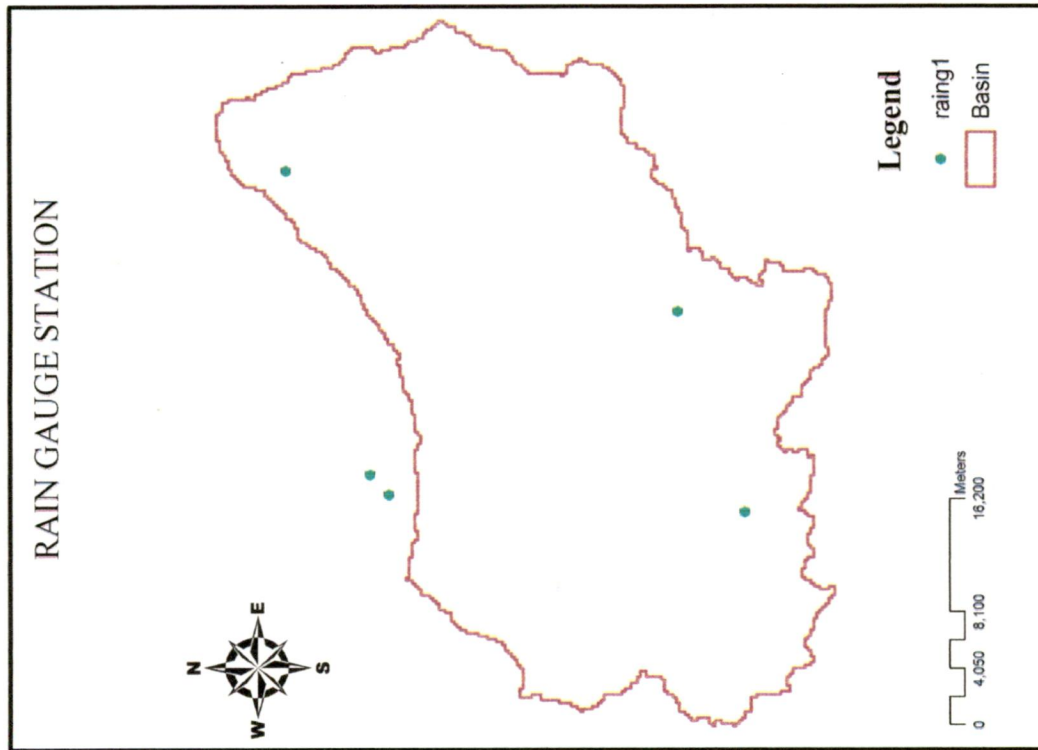
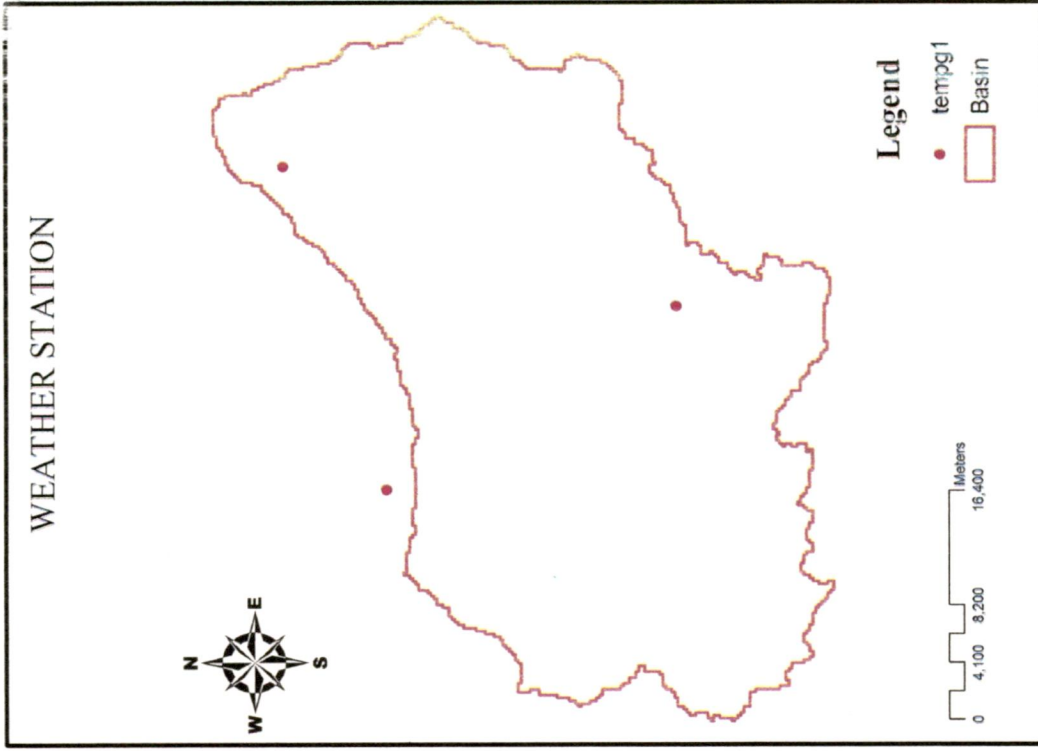
DATE	MAX	MIN
1/1/1984	25.83	22.23
1/2/1984	32.23	27.74
1/3/1984	29.01	24.96
1/4/1984	33.33	28.69
1/5/1984	30.00	25.82
1/6/1984	29.59	25.46
1/7/1984	30.00	25.82
1/8/1984	29.76	25.61
1/9/1984	26.78	23.05
↓	↓	↓

ID	NAME	XPR	YPR	ELEVATION
1	WONOGIRI	490310.560	9135279.480	141.00
2	NGANCAR	503464.031	9115116.491	275.00
3	TAWANGMANGU	513552.231	9142453.982	1000.00

(b) Form of Daily Temperature Data	(b) Form of Weather Station
------------------------------------	-----------------------------

5.2.3. HRU (Hydrologic Response Unit) Processing

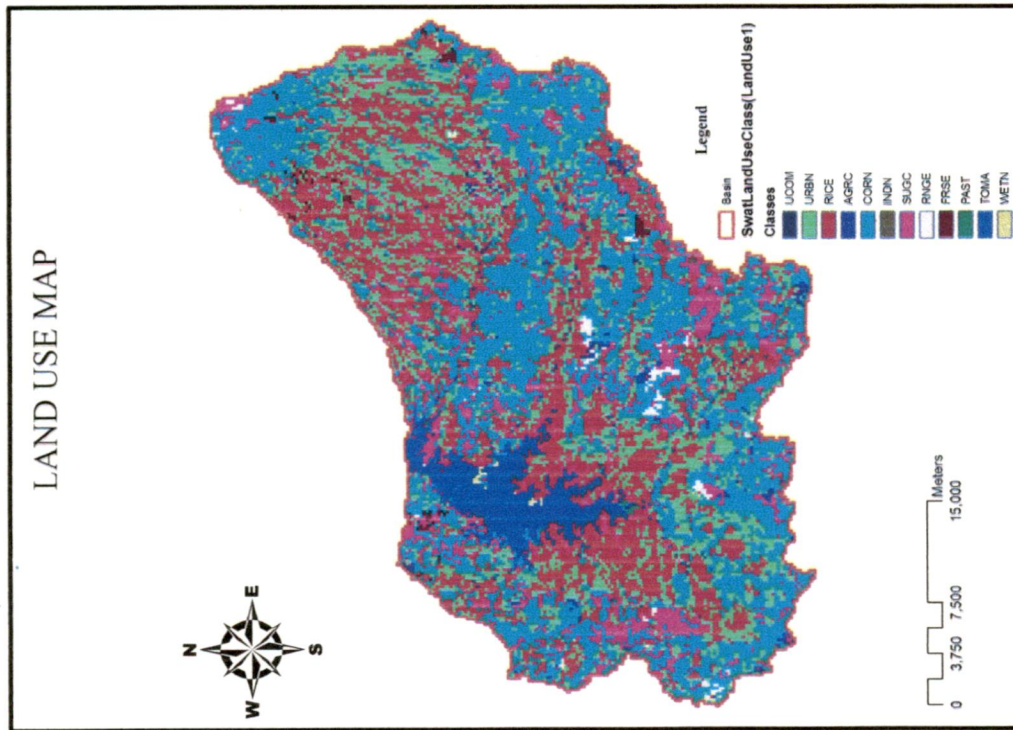
Hydrologic response units are lumped land areas within the subbasin that are comprised of unique land cover, soil, and management combinations (Neitsch, 2005). Runoff is predicted separately for each HRU and routed to obtain the total runoff for the watershed. This increases accuracy and gives a much better physical description of the water balance. Land use, soil, and slope characterization for a watershed is performed using commands from the HRU Analysis menu on the ArcSWAT Toolbar. These tools allow users to load land use and soil layers into the current project, evaluate slope characteristics, and determine the land use/soil/slope class combinations (Figure 5.4 and Figure 5.5) and distributions for the delineated watershed and each respective subwatershed.



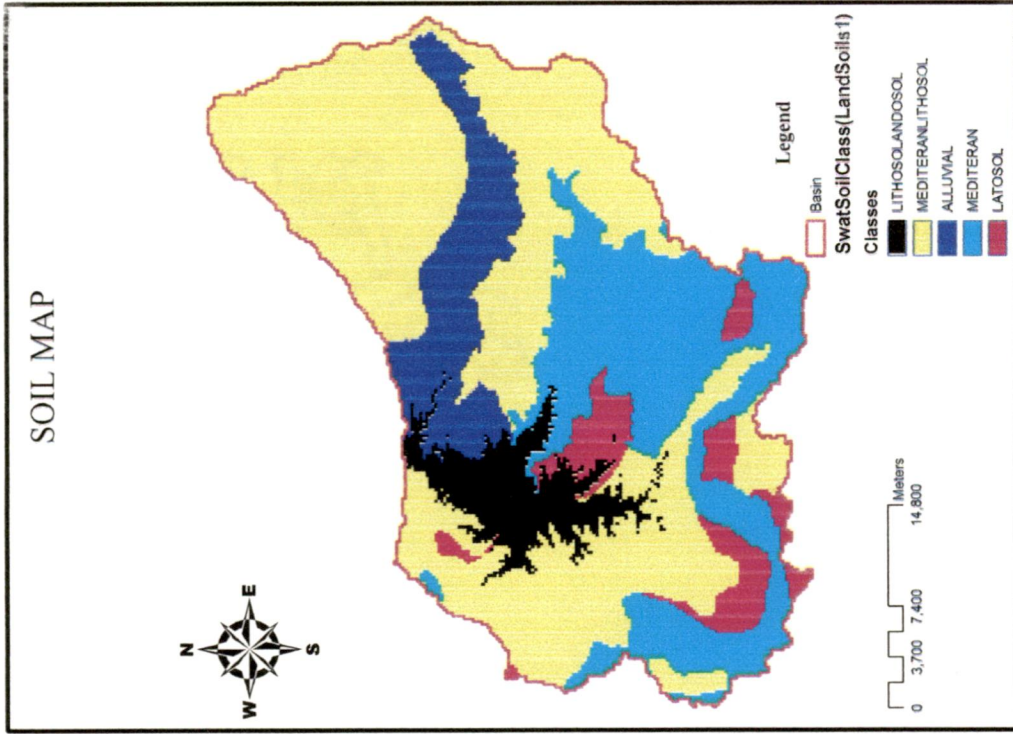
(a) Rain Gauge Map

(b) Weather Station Map

Figure 5.3. Rain Gauge and Weather Station Map

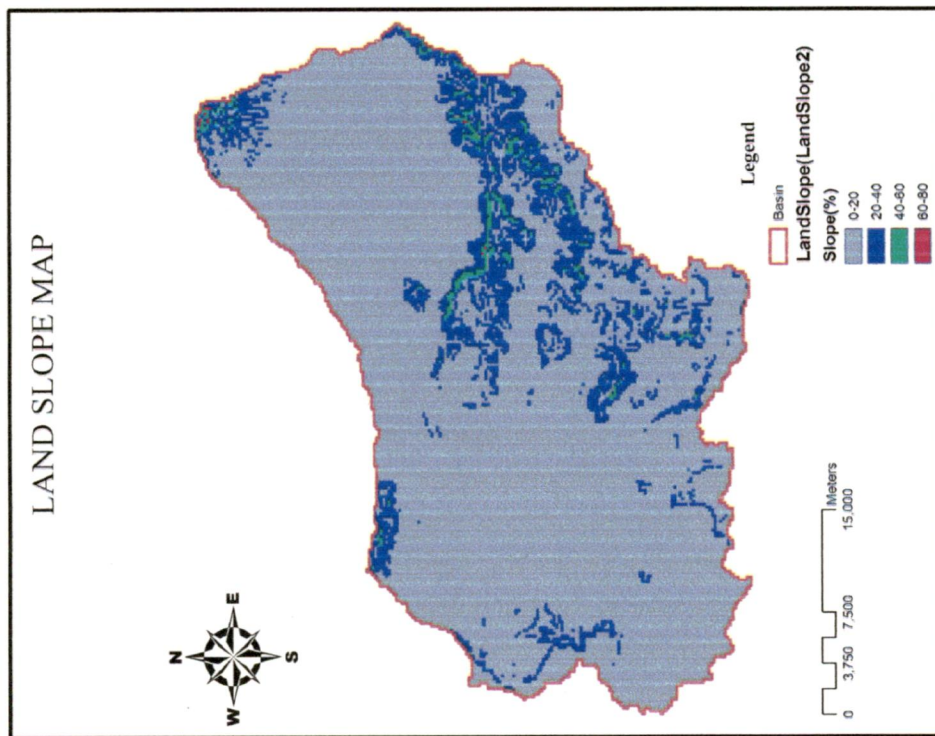


(a) Land Use Map

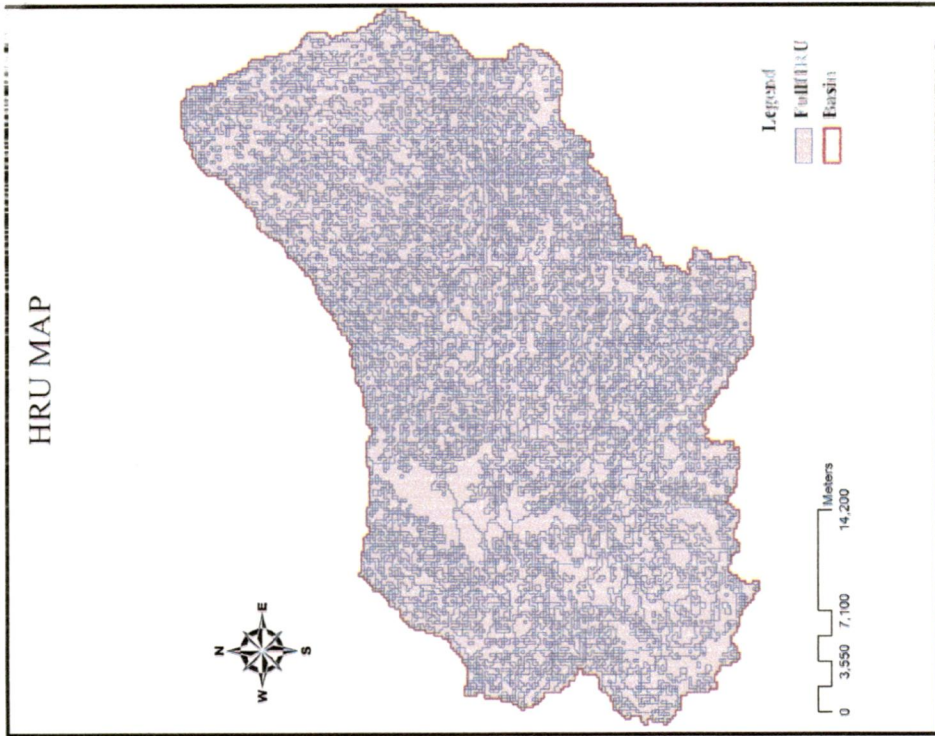


(b) Soil Classification Map

Figure 5.4. Land Use and Soil Classification Map



(a) Land Slope Map



(b) HRU (Hydrologic Response Unit) Map

Figure 5.5. Land Slope and HRU Map

5.2.3.1. Land Use and Soil Definition

Identification of land use and soil type is to know the characteristics of land in each sub-watershed that has been formed as shown in Figure 5.4 . This menu will be automatically active if all processes of watershed delineation are completed. The format input data and result of this step is shown in Figure 5.6.

5.2.4. SWAT Simulation

There are 2 processes that must be done in watershed modeling using SWAT program, namely:

- a Initial flow simulation and calibration, in this step we run the program to obtain the surface runoff using the default parameters that was available on the SWAT program. After we get the discharge of surface runoff, then we compare it with the observed data from the same discharge station, that comparison were used to adjust parameter in the calibration process until we get the same result between observed data and SWAT modeling result.
- b Post Calibration Flow Simulation, in this process we run same data using adjusted parameters that is carried out on the previous step to obtain the result better of SWAT.

5.2.4.1. Initial Flow Simulation

After data the input processing was completed, the next step is the process of running SWAT to study the response of the original parameters of the program on watershed modeling. This process used data from the years 1984-2003, while the observed discharge data are available from 1994-2003. The program was run conducted in the year in which the available observational data, so the results from the SWAT program can be compared with observational data. The observed discharge data of Subbasin 3 (Keduang subbasin) is shown in Table 5.8. The results of modeling using the default values of parameters to produce a discharge inflow modeling for subbasin 3 for calibration year (1994-1999) is shown in Table 5.9.

Table 5.8. Measured Discharge (m³/sec) for Keduang Subbasin

Month/Year	1994	1995	1996	1997	1998	1999	2000	2001	2002	2003
January	46.6	30.0	56.5	58.5	8.3	86.0	31.7	70.5	64.2	53.6
February	43.5	100.0	60.7	78.2	51.4	68.3	53.1	53.9	101.4	73.6
March	100.0	52.5	28.0	17.4	46.8	53.0	71.2	43.5	72.6	36.6
April	24.0	11.8	18.0	30.5	37.5	22.7	98.8	31.7	80.9	4.1
May	2.3	12.7	1.6	7.4	10.5	17.4	19.2	9.5	12.5	3.1
June	0.0	23.6	1.5	0.2	24.6	1.7	0.6	6.9	3.4	5.7
July	0.0	5.4	1.1	0.0	10.1	0.3	0.0	10.4	0.1	0.1
August	0.0	0.2	4.5	0.0	0.1	6.0	0.0	0.2	0.0	0.0
September	0.0	2.0	0.6	0.0	13.6	0.1	0.0	4.7	0.0	0.0
October	0.0	16.5	21.5	0.0	17.7	15.1	34.6	42.2	0.0	5.9
November	5.7	67.6	15.1	4.8	37.8	83.9	55.1	48.2	14.8	20.4
December	3.4	85.0	33.2	9.0	46.2	93.8	18.2	10.8	35.2	25.8

Source: PBS

Table 5.9. SWAT Output Discharge (m³/sec) for Calibration Year (1994-1999) at Subbasin 3

Month/Year	1994	1995	1996	1997	1998	1999
January	23.8	34.6	40.1	40.5	29.6	55.4
February	31.9	70.9	48.7	52.8	36.2	49.4
March	57.2	39.1	24.8	17.6	35.2	40.1
April	24.0	14.5	16.5	21.5	28.9	21.3
May	8.9	11.0	5.0	8.6	12.9	16.0
June	3.9	13.1	2.2	3.2	17.3	4.0
July	1.1	4.9	0.6	0.9	8.7	1.1
August	0.2	1.2	1.2	0.2	2.6	2.4
September	0.1	1.4	0.1	0.1	6.4	0.1
October	0.0	8.1	8.4	0.2	9.4	5.8
November	1.5	41.2	34.8	2.3	22.6	52.8
December	10.4	29.7	24.6	23.5	29.7	59.9

5.2.4.2. SWAT Calibration & Validation

Calibration and validation is the process undertaken to obtain the parameter values in accordance with actual conditions, by comparing the modeling results with observed data. The observed discharge data pertain to 1994-2003 period, and it was divided in 2 parts for calibration and validation purposes. For calibration process, data from the years 1994 through 1999 (6 years) was used, whereas the data used for the validation process is 4 years data (2000-2003). Table 5.10 and Figure 5.6 shows the time series of observed and simulated monthly stream flow during the period of 1994-1999.

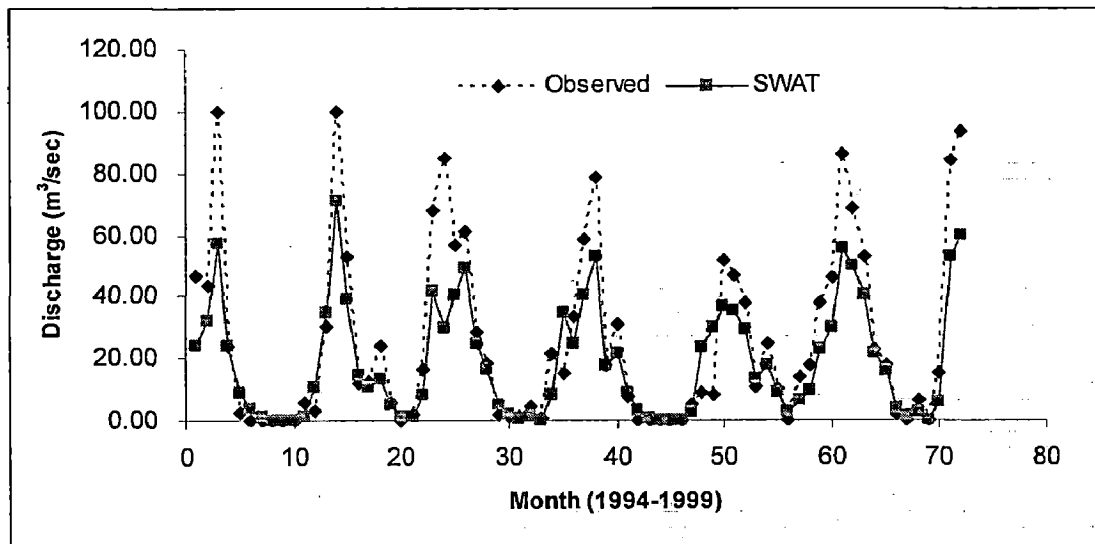


Figure 5.6. Comparison of Observed and Modeling Discharge for Calibration Year

From Figure 5.6 we can see that the SWAT result is less than the observed data. There is some factor that affecting the model is not close to the reality because of data related aspect, such as:

- The measurement stations (hydrological or meteorological) are not representative
- Localized storm
- Malfunctioning gauges (hydrological or meteorological)
- Too little data (monitoring period too short)
- Low accuracy of land use or soil data prediction
- Adjustment of the wrong parameters

In this study, besides the graphical plots and tabular results, three standard statistical techniques, Nash-Sutcliffe coefficient (E), coefficient of determination (R^2), and relative error (RE%) are used to test the model performance and the results are given in Table 5.11. The discharges (observed and computed) before the calibration are presented in Figure 5.7.

Table 5.10. Comparison of Observed and Modeling Discharge for Calibration Year

Year	Month	Observed	SWAT	Year	Month	Observed	SWAT
1994	Jan	46.58	23.75	1997	Jan	58.50	40.47
	Feb	43.50	31.86		Feb	78.24	52.82
	Mar	100.00	57.24		Mar	17.40	17.65
	Apr	24.00	23.99		Apr	30.50	21.51
	May	2.30	8.88		May	7.43	8.57
	Jun	0.00	3.87		Jun	0.17	3.22
	Jul	0.00	1.12		Jul	0.00	0.90
	Aug	0.00	0.23		Aug	0.00	0.25
	Sep	0.00	0.07		Sep	0.03	0.08
	Oct	0.00	0.05		Oct	0.02	0.20
	Nov	5.70	1.48		Nov	4.82	2.33
	Dec	3.45	10.42		Dec	9.01	23.51
1995	Jan	29.95	34.58	1998	Jan	8.27	29.55
	Feb	100.00	70.91		Feb	51.40	36.23
	Mar	52.50	39.14		Mar	46.77	35.20
	Apr	11.79	14.50		Apr	37.53	28.89
	May	12.67	10.99		May	10.47	12.94
	Jun	23.58	13.14		Jun	24.58	17.30
	Jul	5.37	4.94		Jul	10.10	8.72
	Aug	0.19	1.20		Aug	0.11	2.63
	Sep	2.00	1.37		Sep	13.59	6.41
	Oct	16.49	8.06		Oct	17.67	9.36
	Nov	67.58	41.22		Nov	37.77	22.58
	Dec	85.00	29.65		Dec	46.15	29.69
1996	Jan	56.50	40.14	1999	Jan	85.96	55.36
	Feb	60.73	48.73		Feb	68.33	49.35
	Mar	28.00	24.76		Mar	52.98	40.12
	Apr	18.00	16.53		Apr	22.66	21.27
	May	1.60	4.99		May	17.41	16.01
	Jun	1.50	2.15		Jun	1.72	3.99
	Jul	1.05	0.56		Jul	0.31	1.09
	Aug	4.50	1.18		Aug	6.04	2.40
	Sep	0.60	0.14		Sep	0.06	0.09
	Oct	21.50	8.42		Oct	15.07	5.83
	Nov	15.13	34.77		Nov	83.91	52.83
	Dec	33.24	24.65		Dec	93.79	59.95

Table 5.11. Statistical Calculation of model performance

Statistical Parameter	Value
E	-0.34938
RE%	25.89189
R ²	0.8489

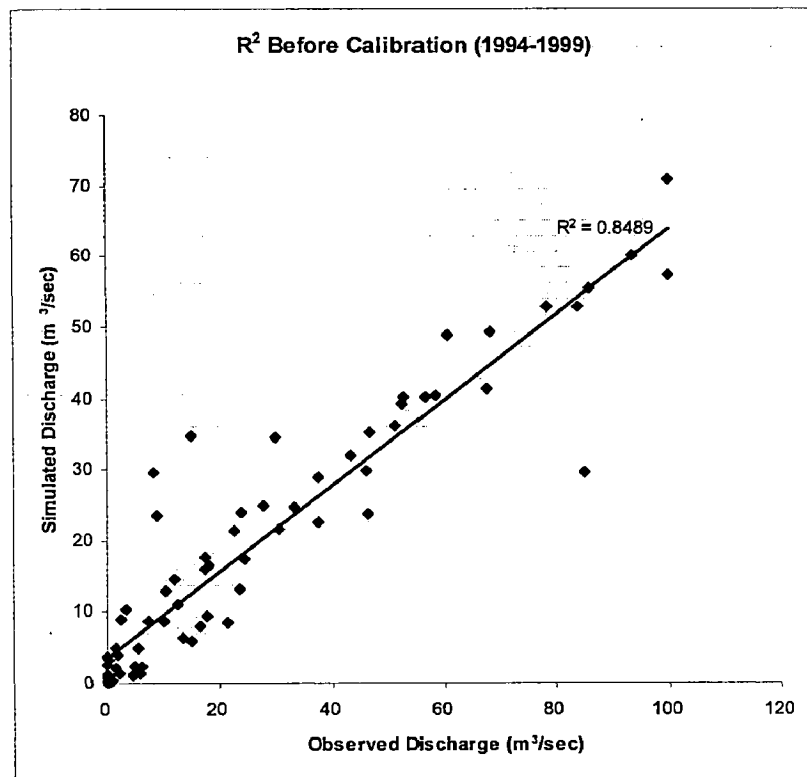


Figure 5.7. R² of Observed and Modeling Discharge before Calibration Process

From statistical calculation (Table 5.11) shows that Relative Error (RE%) is more than 10%, this value indicate that the model does not represent the actual condition of stream flow. For this problem, we need some adjustment of SWAT parameters as follows:

- Carefully review precipitation and flow data for the particular duration, this step is aimed to make sure that data input was correct, because in some case wrong input may be given to the program because of human error on inputting data.
- Curve number for different land uses was increased by 10% (CN2 in .mgt file). Because of the SWAT output showing lower result than observed, than by increasing curve number expected the stream runoff will be increase
- Decreasing soil available water (SOL_AWC in.sol), deep percolation loss (adjust threshold depth of water shallow aquifer required for base flow to occur) (GWQMN in.gw), and groundwater revap coefficient (GW_REVAP in.gw), by decreasing ground water parameter so that the surface water is expected to be increase.

Repeat the adjustment until values are acceptable. It may take several iterations to get the surface runoff and baseflow corrected. The complete parameters that can be adjusted in SWAT program are shown in Table 5.12. Table 5.13 shows the parameter changes made in this study, and the results of the calibration process is shown in Table 5.14 and Figure 5.8.

Table 5.12. Range of Parameters on SWAT Program

CODE	RANGE		DEFINITION
	MIN	MAX	
Ground Water Data (.GW)			
SHALLST	0	1000	Initial depth of water in the shallow aquifer.
DEEPST	0	3000	Initial depth of water in the deep aquifer .
GW_DELAY	0	500	Groundwater delay.
ALPHA_BF	0	1	Baseflow alpha factor.
GWQMN	0	5000	Threshold depth of water in the shallow aquifer required for return flow to occur.
GW_REVAP	0.02	0.2	Groundwater "revap" coefficient.
REVAPMN	0	500	Threshold depth of water in the shallow aquifer for "revap" to occur.
RCHRG_DP	0	1	Deep aquifer percolation fraction.
Management Input Data (.MGT)			
CN2	35	98	SCS runoff curve number factor
Hydrologic Response Units Data (.HRU)			
LAT_TTIME	0	180	Lateral flow travel time.
SLSOIL	0	150	Slope length for lateral subsurface flow.
ESCO	0	1	Soil evaporation compensation factor.
Main Channel Input Data (.RTE)			
CH_N2	-0.01	0.3	Manning's "n" value for the main channel.

Source : SWAT Database

Table 5.13. Adjusted Parameters

Scenario	Changing Parameter	Initial Value	Recommendation	Subbasin
Simulation 1	Default Value	Default Value	Default Value	ALL
Simulation 2	Adjustment CN2	Variate	Variate	ALL
Simulation 3	ALPHA_BF = 1	0.048	1	ALL
Simulation 4	GW_DELAY = 0	31	0	ALL
Simulation 5	GW_REVAP = 0	0.02	0	ALL
Simulation 6	GWQMN = 1000	0	1000	ALL
Simulation 7	RCHRG_DP = 0	0.05	0	ALL
Simulation 8	REVAPMN = 0	1	0	ALL
Simulation 9	CH_N2 = 0.3	0.014	0.3	ALL
Simulation 10	LAT_TIME = 180	0	180	ALL
Simulation 11	SLSOIL = 150	0	150	ALL

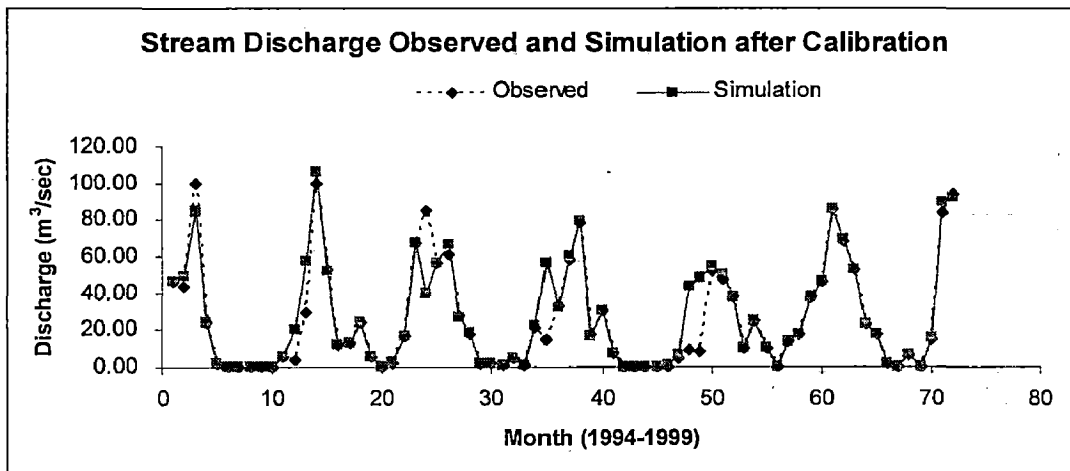


Figure 5.8: Stream Discharge of Observed and Simulation after Calibration Process

Table 5.13 shows that many ground water parameters was adjusted, this adjustment aimed to decrease the amount of water that infiltrated into the soil and become sub surface water so that the runoff will increase. Data in Figure 5.8 represents the monthly modeled discharge compared with the observed data. The model predictions generally followed the pattern of measured monthly outflows with some over predictions in some years and under prediction in the other years. We can not get 100% similar result between model and observation that is because some assumption and adjustment about land and soil characteristic that we make in modeling can not be same with the reality conditions.

In the validation process parameters used that have been calibrated in the previous process for use in the period 2000-2003, the results of validation process is shown in Table 5.15 and Figure 5.9. This validation process aimed to make sure that parameter that was adjusted in the calibration process can be applied for another data in the same area.

Table 5.14.: Comparison Observed and Modeling Discharge after Calibration

Year	Month	Observed	SWAT	Year	Month	Observed	SWAT
1994	Jan	46.58	45.77	1997	Jan	58.50	59.68
	Feb	43.50	49.26		Feb	78.24	79.46
	Mar	100.00	84.98		Mar	17.40	16.91
	Apr	24.00	23.89		Apr	30.50	30.66
	May	2.30	2.22		May	7.43	7.40
	Jun	0.00	0.07		Jun	0.17	0.17
	Jul	0.00	0.05		Jul	0.00	0.10
	Aug	0.00	0.03		Aug	0.00	0.04
	Sep	0.00	0.03		Sep	0.03	0.03
	Oct	0.00	0.07		Oct	0.02	0.65
	Nov	5.70	5.60		Nov	4.82	6.73
	Dec	3.45	20.50		Dec	9.01	43.75
1995	Jan	29.95	57.47	1998	Jan	8.27	48.32
	Feb	100.00	106.30		Feb	51.40	54.53
	Mar	52.50	51.35		Mar	46.77	50.04
	Apr	11.79	11.79		Apr	37.53	37.53
	May	12.67	12.67		May	10.47	10.47
	Jun	23.58	23.58		Jun	24.58	24.58
	Jul	5.37	5.23		Jul	10.10	10.10
	Aug	0.19	0.19		Aug	0.11	0.11
	Sep	2.00	2.55		Sep	13.59	13.59
	Oct	16.49	16.49		Oct	17.67	17.67
	Nov	67.58	67.58		Nov	37.77	37.77
	Dec	85.00	39.86		Dec	46.15	46.15
1996	Jan	56.50	56.75	1999	Jan	85.96	85.96
	Feb	60.73	66.06		Feb	68.33	68.86
	Mar	28.00	27.21		Mar	52.98	52.29
	Apr	18.00	18.38		Apr	22.66	22.66
	May	1.60	1.53		May	17.41	17.41
	Jun	1.50	1.43		Jun	1.72	1.72
	Jul	1.05	1.03		Jul	0.31	0.31
	Aug	4.50	4.73		Aug	6.04	6.04
	Sep	0.60	0.58		Sep	0.06	0.06
	Oct	21.50	21.89		Oct	15.07	15.38
	Nov	15.13	56.29		Nov	83.91	89.11
	Dec	33.24	32.44		Dec	93.79	92.25

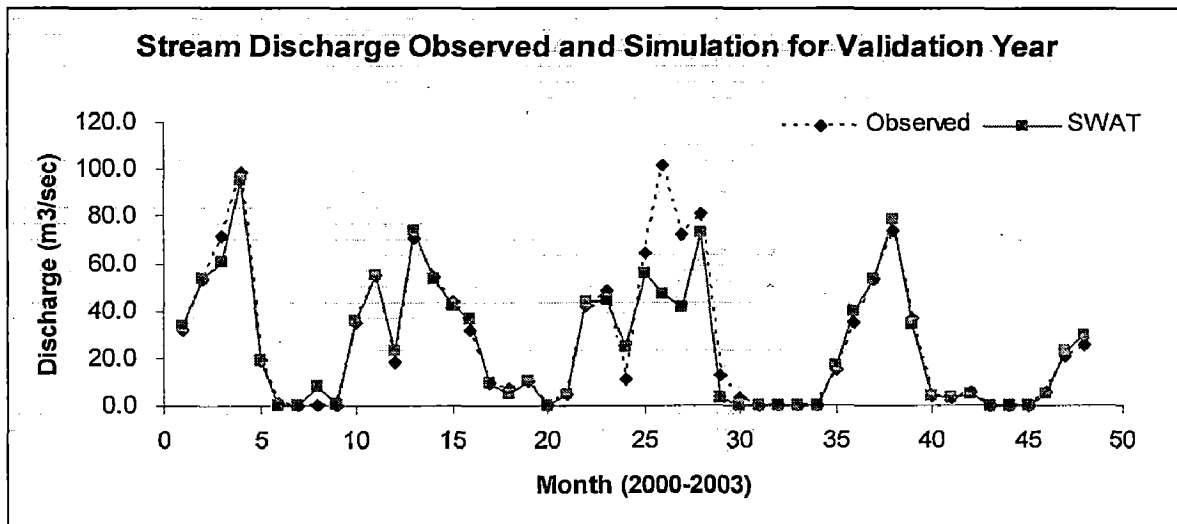


Figure 5.9: Stream Discharge Observed and Simulation for Validation Year

Table 5.15.: Comparison of Observed and Modeling Discharge for Validation

Year	Month	Observed	SWAT	Year	Month	Observed	SWAT
2000	Jan	31.7	33.05	2002	Jan	64.2	55.5
	Feb	53.1	53.15		Feb	101.4	46.75
	Mar	71.2	60.35		Mar	72.6	41.58
	Apr	98.8	95.74		Apr	80.9	72.93
	May	19.2	18.68		May	12.5	2.88
	Jun	0.6	0.1352		Jun	3.4	0.3103
	Jul	0.0	0.06055		Jul	0.1	0.07375
	Aug	0.0	7.988		Aug	0.0	0.05739
	Sep	0.0	0.4951		Sep	0.0	0.0406
	Oct	34.6	35.45		Oct	0.0	0.1365
	Nov	55.1	54.73		Nov	14.8	16.76
	Dec	18.2	22.75		Dec	35.2	39.45
2001	Jan	70.5	74.01	2003	Jan	53.6	53.35
	Feb	53.9	53.22		Feb	73.6	78.64
	Mar	43.5	42.06		Mar	36.6	34.05
	Apr	31.7	36.78		Apr	4.1	4.072
	May	9.5	9.739		May	3.1	3.378
	Jun	6.9	4.949		Jun	5.7	5.022
	Jul	10.4	10.35		Jul	0.1	0.05716
	Aug	0.2	0.05468		Aug	0.0	0.04254
	Sep	4.7	4.572		Sep	0.0	0.03569
	Oct	42.2	43.58		Oct	5.9	4.735
	Nov	48.2	44.21		Nov	20.4	22.8
	Dec	10.8	24.41		Dec	25.8	29.04

The model almost accurately predicted the outflows including the zero flows in the validation year of 2000-2003. This was also supported by the data from statistical

calculation, after correction in the SWAT model, we get better result that shows by relative error (RE%) that decreasing until less than 10% (Table 5.16), it is indicate that is not much different between model result and observed data. For the calibration and validation period simulated discharges corresponding to observed one are presented in Figure 5.10.

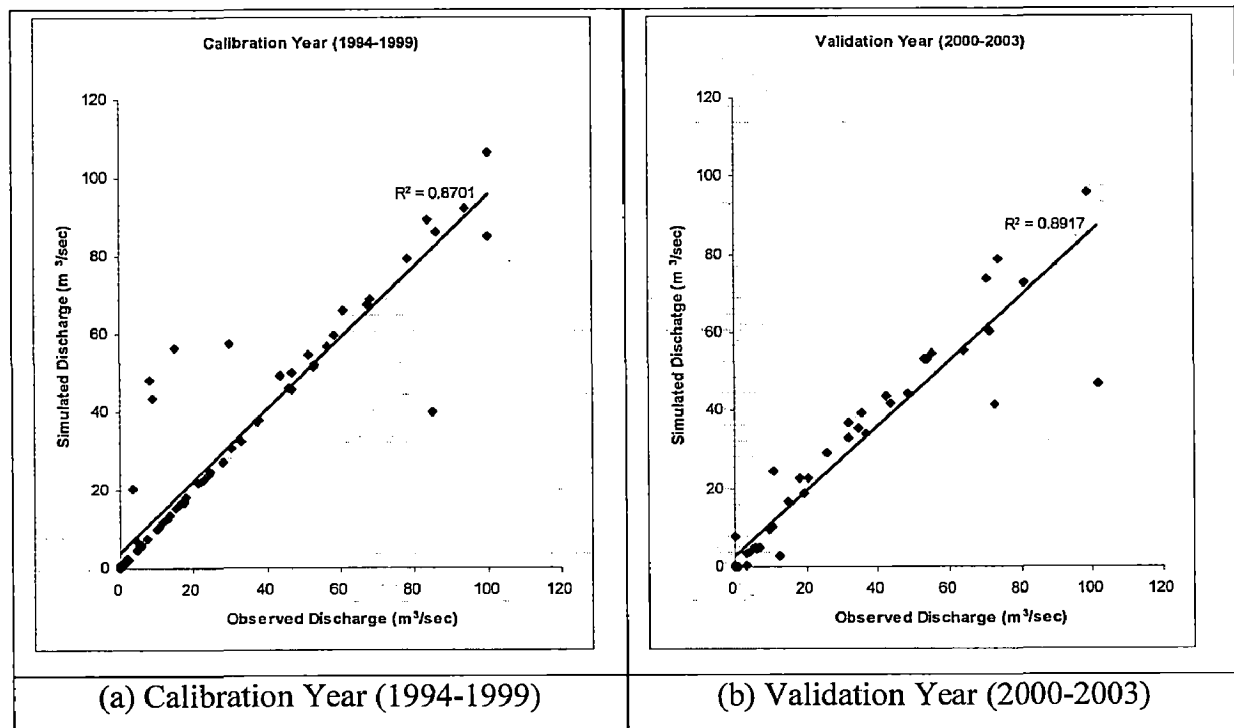


Figure 5.10. R^2 for Observed and Modeling Discharge

Table 5.16. Statistical Calculation of Model Performance after Correction

SCENARIO	E	RE%	R^2
CALIBRATION YEAR (1994-1999)	0.924001	-7.12073958	0.8701
VALIDATION YEAR (2000-2003)	0.9390709	6.539382001	0.8917

We can see the change of coefficient of determination (R^2) every year during calibration period (1994-1999) as shown in Figure 5.11 and 5.12. Those figure shows that R^2 before and after calibration in some year was low (< 0.85). It is because in watershed modeling it was used same land use map because of the data for land use is not available in yearly. Susilowati (2006) was recommended that during 1992–1996 the land use at Bengawan Solo catchment was changing 1.81% averagely (Table 5.17). But

generally the watershed modeling is close to the actual condition with R^2 0.87 and 0.89 respectively for calibration and validation year (Table 5.16).

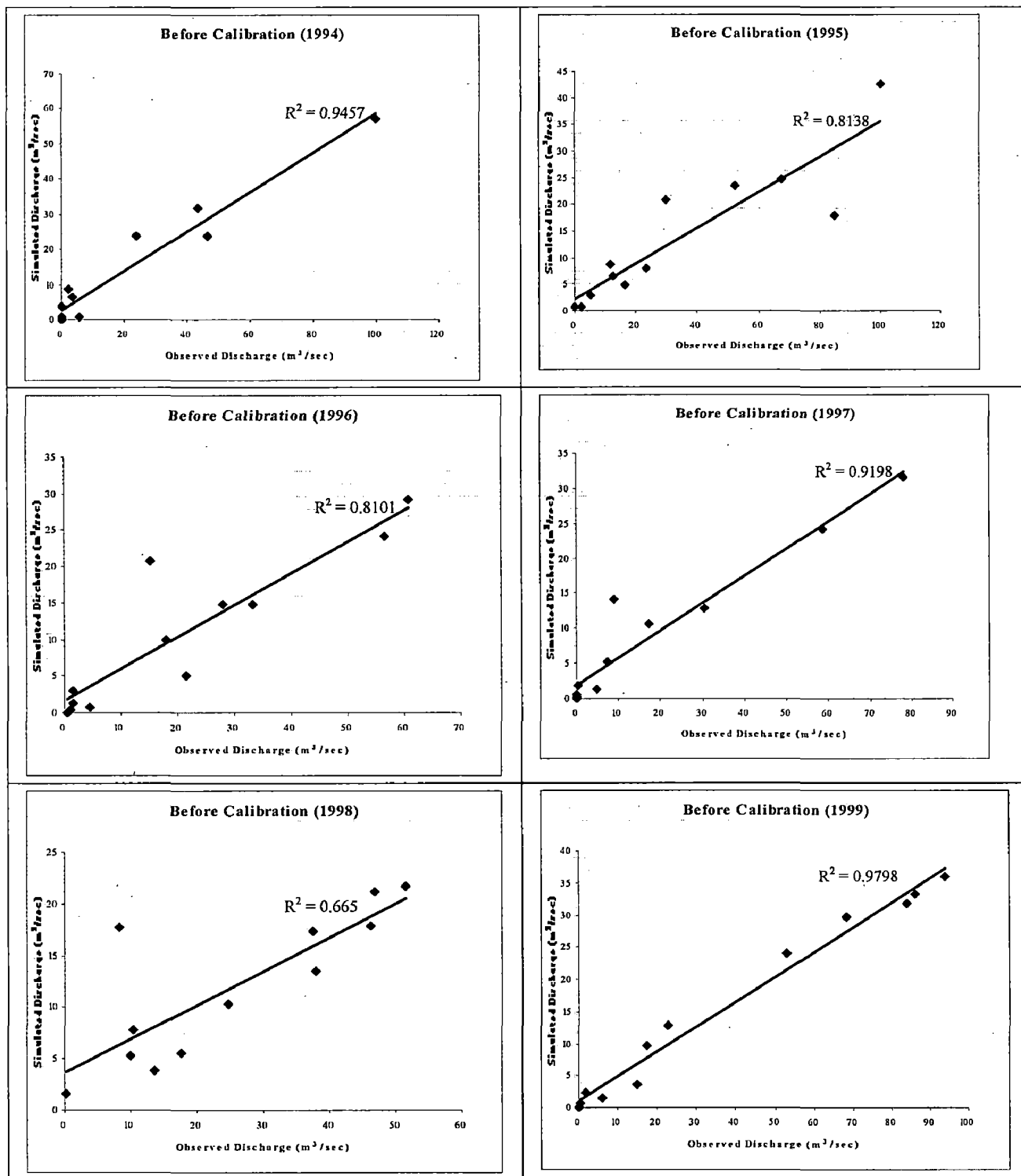


Figure 5.11. Yearly R^2 Before Calibration (1994-1999)

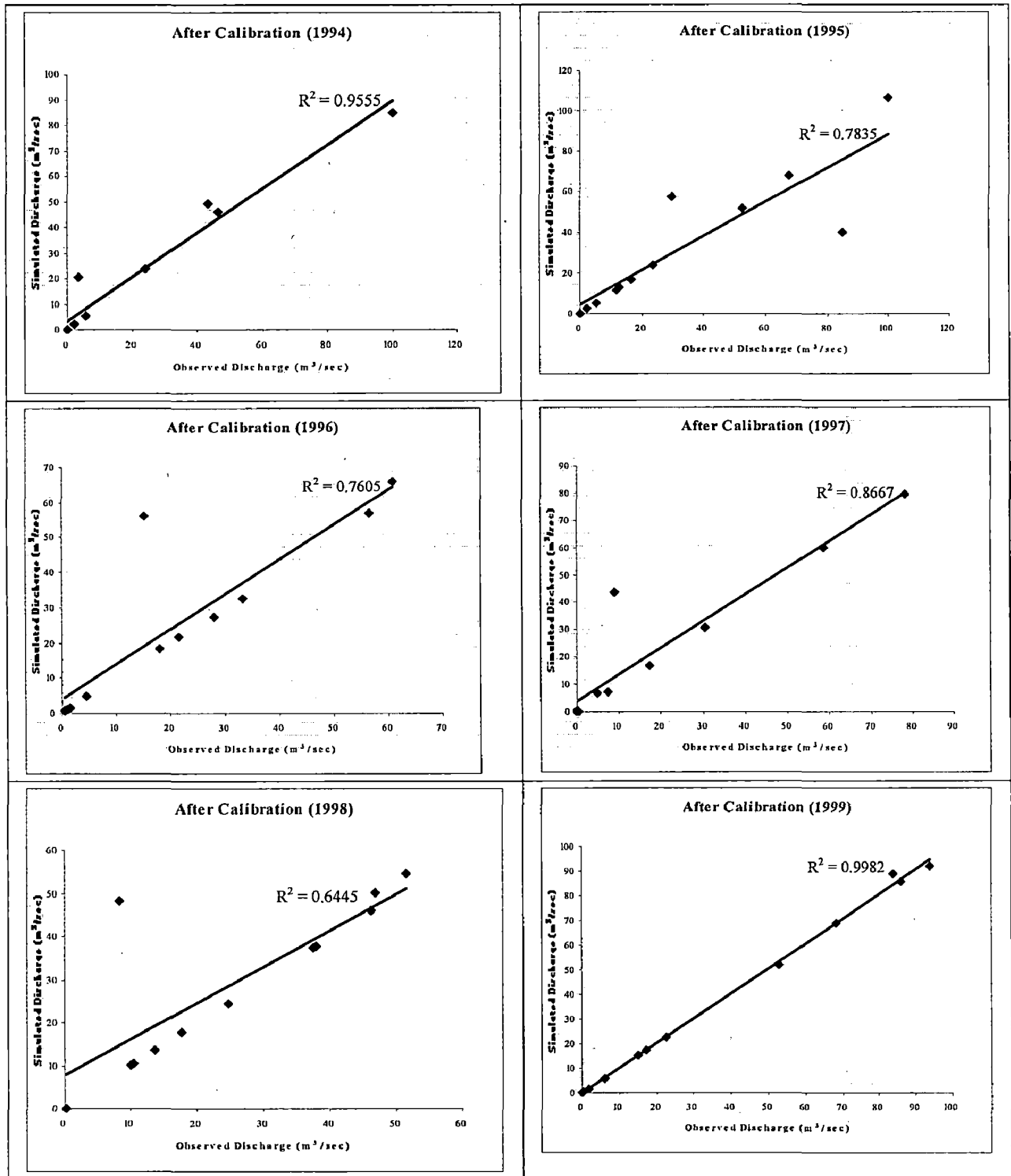


Figure 5.12. Yearly R² After Calibration (1994-1999)

Table 5.17. Land Use Change at Bengawan Solo Catchment

Land Use	Change Area	% Change
	(Ha)	
Road	0.59	0.50
Industrial	4.54	3.08
Commercial	0.80	0.65
Residential	10.71	1.58
Public Service	5.26	4.53
Open Area	5.18	6.55

Source : Susilowati, 2006

5.3. Climate Change Scenario

Calculation of assessment of climate change (Table 5.4) shows that precipitation is likely to change by -3% to 3% for medium-term scenario and change by -12% to 12% for long-term scenario, while temperature was change by -5°C to 2.32°C for medium-term scenario and was change by 3.61°C to 3.92°C for long-term scenario. This study is trying to compare both IPCC 2007 and calculation to get more comprehensive result in predicting impact of climate change on hydropower generation. Using parameters that have been calibrated on previous step, the stream discharge is calculated by SWAT program with changing on precipitation and temperature data following the climate scenario (Table 5.18).

From Table 5.18 shows that minimal change indicate reducing in precipitation, but in temperature decreasing only shows in the medium-term scenario, while in the long-term scenario calculation of trend analysis can not be done, because of the data is not available for temperature, than this study using IPCC 2007 recommendation, that is why there is no variation in the temperature data for long-term scenario. The statistical description of simulation result base on climate scenario is shown in Table 5.19.

Table 5.19 shows that the medium-term scenario does not show significant effect of climate change, discharge changes only by range 0.02-0.20 m³/sec. The average discharge of scenario II of medium-term is higher than average discharge of scenario I. It is because in scenario I the evapotranspiration is higer than in scenario II. However, in the long-term scenario shows significant effect of climate change by increasing average discharge by 7.8 m³/sec in the scenario I and by decreasing 5.02 m³/sec in the scenario II.

Table 5.18. Climate Scenario used for Simulation

Scenario	Year	Seasons	Change		
			Precipitation (%)	Temperature (°C)	
I	Observed	1984 - 2003	DJF	Observed	Observed
			MAM	Observed	Observed
			JJA	Observed	Observed
			SON	Observed	Observed
II	Medium-Term (Scenario II)	2024 - 2043	DJF	-3	-0.1
			MAM	0	0.4
			JJA	-1	-0.5
			SON	-3	0.7
III	Medium-Term (Scenario I)	2024 - 2043	DJF	2	2.25
			MAM	3	2.32
			JJA	0	2.13
			SON	-1	1.32
IV	Long-Term (Scenario II)	2074 - 2093	DJF	-12	3.92
			MAM	-1	3.83
			JJA	-3	3.61
			SON	-9	3.72
V	Long-Term (Scenario I)	2074 - 2093	DJF	8	3.92
			MAM	12	3.83
			JJA	9	3.61
			SON	9	3.72

Table 5.19. Statistical Description of Simulation Result Based on Climate Scenario

Parameter	Scenario									
	Observed Year		Medium Term 2024-2043				Long Term 2074-2093			
	1984-2003		Scenario I		Scenario II		Scenario I		Scenario II	
	Discharge (m ³ /sec)	Precip. (mm)	Discharge (m ³ /sec)	Precip. (mm)	Discharge (m ³ /sec)	Precip. (mm)	Discharge (m ³ /sec)	Precip. (mm)	Discharge (m ³ /sec)	Precip. (mm)
Mean	53.36	5.63	53.38	5.72	53.56	5.51	61.16	6.15	48.34	5.18
Standart Deviation	55.31	13.53	55.73	13.77	55.05	13.25	61.18	14.79	48.75	12.46
Max.	267.02	232.00	267.69	236.64	264.56	225.04	288.30	250.56	230.48	204.16
Min.	0.03	0.00	0.00	0.00	0.00	0.00	0.00	0.00	0.00	0.00
Mean Dry Month	18.25	2.39	17.99	2.43	18.63	2.37	22.26	2.42	17.80	2.11
Mean Wet Month	102.52	10.20	102.94	10.38	102.46	9.96	115.62	4.84	91.10	4.03
>100	51	49.00	51	55.00	51	46.00	62	92.00	43	33.00
<10	74	30357.0	76	30417.0	72	30582.0	67	30205.0	73	30819.0
Mean Temperature (°C)	25.16		27.17		25.29		28.93		28.93	
Mean Potential Evaporation (mm)	177.73		189.14		178.33		199.20		199.27	
Mean Evapotranspiration (mm)	51.333		53.572		48.148		50.607		50.124	
Scenario										
Precipitation (%)										
DJF	Observed		+2		-3		+8		-12	
MAM	Observed		+3		0		+12		-1	
JJA	Observed		0		-1		+9		-3	
SON	Observed		-1		-3		+9		-9	
Temperature (°C)										
DJF	Observed		+2.25		-0.1		+3.92		+3.92	
MAM	Observed		+2.32		+0.4		+3.83		+3.83	
JJA	Observed		+2.13		-0.5		+3.61		+3.61	
SON	Observed		+1.32		+0.7		+3.72		+3.72	

5.4. Simulation of Reservoir Operation for Hydropower Generation

This study aimed to determine the energy that can be generated and the reliability of hydropower corresponding to different scenario of climate change. For this purpose, two steps were followed. The first step is determining the firm power that can be generated by the hydropower plant. Second is simulating the reservoir operation with given firm power to determine the amount of energy that can be generated and the associated reliability. The data that was needed for this simulation are:

1. Inflow discharge to the reservoir
2. Monthly depth of evaporation
3. Minimum and maximum reservoir capacity, initial reservoir storage
4. Power plant capacity and efficiency
5. Elevation – Area – Capacity Table of reservoir

The steps to determine firm power are as shown in Figure 5.13. After knowing the firm energy that can be generated by hydropower plant, the next step is simulation of reservoir operation to determine reliability of the energy that can be generated (Figure 5.14). The result of reservoir simulation to determine possible firm energy that can be generated is shown in Table 5.20 and the result of hydropower simulation to determine the energy reliability is shown in Table 5.21.

Table 5.20 shows that the possible firm energy that can be generated by Wonogiri hydropower plant is almost the same under different scenarios of climate change, except for long-term scenario I that shows significant increase in possible firm energy and corresponding firm power. We can see that the firm energy and corresponding firm power in long-term period scenario II is higher than in observed period even the other factors is likely to decrease, for analyze those phenomena we can see the critical period that affecting the firm power at both periods as shown in Table 5.21. The corresponding firm power shows the minimum capacity that needed by power plant to generate the energy. From Table 5.20 we can see that hydropower generation will be affected by climate change through reservoir inflow.

Table 5.20. Possible Firm Energy and Corresponding Firm Power of Wonogiri Hydropower Plant

Scenario		Annual Reservoir Inflow		90% Dependable Flow (m ³ /sec)	Possible Firm Energy	Corresponding Firm Power
		Maximum	Standard Deviation		MW-hr	MW
1984 - 2003		267.02	55.31	0.185904	2314.58	3.21
2024 - 2043	Scenario I	267.69	55.73	0.08224	2321.40	3.22
	Scenario II	264.56	55.05	0.115504	2306.87	3.2
2074 - 2093	Scenario I	288.30	61.18	0.163185	2431.04	3.38
	Scenario II	230.48	48.75	0.113033	2334.18	3.24

Table 5.21 (a) Reservoir Simulation: Critical Period for Observed Series (1984-2003)

Scenario	Year	Months	Initial Storage	Inflow	Outflow	Reservoir Volume	Reservoir Level	Effective Head	Spill	Generated Energy
			MCM	MCM	MCM	MCM	m	m	MCM	MWh
1984 - 2003	1994	5	433.00	15.22	50.28	397.94	135.405	19.875	0.00	2314.582
	1994	6	397.94	0.53	52.01	346.46	134.609	19.213	0.00	2314.582
	1994	7	346.46	0.29	54.39	292.35	133.709	18.372	0.00	2314.582
	1994	8	292.35	0.19	57.55	235.00	132.575	17.364	0.00	2314.582
	1994	9	235.00	0.18	62.16	173.02	131.115	16.076	0.00	2314.582
	1994	10	173.02	0.31	69.98	103.35	128.948	14.279	0.00	2314.582
	1994	11	103.35	36.22	81.57	58.00	127.000	12.250	0.00	2314.582
Total				52.94	427.94					

Table 5.21 (b) Reservoir Simulation: Critical Period for Long-Term Period (2074-2093) Scenario II

Scenario	Year	Months	Initial Storage	Inflow	Outflow	Reservoir Volume	Reservoir Level	Effective Head	Spill	Generated Energy
			MCM	MCM	MCM	MCM	m	m	MCM	MWh
2074 - 2093 SCENARIO II	2084	5	433.00	17.99	50.64	400.35	135.447	19.899	0.00	2334.178
	2084	6	400.35	0.00	52.36	347.99	134.635	19.247	0.00	2334.178
	2084	7	347.99	0.00	54.79	293.20	133.727	18.394	0.00	2334.178
	2084	8	293.20	0.00	58	235.20	132.578	17.374	0.00	2334.178
	2084	9	235.20	0.00	62.72	172.48	131.094	16.068	0.00	2334.178
	2084	10	172.48	0.30	70.76	102.02	128.892	14.241	0.00	2334.178
	2084	11	102.02	38.43	82.45	58.00	127.000	12.222	0.00	2334.178
Total				56.72	431.72					

The critical period that means by this simulation is the condition when the reservoir capacity starts from maximum reservoir capacity than decrease to the minimum reservoir capacity in short period due to small water inflow to the reservoir. In both case,

reservoir was full in the month of Mav and attained the dead storage level in the month of November. Table 5.21 (a) shows the sum of inflow and outflow were 52.94 MCM and 427.94 MCM respectively for observed period, while Table 5.21 (b) shows the sum of inflow and outflow of long-term period scenario II were 56.72 MCM and 431.72 MCM respectively. From both table (Table 5.21 (a) and Table 5.21 (b)) we can see that reservoir inflow and outflow in long-term period scenario II is higher than in observed period, which was causes the energy that can be generated in long-term period scenario II is higher than in observed period.

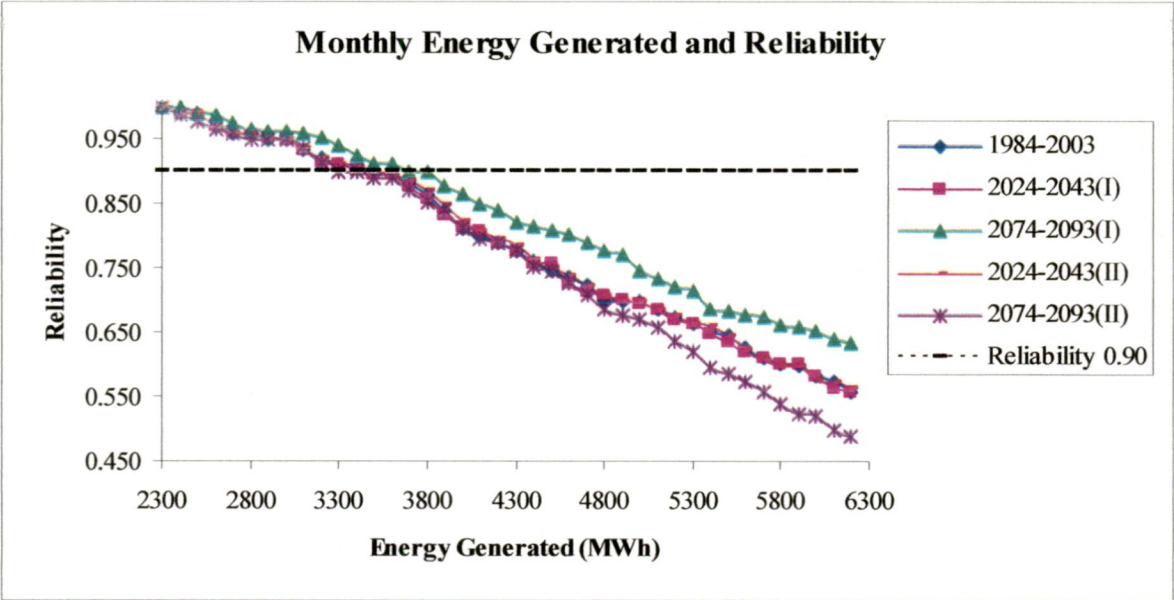


Figure 5.15. Monthly Energy Generated and Reliability

Figure 5.15 shows that for medium-term scenario, the deviation of reliability of monthly energy generated is less from the observed flow scenario than in long-term scenario even from scenario I or scenario II. Note that for reliability values above 0.90 is likely same in almost all scenarios, except in long-term scenario I that shows little higher reliability than the other scenarios. The deviation among the curve increase when the energy generation is more than 4800 MWh (the reliability is less than 0.688). This deviation shows variation of inflow discharge corresponding to climate change. Small deviation means the climate change does not give much impact on variation of discharge that have been generated, so the energy that can be generated using the inflow discharge corresponding with climate change relatively same with observed period. We may highlight that the possibility of operating the power plant at such low reliability is rather small. This

indicates that the variation of reservoir inflow in medium-term scenario is not too much, compared to the variation of reservoir inflow in long-term scenario and for high reliability the changing of climate did not give more impact on hydropower generation than in low reliability.

From the result of climate change calculation and the recommendation of IPCC 2007 as shown in Table 5.4 and Table 5.18, shows that in the study area climate change in the medium-term scenario (40 years) will have small change in precipitation ($\pm 3\%$) and temperature (-0.5°C to $+2.32^{\circ}\text{C}$). For this scenario of climate change, the firm energy that can be generated by hydropower plant at the study area is likely to change by 0.3% to -0.33% respectively for scenario I and scenario II. For long-term scenario, there will be significant change in precipitation and temperature by -12% to $+12\%$ and $+3.61^{\circ}\text{C}$ to $+3.92^{\circ}\text{C}$ (Table 5.4 and Table 5.18) respectively and the firm energy is likely to change by 5.03% to 0.85% respectively for scenario I and scenario II.

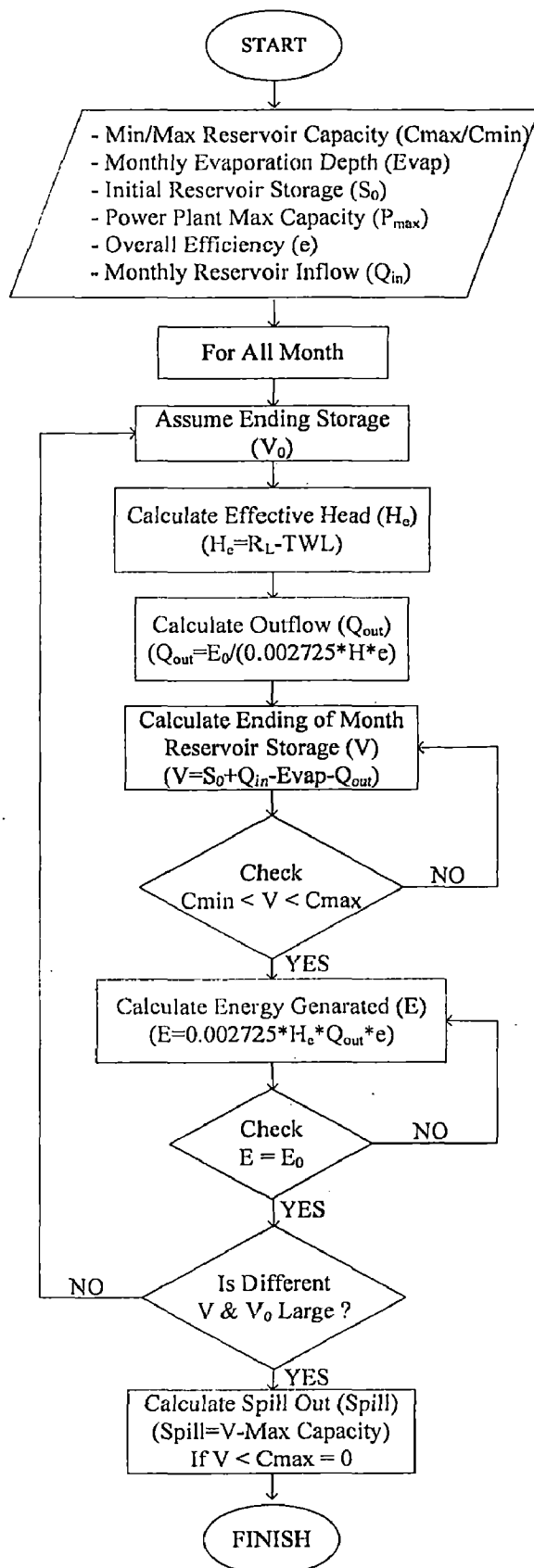


Figure 5.13. Reservoir Simulation Flow Chart for Determining Firm Energy

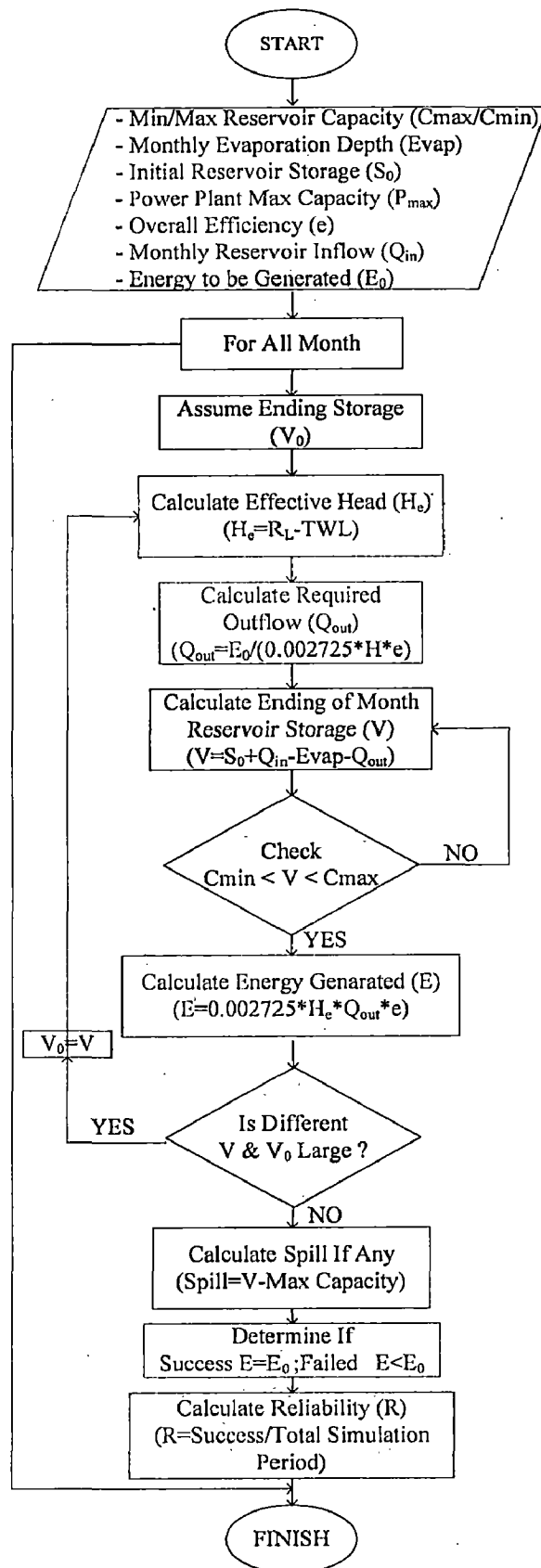


Figure 5.14. Reservoir Simulation Flow Chart for Determining Energy Reliability

Table 5.22: Simulation of Monthly Firm Energy Generated and Reliability

Energy Generation	Scenario											
	Observed Year			Medium-Term				Long-Term				
	1984 - 2003			2024 - 2043		2024 - 2043		2074 - 2093		2074 - 2093		
MW-hr	Failure Months	Reliability	Failure Months	Reliability	Failure Months	Reliability	Failure Months	Reliability	Failure Months	Reliability	Failure Months	Reliability
2300	0	1.000	0	1.000	0	1.000	0	1.000	0	1.000	0	1.000
2400	2	0.992	2	0.992	2	0.992	0	1.000	3	0.988	3	0.988
2500	2	0.992	3	0.988	2	0.992	2	0.992	2	0.992	5	0.979
2600	7	0.971	7	0.971	7	0.971	7	0.971	3	0.988	8	0.967
2700	10	0.958	9	0.962	10	0.958	10	0.958	6	0.975	10	0.958
2800	10	0.958	10	0.958	10	0.958	10	0.958	8	0.967	12	0.950
2900	12	0.950	11	0.954	12	0.950	12	0.950	9	0.962	12	0.950
3000	12	0.950	12	0.950	12	0.950	12	0.950	9	0.962	12	0.950
3100	16	0.933	16	0.933	15	0.938	15	0.938	10	0.958	15	0.938
3200	19	0.921	20	0.917	19	0.921	19	0.921	11	0.954	21	0.913
3300	21	0.913	21	0.913	21	0.913	21	0.913	14	0.942	24	0.900
3400	22	0.908	23	0.904	22	0.908	18	0.925	18	0.925	24	0.900
3500	25	0.896	25	0.896	24	0.900	21	0.913	21	0.913	26	0.892
3600	25	0.896	25	0.896	25	0.896	21	0.913	21	0.913	26	0.892
3700	28	0.883	29	0.879	27	0.887	24	0.900	24	0.900	31	0.871
3800	32	0.867	34	0.858	31	0.871	24	0.900	24	0.900	35	0.854
3900	38	0.842	40	0.833	36	0.850	29	0.879	29	0.879	38	0.842
4000	45	0.813	44	0.817	42	0.825	32	0.867	32	0.867	45	0.813
4100	48	0.800	46	0.808	46	0.808	36	0.850	36	0.850	49	0.796

(Continue)

Table 5.22. Simulation of Monthly Firm Energy Generated and Reliability (Continues)

Energy Generation	Scenario											
	Observed Year		Medium-Term				Long-Term					
	1984 - 2003		2024 - 2043		2024 - 2043		2074 - 2093		2074 - 2093			
MW-hr	Failure Months	Reliability	Failure Months	Reliability	Failure Months	Reliability	Failure Months	Reliability	Failure Months	Reliability		
4200	50	0.792	50	0.792	49	0.796	38	0.842	50	0.792		
4300	53	0.779	53	0.779	51	0.788	43	0.821	53	0.779		
4400	57	0.762	58	0.758	56	0.767	44	0.817	59	0.754		
4500	61	0.746	58	0.758	60	0.750	46	0.808	61	0.746		
4600	63	0.738	65	0.729	62	0.742	47	0.804	65	0.729		
4700	66	0.725	68	0.717	66	0.725	50	0.792	70	0.708		
4800	72	0.700	70	0.708	70	0.708	53	0.779	75	0.688		
4900	72	0.700	71	0.704	72	0.700	55	0.771	77	0.679		
5000	72	0.700	73	0.696	72	0.700	61	0.746	79	0.671		
5100	75	0.688	75	0.688	75	0.688	64	0.733	82	0.658		
5200	78	0.675	79	0.671	77	0.679	67	0.721	87	0.637		
5300	80	0.667	80	0.667	80	0.667	68	0.717	91	0.621		
5400	83	0.654	84	0.650	81	0.663	75	0.688	97	0.596		
5500	85	0.646	87	0.637	85	0.646	76	0.683	99	0.587		
5600	89	0.629	91	0.621	90	0.625	77	0.679	102	0.575		
5700	93	0.613	93	0.613	94	0.608	78	0.675	106	0.558		
5800	95	0.604	95	0.604	96	0.600	81	0.663	110	0.542		
5900	96	0.600	95	0.604	96	0.600	82	0.658	114	0.525		
6000	100	0.583	100	0.583	101	0.578	83	0.654	115	0.521		
6100	102	0.575	104	0.567	102	0.575	86	0.642	120	0.500		
6200	106	0.558	106	0.558	104	0.567	88	0.633	122	0.492		

CHAPTER VI CONCLUSIONS

6.1. Conclusions

This work has analyzed the impact of climate change on the hydrologic response of Wonogiri watershed as well as on hydropower generation. The following conclusions can be drawn from the study:

- The change in precipitation at the study area is likely to range between $\pm 3\%$ in the medium-term scenario (40 years from observed period approximately corresponding to 2024-2043) and $\pm 12\%$ in the long-term scenario (90 years from observed period approximately corresponding to 2074-2093) (Table 5.4 and Table 5.18). Further, the change in temperature in the study area is likely to range between -0.5°C to $+2.32^{\circ}\text{C}$ and $+3.61^{\circ}\text{C}$ to $+3.92^{\circ}\text{C}$ respectively for medium and long term scenario (Table 5.4 and Table 5.18).
- The result of modeling of Wonogiri catchment using SWAT model shows that the statistical properties of inflows to the Wonogiri reservoir are likely to change as shown at Table 6.1. Table 6.1 shows that in the medium-term period, the discharge is not likely to change much. However, in the long-term period, the change is likely to be appreciable.

Table 6.1. Result of Modeling of Wonogiri Catchment

Scenario		Mean Precipitation (mm)	Annual Reservoir Inflow			
			Mean (m3/sec)	Standard Deviation	% Change Over Baseline	Correlation Lag -1
1984 - 2003	Observed	5.63	53.36	55.31	-	-0.08103
2024 - 2043	Scenario I	5.72	53.38	55.73	0.04	-0.06701
	Scenario II	5.51	53.56	55.05	0.37	-0.09197
2074 - 2093	Scenario I	6.15	61.16	61.18	14.62	-0.07305
	Scenario II	5.18	48.34	48.75	-9.41	-0.07089

- In the medium-term scenario, the firm energy that can be generated by Wonogiri hydropower plant is likely to change by 0.3% to -0.33% respectively for scenario I and scenario II. While it may change by 5.03% to 0.85% for long-term scenario I and scenario II respectively.

- Hydropower generation at 0.90 reliability is shown in Table 6.2:

Table 6.2 Hydropower Generation at 0.90 Reliability

Scenario		Hydropower Generation	
		MWh	% Change Over Baseline
1984 - 2003	Observed	3325.30	-
2024 - 2043	Scenario I	3319.22	-0.183
	Scenario II	3344.32	0.572
2074 - 2093	Scenario I	3800.00	14.275
	Scenario II	3400.00	2.246

- Energy generated with reliability above 0.90 is nearly the same in almost all scenarios, except in long-term scenario I that shows higher generation than the other scenarios. Than the deviation from the baseline increase when the energy generation is more than 4800 MWh or the reliability less than 0.688 (Figure 5.15).

Based on the above, we can state that climate change impact need not always give negative impact. In some area climate change may provide a negative impact like decreasing in stream flow, drought, flood, and many other else, but we do not see that in this study area. Mostly, the impact of climate change on the stream flow and hydropower generation at the study area are likely to increase, except for long-term scenario II that shows decreasing in the stream flow by -9.41% (Table 6.1).

6.2. Suggestions for Future Research

- Climate change in the study area may be predicted using down-scaling technique.
- Watershed modeling (using SWAT or any suitable model) with consideration of change in land use and land cover, beside climate is necessary to get a better estimate of likely inflows and hydropower generation.
- Long series of data will be necessary to get better calibration and validation of the hydrologic models and predict the climate change impact.

REFERENCES

- Arnell, Nigel, 1997, *Global Warming, River Flows and Water Resources*, John Wiley & Sons Ltd, Baffins Lane, Chchester, West Sussex PO19 1UD, England.
- Arnell, N.W., Liu, C., Compagnucci, R., da Cunha, L., Hanaki, K., Howe, C., Mailu, G., Shiklomanov, I., Stakhiv, E., 2001. Hydrology and water resources. In: McCarthy, J.J., Canziani, O.F., Leary, N.A., Dokken, D.J., White, K.S. (Eds.), *IPCC Climate Change 2001: Impacts, Adaptation & Vulnerability, The Third Assessment Report of Working Group II of the Intergovernmental Panel on Climate Change (IPCC)*, 1000. Cambridge University Press, Cambridge, UK, pp. 133–191 (1000 pages).
- Barrows, H.K., 1978; *Water Power Engineering*, McGraw-Hill Books Company, Inc. New Delhi.
- Barry, R.G. and R.J. Chroley, 1995; *Atmosphere, Weather and Climate*, Routledge, London and New York.
- Booij, M.J., 2005; *Impact of Climate Change on River Flooding Assessed with Different Spatial Model Resolutions*, *Journal of Hydrology* 303, 176-19
- Bouwer, H. 1969. Infiltration of Water into Non Uniform Soil. *Journal Irrigation and Drainage Div.*, ASCE 95(IR4):451-462.
- Bouwer, Herman, 2002. Integrated Water Management for the 21st Century: Problem and Solution., *Journal of Irrigation and Drainage Engineering*. Vol. 128 No.4, August 1, 2002.
- Bouwer, L. M., Aerts, J. C. J. H., Droogers, P. and Dolman, A. J., 2006. Detecting the Long-Term Impacts from Climate Variability and Increasing Water Consumption on Runoff in The Krishna River Basin (India). *Hydrology Earth System Science*, 10, 703–713.
- Chaudhari, Q.Z., 1994, *Pakistan's Summer Monsoon Rainfall Associated with Global and Regional Circulation Features and its Seasonal Prediction*. In: *Proceedings of the International Conference on Monsoon Variability and Prediction*, Trieste, Italy, May 9-13.
- Chen, L., Dong, M., and Shao, Y. (1992). The Characteristics of Interannual Variations on the East Asian Monsoon. *Journal of the Meteorological Society of Japan* 70, 397–421.
- Christensen, N.S and Lettenmainer, D.P., 2007. A Multimodel Ensemble Approach to Assessment of Climate Change Impacts on the Hydrology and Water Resources of the Colorado River Basin. *Hydrology & Earth System Science* 11, 1417-1434.
- DelGenio, A.D., Lacis, A.A., Ruedy, R.A., 1991. Simulations of the Effect of a Warmer Climate on Atmospheric Humidity. *Nature* 351, 382–385.

- Dibike, Yonas B. and Coulibaly, Paulin, 2005. Hydrologic Impact of Climate Change in the Saguenay Watershed: Comparison of Downscaling Methods and Hydrologic Models. *Journal of Hydrology* 307 (2005) 145–163
- Dragoni, W. and Sukhija, B.S., 2008: Climate Change and Groundwater: A Short Review., Geological Society, London, Special Publications 2008; v. 288; p. 1-12. doi:10.1144/SP288.1
- Du, J., and Ma, Y.C. (2004). Climatic Trend of Rainfall over Tibetan Plateau from 1971 to 2000. *Acta Geographica Sinica* 59(3), 375-382.
- EIA, 1999. International Energy Annual 1999:electricity. US Energy Information Administration, Department of Energy, <http://www.eia.doe.gov/emeu/iea/elec.html>.
- FAO (Food and Agriculture Organization), 2003: *World Agriculture: Towards 2015/2030. An FAO Perspective*. Bruinsma, Ed., FAO, Rome and Earthscan, London.
- FAO (Food and Agriculture Organization), 2004a: Yearbook of Fishery Statistics 2002: Capture Production, Vol. 94/1, Food and Agriculture Organization of the United Nations, Rome.
- FAO (Food and Agriculture Organization), 2004b: Yearbook of Fishery Statistics 2002: Aquaculture Production, Vol. 94/2, Food and Agriculture Organization of the United Nations, Rome.
- FAO (Food and Agriculture Organization), 2004c: Data Base. Food and Agriculture Organization of the United Nations, Rome.
- FAO (Food and Agriculture Organization), 2005: Special event on impacts of climate change, pests and diseases on food security and poverty reduction. Background document 31st Session of the Committee on World Food Security, Rome.
- FAO/WFP (Food and Agriculture Organization/World Food Programme), 2000: FAO/WFP Crop and Food Supply Assessment Mission to Cambodia. Special Report X9237/E, 29 December 2000, FAO Global Information and Early Warning System on Food and Agriculture/World Food Programme.
- Goyal, R.K., 2004. Sensitivity of Evapotranspiration to Global Warming: A Case Study of Arid Zone of Rajasthan (India), *Agricultural Water Management* 69 (2004) 1–11
- Harrison, Gareth P. and Whittington, H. (Bert) W., 2007. Susceptibility of the Batoka Gorge Hydroelectric Scheme to Climate Change. *Hydrology Earth System Science*, 11(3), 1191-1205, 2007
- Held, I.M., Soden, B.J., 2000. Water Vapor Feedback and Global Warming. *Annu. Rev. Energy Environ.* 25, 441–475.
- Huntington, Thomas G., 2006. Evidence for Intensification of The Global Water Cycle: Review and Synthesis. *Journal of Hydrology* 319 (2006) 83–95
- Hu, Z.Z., Yang, S., and Wu, R. (2003). Long-Term Climate Variations in China and Global Warming Signals. *Journal of Geophysical Research* 108, doi:10.1029/2003JD003651

<http://www.globalwarming.org.in/>

http://www.philly.com/inquirer/front_page/20100423_Iceland_a_hot_spot_of_volcanic_activity.html#axzz0nvwppkUo

IEA, 1999; Key World Energy Statistics. International Energy Agency, Paris.

IPCC, 2007a; Climate Change 2007: The Physical Science Basis, Cambridge University Press, UK.

IPCC, 2007b; Climate Change 2007: Impact, Adaptation and Vulnerability, Cambridge University Press, UK.

IPCC, 2007c; Climate Change 2007: Mitigation of Climate Change, Cambridge University Press, UK.

Jain, SK and Singh, V.P., 2003: Water Resources System Planning and Management, Elsevier Science B.V. Sara Burgerhartstraat 25 – P.O. Box 211, 1000 AE Amsterdam, The Netherlands

Kilsby, CG., Tellier, S.S., Fowler, H.J. and Howels, T.R., 2007. Hydrological Impacts of Climate Change on the Tejo and Guadiana Rivers. *Hydrology & Earth System Science* 11(3), 1175-1189.

Kirk, Robert W. Van and Naman, Seth W., 2007, Separating Effects of Water-Use and Climatic Changes on Base Flow in the Lower Klamath Basin, U.S. Fish and Wildlife Service Arcata Fish and Wildlife Office 1655 Heindon Road Arcata, California 95521

Koch, Franch H., 2002; Hydropower-The Politics of Water and Energy: Introduction and Overview, *Energy Policy* 30 (2002) 1207-1213, http://www.sciencedirect.com/science?_ob=MIimg&_imagekey=B6V2W-461XG91-2-1&_cdi=5713&_user=1143371&_orig=search&_coverDate=11%2F30%2F2002&_sk=999699985&view=c&wchp=dGLbVtz-zSkzV&md5=ee2b0f103bb96eddc1eca8498392de35&ie=/sdarticle.pdf

Labat D, Godderis Y, Probst JL, Guyot JL. Evidence for Global Runoff Increase Related to Climate Warming. *Adv Water Resour* 2004:631–42.

Landsea, C.W., Harper, B.A., Hoarau, K.H., and Knuff, J.A. (2006). Can We Detect Trends in Extreme Tropical Cyclones? *Science* 313, 452-454.

Legates, David R., Lins, Harry F. and McCabe, Gregory J., Comments on “Evidence for Global Runoff Increase Related to Climate Warming” by Labat et al., *Advances in Water Resources* 28 (2005) 1310–1315

Lehner, Bernard, Czisch, Gregor and Vassolo, Sara, 2005; The Impact of Global Climate Change on the Hydropower Potential of Europe : A Model-Based Analysis, *Energy Policy* 33 (2005) 839-885, http://www.sciencedirect.com/science?_ob=MIimg&_imagekey=B6V2W-4B8BMS B-1-&_cdi=5713&_user=1143371&_orig=search&_coverDate=05%2F31%2F2005&_sk=999669992&view=c&wchp=dGLbVtzzSkzV&md5=621990f185a78d84da9413e84db1dc4e&ie=/sdarticle.pdf

- Liepert, J., Roeckner, E., Lohmann, U., Liepert, B.G., 2004. Aerosols Dampen the Water Cycle in a Warmer and Moister World. *Geophys. Res. Lett.* 31. doi:10.1029/2003GL0190660.
- Linde, A. H. te, Aerts, J. C. J. H., Hurkmans, R. T. W. L., and Eberle, M., 2008. Comparing Model Performance of Two Rainfall-Runoff Models in the Rhine Basin using Different Atmospheric Forcing Data Sets. *Hydrology & Earth System Science* 12, 943-957.
- Loaciga, H.A., Valdes, J.B., Vogel, R., Garvey, J., Schwarz, H., 1996. Global Warming and the Hydrologic Cycle. *J. Hydrol.* 174, 83–127.
- Lucena, Andre Frossard Pereirade, et al., 2009. The Vulnerability of Renewable Energy to Climate Change in Brazil. *Energy Policy* 37 (2009) 879–889
- Mein, R.G. and C.L. Larson. 1973. Modeling Infiltration during a Steady Rain. *Water Resources Research* 9(2):384-394
- Mishra, Surendra Kumar and Singh, Vijay P., 2003. Soil Conservation Service Curve Number (SCS-CN) Methodology., Kluwer Academic Publishers – Netherlands.
- Morlot, Jan Corfee, and Hohne, Niklas, 2003, Climate Change: Long-Term Targets and Short-Term Commitments, *Global Environmental Change* 13 (2003) 277–293
- Nearing, M.A., B.Y. Liu, L.M. Risse, and X. Zhang. 1996. Curve Number and Green-Ampt Effective Hydraulic Conductivities. *Water Resources Bulletin* 32:125-136.
- Neitsch, S.L., Arnold, J.G., Kiniry, J.R., Williams, J.R., 2005., Soil and Water Assessment Tool Theoretical Documentation Version 2005., Grassland, Soil and Water Research Laboratory - Agricultural Research Service 808 East Blackland Road - Temple, Texas 76502
- Nieuwolt , Simon and McGregor, Glenn R. , 1998; *Tropical Climatology: An Introduction to the Climates of the Low Latitudes*, Wiley, John & Sons, Incorporated.
- Nyenje, Philip M. and Batelaan, Okke, 2009, Estimating the Effects of Climate Change on Groundwater Recharge and Baseflow in the Upper Ssezibwa Catchment, Uganda, *Hydrological Sciences–Journal–des Sciences Hydrologiques*, 54(4) August 2009 Special issue: Groundwater and Climate in Africa.
- Oud, Engelbertus, 2002; The Evolving Context for Hydropower Development, *Energy Policy* 33 (2005) 1215-1223, http://www.sciencedirect.com/science?_ob=MIimg&_imagekey=B6V2W-461XG91-3-5&_cdi=5713&_user=1143371&_orig=search&_coverDate=11%2F30%2F2002&_sk=999699985&view=c&wchp=dGLbVtz-zSkzV&md5=9174b3482ca67e9fb7dae6496a47885d&ie=/sdarticle.pdf
- Polhemus, Dan A., 2009, Climate Change in New Guinea and its Potential Effects on Freshwater Ecosystems, Bishop Museum Technical Report 42(3) January 2009.
- Polhemus, D. A. and G. A. Allen. 2007. Inland Water Ecosystems in Papua: Classification, Biota and Threats, pp. 858–900 in *Ecology of Papua, Part 2* (A. J. Marshall and B. M. Beehler, eds.). Periplus Editions (HK) Ltd., Singapore. xv + 753–1467 pp.

- Preston, Benjamin L., et al., 2006, *Climate Change in the Asia/Pacific Region : A Consultancy Report Prepared for the Climate Change and Development Roundtable, Commonwealth Scientific and Industrial Research Organization (CSIRO) Australia.*
- Ramanathan, V., Krutzen, P.J., Kiehl, J.T., Rosenfeld, D., 2001. Aerosols, Climate, and the Hydrologic Cycle. *Science* 294, 2119–2124.
- Ren, G., Wu, H., and Chen, Z. (2000). Spatial Pattern of Precipitation Change Trend of the Last 46 Years over China. *Journal of Applied Meteorology* 11(3), 322-330.
- Schaeffer, Roberto and Szklo, Alexandre Salem, 2001. Future Electric Power Technology Choices of Brazil: A Possible Conflict Between Local Pollution and Global Climate Change. *Energy Policy* 29 (2001) 355-369
- Schaeffli, Bettina, Hingray, Benoit and Musy, Andre, 2007. Climate Change and Hydropower Production in the Swiss Alps: Quantification of Potential Impacts and Related Modelling Uncertainties. *Hydrology Earth System Science*, 11(3), 1191-1205, 2007
- Shi, Y. F., Shen Y.P., and Hu R.J. (2002). Preliminary Study on Signal, Impact and Foreground of Climatic Shift from Warm-Dry to Warm-Humid in Northwest China, *Journal of Glaciology Geocryology* 24(3), 219-226.
- Stanhill, G., Cohen, S., 2001. Global dimming: A Review of the Evidence for a Widespread and Significant Reduction in Global Radiation with Discussion of its Probable Causes and Possible Agricultural Consequences. *Agric. Forest Meteorol.* 107, 255–278.
- Susilowati dan Satina, Tima, 2006. Analisis Perubahan Tata Guna Lahan dan Koefisien Limpasan terhadap Debit Drainase Perkotaan., *Media Teknik Sipil – Januari 2006.*
- Trenberth, K.E., 1999. Conceptual Framework for Changes of Extremes of the Hydrological Cycle with Climate Change. *Climatic Change* 42, 327–339.
- Singh, Savindra, 2005; *Climatology*, Prayag Pustak Bhawan, Allahabad
- UNFCCC, 2007; *Climate Change: Impacts, Vulnerabilities and Adaptation in Developing Countries*, Climate Change Secretariat (UNFCCC) Martin-Luther-King-Strasse 853175 Bonn, Germany.
- Wang, S et all, 2006, The Impact of the Climate Change on Discharge of Suir River Catchment (Ireland) under Different Climate Scenarios, *Natural Hazards Earth System Science*, 6, 387–395, 2006, Met Eireann, Glasnevin Hill, Dublin 9, Ireland.
- Wild, M., Ohmura, A., Gilgen, H., Rosenfeld, D., 2004, On the Consistency of Trends in Radiation and Temperature Record and Implications for the Global Hydrologic Cycle. *Geophys. Res. Lett.* 31, L11201 doi: 10.11029/2003L091188.

- Winchell, M., Srinivasan, R., Di Luzio, M. and Arnold, J., 2009, ARCSWAT 2.3.4 Interface for SWAT2005 - User's Guide, Blackland Research Center Texas Agricultural Experiment Station 720 East Blackland Road - Temple, Texas 76502 and Grassland, Soil And Water Research Laboratory USDA Agricultural Research Service 808 East Blackland Road - Temple, Texas 76502
- White, Kati L. and Chaubey, Indrajeet, 2005., Sensitivity Analysis, Alibration, and Validations for a Multisite and Multivariable SWAT Model., Journal Of The American Water Resources Association - American Water Resources Association
- World Bank, 2005, India's Water Economy: Branching for a Turbulent Future, World Bank October 2005
- World Bank, 2009, South Asia: Shared Views on Development and Climate Change, South Asia Region Sustainable Development Department International Bank for Reconstruction and Development/The World Bank 1818 H Street NW Washington DC 20433 U.S.A.
- Zhao, L., Ping, C.L., Yang, D., Cheng, G., Ding, Y., and Liu, S. (2004). Changes of Climate and Seasonally Frozen Ground over the Past 30 years in Qinghai-Xizang (Tibetan) Plateau, China. *Global and Planetary Change* 43, 19-31.